Neutrino oscillations in matter

T. K. Kuo

Department of Physics, Purdue University, West Lafayette, Indiana 47907

James Pantaleone

Department of Physics, University of California at Riverside, Riverside, California 92521

Nonzero neutrino masses would provide new, unique information on particle physics beyond the standard model. Neutrino flavor oscillations provide the most sensitive method for directly testing for small neutrino masses. When the oscillations occur in matter, a resonance can occur that dramatically enhances the flavor mixing and can lead to conversion from one neutrino flavor to another. This is an attractive solution to the long-standing "solar neutrino problem." The phenomenon of neutrino oscillations in matter is reviewed. Analytic descriptions of the neutrino flavor survival probability in matter are considered in detail. A discussion is given for applications of neutrino oscillations in matter for the sun, Earth, supernovae, and the early universe.

CONTENTS

I. GENERALITIES

A. Introduction

It has been three decades since the possibility of neutrino oscillations was first suggested (Pontecorvo, 1958, 1969; Maki *et al.*, 1962). Even though no firm experimental evidence for their existence has been established, the search for neutrino flavor mixings has been conducted with ever increasing vigor. The main reason for this enthusiasm is that the idea seems extremely reasonable in the framework of our current theoretical understanding of elementary-particle physics.

Theoretically, in the standard model of particle physics, neutrinos are usually assumed to be purely left handed and massless. However, there is no compelling reason to assume this. The standard model, with its numerous arbitrary parameters, is considered by many as the low-energy limit of a more complete theory. In such unified theories, one generally does have massive neutrinos. If neutrinos are massive, then there should be a leptonic mixing matrix corresponding to the Cabibbo-Kobayashi-Maskawa (CKM) matrix. The lepton-quark analogy is now complete.

Experimentally, the phenomenology of light neutrinos is very hard to distinguish from that of massless neutrinos. However, with small neutrino masses come small neutrino mass differences and the possibility of macroscopic oscillation wavelengths. The phenomenon of oscillation is very common in classical as well as in quantum-mechanical systems. A familiar example is that of K_0-$\bar{K}_0$ oscillations. Because of the CKM mixing matrix, weak interactions induce transitions between K_0 and

$\bar{K}_0$. Thus the mass eigenstates are admixtures of K_0 and $\bar{K}_0$. As a consequence, if we start with a beam of, say, K_0, as it propagates in time it will oscillate between the states K_0 and $\bar{K}_0$. However, there are some differences between kaon and neutrino oscillations. K_0-$\bar{K}_0$ mixing is expected to be maximal, but the amplitude of neutrino mixing is bounded by the lepton mixing matrix. Furthermore, the kaons decay while the lifetimes of neutrinos with small masses are negligible.

Having established the qualitative aspects of neutrino oscillations, it remains to treat the problem quantitatively. Unfortunately, not much is certain about neutrino mass and mixing parameters. Experimentally, bounds on the masses and mixing angles exist, but no definitive evidence for a nonzero neutrino mass has been established. Theoretically, there seems to be a consensus that the "seesaw" model provides a nice explanation for why neutrino masses are small. Generally, this model gives a hierarchy of neutrino masses and small mixing angles. In the analysis to follow, we shall occasionally fall back on this general expectation as a guide for discriminating between the many logical possibilities for neutrino mass and mixing parameters.

So far, we have tacitly assumed that the neutrinos are propagating in vacuum. Since the neutrino cross section is proportional to G_F^2, the mean free path of a neutrino is so large that there seems little chance for the medium to influence the neutrino propagation. This turns out not to be the case, as pointed out by Wolfenstein (1978a, 1978b, 1979). The point is that for neutrino oscillations the relevant quantity is the phase of the neutrino wave function. Since the phase is altered to order G_F by the medium, neutrino oscillations can be influenced greatly. As we shall discuss later, the characteristic length for phase alteration is about 10^9 cm, for a medium with a density of 1 g/cm^3, versus the mean free path, about 10^{17} cm in the same medium. Thus neutrino oscillations in an astrophysical setting can be very different from that in vacuum. Even more interesting is the fact that the oscillation effect takes on a resonance form, as pointed out by Mikheyev and Smirnov (1985, 1986a, 1986b). If the conditions for a resonance are met, the neutrino flavor mixing can become maximal. If the neutrino propagates adiabatically through the resonance, the initial flavor of the neutrino is converted to another flavor. This is known as the MSW (Mikheyev, Smirnov, and Wolfenstein) effect.

A prime motivation for the study of neutrino oscillations has been the long-standing "solar neutrino problem." The theory of the dynamics of the sun has been in place for a long time and has settled down in the form of a "standard solar model." However, the ^{37}Cl experiment (Davis, 1988), which has been running for two decades, has found a consistent discrepancy between the predicted and the observed solar neutrino fluxes. During this long period, both the ^{37}Cl experiment and the model of the sun have undergone thorough reinvestigation. There appears to be a real effect in the ratio of $\frac{1}{3}$ to $\frac{1}{4}$ between measured versus predicted flux. More recently, in the water Cherenkov detector Kamiokande II, an upper bound of about $\frac{1}{2}$ has been established for the same ratio (Mann *et al.*, 1988). Among the many theoretical ideas proposed, neutrino oscillations seem to offer the most reasonable solution.

It has long been realized that vacuum neutrino oscillations could solve the solar neutrino problem. Vacuum oscillations could reduce the solar neutrino flux by $\frac{1}{3}$ or $\frac{1}{4}$ if the mixing were maximal between three or four flavors, respectively. This is somewhat distasteful since, as mentioned previously, the general expectation is that the mixing angles are small. However, with the inclusion of matter effects, large reductions are possible for very small vacuum mixing. It turns out that for the solar neutrinos, the resonance conditions would be met for a "ν_μ" or a "ν_τ" neutrino mass of 10^{-2}–10^{-4} eV and for mixing angles $\sin\theta > 10^{-2}$. Both of these quantities are easily within the bounds of theoretical estimates. This is why the neutrino oscillation, and, in particular, the MSW effect, is regarded as the most plausible candidate for the solution of the solar neutrino problem.

There are other ways to solve the solar neutrino problem (for a short review see, e.g., Weneser and Friedlander, 1987) through extending the properties of neutrinos. One such proposal is to give the ν_e an extremely large magnetic moment. Then the left-handed neutrino that is produced can rotate into a right-handed neutrino that does not interact in a detector. Another proposal is that the solar neutrinos can oscillate into sterile neutrino states. In general, these proposals require radical extensions of the standard model, and we shall not consider their details further.

There exists an earlier, methodical review of neutrino oscillations in matter by Mikheyev and Smirnov (1987c). In the short time since that review there has been considerable progress. For example, the analytic description of the MSW effect has improved. There is a new, independent measurement of the solar neutrino flux, and the neutrinos have been detected from a nearby supernova. In the present paper we have tried to give a comprehensive review of neutrino oscillations in matter with an emphasis on practical, physical applications.

This review is divided into four parts. In Sec. I we present a very brief overview of the current status of neutrino physics. Section I.B reviews the dominant theoretical model for neutrino masses, the seesaw mechanism. Section I.C summarizes the results of experimental limits on neutrino masses. The remainder of the review concentrates on neutrino oscillations in matter.

In Sec. II we develop the tools to describe quantitatively the MSW effect. Section II.A reviews the theory of neutrino oscillations in vacuum. Section II.B derives the wave equation for neutrinos propagating in matter. The next two sections then discuss analytical techniques for solving this equation, for two neutrino flavors in Sec. II.C and for three neutrino flavors in Sec. II.D.

In Sec. III we apply the result of Sec. II to different media and different sources of neutrinos. Section III.A

discusses resonant conversion of neutrinos in the sun and the neutrino parameters that solve the solar neutrino problem. Section III.B reviews matter-enhanced mixing of neutrinos propagating through the Earth for various sources of neutrinos. Section III.C discusses aspects of resonant conversion of supernova neutrinos: what can be learned from SN 1987A or possibly from the next supernova? Section III.D reviews neutrino oscillations in the early universe.

Section IV consists of a summary of our review, with conclusions.

B. "Expected" neutrino parameters

In the $SU_C(3)\times SU_L(2)\times U_Y(1)$ standard model the neutrinos can be massless. When one considers extensions of the standard model, such as in many unified theories, the neutrinos usually pick up masses. Although there are many schemes (Langacker, 1981) to explain why these masses should be small, most are just variations on one basic theme—a seesaw mechanism (Gell-Mann, *et al.*, 1979; Yanagida, 1979). To illustrate these schemes and their predictions we shall discuss one simple version of the seesaw mechanism. However, our examination of neutrino mixing in matter will not be restricted to any particular neutrino mass mechanism. The discussion here is meant to serve as a guide to what present-day wisdom gives as the favored neutrino parameters.

For three generations of left- and right-handed neutrinos the seesaw mechanism suggests the following 6×6 neutrino mass matrix,

$$M=\begin{bmatrix} 0 & m_D/2 \\ m_D^T/2 & M_R \end{bmatrix} . \tag{1.1}$$

Here m_D is a 3×3 Dirac mass matrix and M_R is a 3×3 Majorana mass matrix. The neutrino Dirac mass matrix m_D is expected to be similar to the quark and charged-lepton mass matrices, so the generation structure of the known fermions implies that $\mu_3 \gg \mu_2 \gg \mu_1$, where μ_i are the three eigenvalues of m_D. m_D can be diagonalized by two unitary transformations Y and V, $Ym_DV \equiv \mu_i\delta_{ij}$. M_R is a different type of mass term that cannot occur for charged fermions. This term breaks the global U(1) symmetry, the lepton number, and is expected to be generated at some large unification scale, $\Lambda \gg \mu_i$.

As an example, let us assume that there is only one heavy scale and that M_R is diagonal, so that $M_R=\Lambda$ times the identity matrix. In this case the algebra simplifies. The mass eigenvalues are given, in general, by

$$\pm[(\Lambda^2+\mu_i^2)^{1/2}\pm\Lambda]/2 . \tag{1.2}$$

For the light eigenvalues this takes the approximate form

$$m_i \approx \mu_i^2/\Lambda . \tag{1.3}$$

The mass matrix M in Eq. (1.1) is diagonalized exactly by the unitarity transformation W, such that $W^TMW=$diagonal. The matrix W is given by

$$W=\begin{bmatrix} Y^T & 0 \\ 0 & V \end{bmatrix}\begin{bmatrix} \tilde{C} & \tilde{S} \\ -\tilde{S} & \tilde{C} \end{bmatrix} , \tag{1.4}$$

where Y and V are the matrices that diagonalize m_D and $\tilde{C}=\cos\theta_i\delta_{ij}$, $\tilde{S}=\sin\theta_i\delta_{ij}$ with $\tan 2\theta_i=\mu_i/\Lambda$ (see, e.g., Cheng and Li, 1980). The heavy neutrino coupling to the charged weak currents is suppressed by $\sin\theta_i=\mu_i/\Lambda$, but the light-neutrino mixing matrix depends on $\cos\theta_i\approx 1$ and hence is relatively unaffected by the seesaw mechanism.

Since m_D is expected to be similar to the charged-fermion mass matrices, the light-neutrino mixing matrix is expected to be similar to the mixing matrix in the quark sector. We shall define the light-neutrino mixing matrix as

$$\nu_\alpha = U_{\alpha i}\nu_i , \tag{1.5}$$

so that the charged-lepton current is proportional to $\bar{l}_\alpha U_{\alpha i}\nu_i$. Comparing this with the quark weak current, we see from the above discussion that a reasonable order-of-magnitude guess for the neutrino mixing matrix is

$$U \approx U_{\rm KM}^\dagger , \tag{1.6}$$

where $U_{\rm KM}$ is the Cabibbo-Kobayashi-Maskawa quark mixing matrix. This neglects the mixing with the heavy-neutrino states.

What to expect for the light-neutrino masses, Eq. (1.3), is less certain than what to expect for the light-neutrino mixings, Eq. (1.6). The largest uncertainty lies in what to choose for the heavy-mass scale Λ. There are a number of choices for the scale Λ, leading to different values for m_i. If we take Λ to be 10^{14} GeV, a typical grand unification scale, and $\mu_3 \approx m_\tau$, then $m_3 \approx 10^{-4}$ eV. This mass value can be smaller or larger by several orders of magnitude, since we may identify the large mass with $\alpha^2\Lambda$ (assuming it is radiatively generated) or with $\Lambda_{\rm PLANCK}$ ($\approx 10^{19}$ GeV). These mass values are thus easily compatible with the ranges required in the MSW effect.

Another uncertainty for the neutrino masses concerns what to expect for the nature of the neutrino mass hierarchy. Equation (1.3) predicts that the light-neutrino masses should vary approximately as the square of the charged-fermion masses. However, this can change if one does not make the assumption that M_R is a diagonal mass matrix. Then the three light-neutrino mass eigenstates that couple to the charged leptons would have the approximate mass matrix

$$m_\nu = m_D M_R^{-1} m_D^T \tag{1.7}$$

(see, e.g., Terry and Kuo, 1981). Structure in M_R would change the predictions of Eq. (1.3). It is not unreasonable to expect that a hierarchical structure in M_R could

exist and that the variation of the light-neutrino masses with the charged-fermion masses would be linear, cubic, or something else. Such structure in M_R would similarly affect the neutrino mixing matrix. The hierarchy in mixing angles expected in Eq. (1.6) could be increased or decreased, analogous to the change in the neutrino mass ratio.

C. Experimental constraints on neutrino masses and mixings

Here we shall give a brief review of the present experimental limits on neutrino masses. We shall emphasize limits on light neutrinos and shall not discuss limits on heavy, fourth-generation neutrinos. For details on this subject, see, e.g., Gronau *et al.* (1984); Gilman (1986); Babu *et al.* (1989), and references therein. We shall also not discuss limits on neutrino masses from cosmology.

1. Kinematic limits

A list of limits on neutrino masses from kinematics is given in Table I. Here $m(\nu_\alpha)$ denotes the mass of the neutrino that couples dominantly to the charged lepton of species α. The first four entries are from observation of the electron spectrum from tritium decay. A nonzero neutrino mass means that less kinetic energy is available for the electron, so that the high energy end point of the spectrum is decreased. The first entry in the table indicates a possible nonzero neutrino mass observation by ITEP (the Institute of Theoretical and Experimental Physics; see Boris *et al.*, 1987). However, this possibility has not been confirmed and, in fact, is barely compatible with other studies of tritium decay; Zurich (Fritschi *et al.*, 1986), LANL (Los Alamos National Laboratory; see Wilkerson *et al.*, 1987), and INS-Tokyo (the Institute for Nuclear Study–University of Tokyo; see Kawakami *et al.*, 1987).

A limit on $m(\nu_e)$ comparable to these comes from the recent observation on neutrinos emitted from the supernova 1987A in the Large Magellanic Cloud. The neutrinos were detected with energies of tens of MeV on a time scale of a few seconds. This agrees with the theoretical models for supernova collapse. The hot neutron star produced just after the collapse of the core is expected to thermally emit neutrinos with a temperature of a few MeV on a time scale of a few seconds. If the neutrinos had a mass, the signal would be distorted in time, since the neutrinos are emitted with a range of energies and hence a range of velocities. The difference in the time of flight δt for two neutrinos emitted from the supernova with different energies but the same mass is given by

$$\delta t \approx L\delta v \approx L\delta\gamma/\gamma^3 \approx L(m/E)^3\delta E/m \ . \tag{1.8}$$

Taking δt to be a few seconds and $\delta E \approx E \approx$ tens of MeV, and using that the distance from the supernova to Earth, L, is approximately 170 000 light years, yields the limit on the neutrino mass m given in Table I. This limit has been much discussed in the literature and may be improved by a factor of 2 to 4 if one incorporates specific features of hot neutron star models. However, it is not clear how reliable these models are.

The kinematic limits on $m(\nu_\mu)$ and $m(\nu_\tau)$ are obtained in a fashion similar to the limits on $m(\nu_e)$ from tritium decay. The limit on $m(\nu_\tau)$ is from the study of the pion spectrum of the decay $\tau \to 5\pi + \nu_\tau$ (Albrecht *et al.*, 1988). The limit on $m(\nu_\mu)$ is from the study of the muon spectrum in $\pi \to \mu + \nu_\mu$ decay (Abela *et al.*, 1984).

TABLE I. Current experimental limits on the neutrino masses from kinematics.

$17 < m(\nu_e) < 40$ eV	ITEP
$m(\nu_e) < 18$ eV	Zurich
$m(\nu_e) < 27$ eV	LANL
$m(\nu_e) < 32$ eV	INS-Tokyo
$m(\nu_e) < 20$ eV	SN 1987A
$m(\nu_\mu) < 250$ keV	SIN
$m(\nu_\tau) < 35$ MeV	ARGUS

2. Vacuum oscillations

A detailed theoretical description of vacuum oscillations will be developed in the next section. Here we merely summarize the existing level of experimental sensitivity in Fig. 1. The data are analyzed under the simplifying assumption of only two neutrino flavors, because no firm evidence for neutrino vacuum mixing has ever been found. The graphs plot the experimental constraints on the effective two-flavor mass difference versus mixing for $\nu_e \rightleftarrows \nu_x$ and $\nu_\mu \rightleftarrows \nu_x$ oscillations. Accelerators, nuclear reactors, and cosmic rays are used as sources of neutrinos.

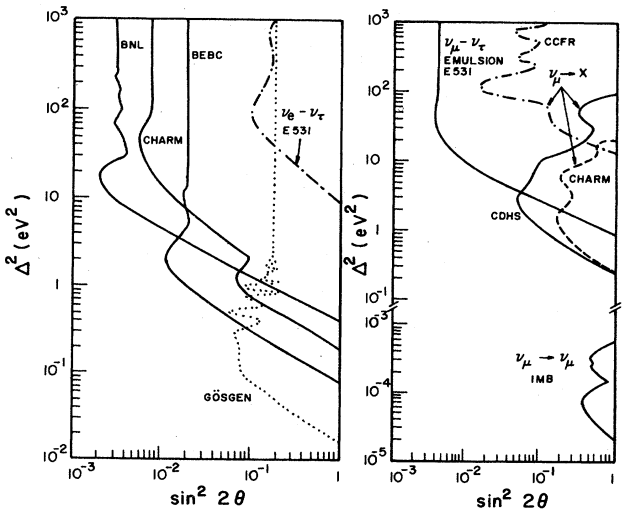

FIG. 1. Limits (90% C.L.) on $\nu_\mu \to \nu_e$, $\nu_e \to \nu_\tau$, and $\bar{\nu}_e \to x$ (left) and $\nu_\mu \to x$ and $\nu_\mu \to \nu_\tau$ (right). The allowed areas are to the left of the curves (Eichler, 1988).

3. Neutrinoless double-beta decay

If the neutrino has a Majorana mass, then lepton number is no longer a conserved quantum number. Decays that violate lepton number can then occur and would be evidence for a neutrino mass. One such decay that is often sought is the neutrinoless decay of a nucleus with two positrons emitted—neutrinoless double-beta decay. Double-beta decay with two-neutrino emission is allowed by lepton number conservation and has recently been observed directly (Elliot *et al.*, 1987). Neutrinoless double-beta decay enjoys a significant enhancement from phase space over the lepton-number-conserving process. Thus the failure to observe neutrinoless double-beta decay can put meaningful limits on the neutrino mass. For a review of the experimental constraints on double-beta decay see Caldwell (1988).

The present limit on the neutrino mass from neutrinoless double-beta decay is

$$\langle m(\nu_e)\rangle < 1 \text{ eV} . \tag{1.9}$$

The nuclear physics is quite complicated, so the exact limit is uncertain by about an order of magnitude. However, the recent observation of double-beta decay with neutrino emission should greatly help to decrease this uncertainty. The quantity $\langle m(\nu_e)\rangle$ represents a sum of the amplitude over all mass eigenstates that couple to the electron. It is given approximately by

$$\langle m(\nu_e)\rangle \equiv \sum_i U_{ei}^2 \chi_i m_i + \sum_j U_{ej}^2 \chi_j \sigma^2 / M_j ; \tag{1.10}$$

U_{ei} is the mixing matrix between the electron neutrino and the ith mass eigenstate, χ_i is the CP eigenvalue of that eigenstate, m_i and M_i are neutrino masses, and σ is a hadronic mass scale. The first sum in Eq. (1.10) is valid for light neutrinos; the second sum is valid for heavy neutrinos.

For light neutrinos, the dominant physical process is similar to double-beta decay with neutrino emission; that is, two neutrons decay, but now their two neutrinos annihilate each other. The annihilation requires a Majorana mass term in the numerator of the amplitude, however, if the neutrino has a mass less than the inverse of the nuclear radius, then the effect of the mass in the denominator of the amplitude (neutrino propagation effects) can be neglected. This is how the first sum in Eq. (1.10) is obtained.

Neutrinoless double-beta decay invoked by a heavy neutrino involves a different process (see the theoretical review by Haxton and Stephenson, 1984). If the neutrino mass is much larger than the scale of hadronic structure σ, then the neutrino annihilation is essentially a pointlike process. The neutrino masses in the denominator from the two neutrino propagators are no longer negligible and now give a M_j^2 in the denominator in addition to the factor of M_j in the numerator mentioned previously. The effective Lagrangian for this process involves two pion fields and two electron fields. This is how the second sum in Eq. (1.10) is obtained. The quantity σ in this sum is a nuclear scale that is not well calculated. A naive estimate for it is $10 < \sigma < 500$ MeV.

Using the expression in Eq. (1.10) for the heavy-neutrino contribution and $\sigma \approx 100$ MeV, we see that limits can be put on the electron-neutrino mixing matrix element for heavy neutrinos with masses up to about 10^7 GeV. Thus one might suspect that double-beta decay could be sensitive to the heavy neutrinos in the seesaw mechanism. However, in the mechanism described in Sec. I.B, there is an additional suppression of the heavy-neutrino contribution in the flavor mixing matrix. Using Eq. (1.4) and taking a typical Dirac mass μ_i to be about 1 GeV, we find that, the largest heavy-neutrino mass Λ to which double-beta decay is expected to be sensitive becomes about 100 GeV.

II. THEORY

A. Neutrino oscillations in vacuum

Neutrino oscillations in vacuum have been extensively reviewed by Bilenky and Pontecorvo (1977) and Bilenky and Petcov (1987). In the following we shall briefly summarize the main results in this topic.

1. The standard model

In the standard model, neutrinos are massless, chargeless fermions. They only interact with other particles via the electroweak interactions. The effective Hamiltonian for weak interactions can be written as

$$H = (1/\sqrt{2}) G_F (J_c^\mu J_{c\mu}^\dagger + J_N^\mu J_{N\mu}) , \tag{2.1}$$

where $G_F = 1.166\,37 \times 10^{-5}$ GeV^{-2}; J_c^μ is the charged current

$$J_c^\mu = (\bar{d}\,\bar{s}\,\bar{b})\gamma^\mu(1-\gamma^5)K^\dagger \begin{pmatrix} u \\ c \\ t \end{pmatrix} + (\bar{e}\,\bar{\mu}\,\bar{\tau})\gamma^\mu(1-\gamma^5) \begin{pmatrix} \nu_e \\ \nu_\mu \\ \nu_\tau \end{pmatrix} , \tag{2.2}$$

which is mediated by W exchange. J_N^μ is the neutral-current interaction mediated by Z exchange. By omitting the heavy-fermion terms and using only the first-generation fermions, the neutral current is

$$\begin{aligned} J_N^\mu &= J_3^\mu - 2\sin^2\theta_w J_{\rm em}^\mu , \\ J_3^\mu &= \tfrac{1}{2}[\,\bar{u}\gamma^\mu(1-\gamma^5)u - \bar{d}\gamma^\mu(1-\gamma^5)d \\ &\quad + \bar{\nu}\gamma^\mu(1-\gamma^5)\nu - \bar{e}\gamma^\mu(1-\gamma^5)e] , \\ J_{\rm em}^\mu &= \tfrac{2}{3}\bar{u}\gamma^\mu u - \tfrac{1}{3}\bar{d}\gamma^\mu d - \bar{e}\gamma^\mu e . \end{aligned} \tag{2.3}$$

The weak charge current J_c^μ and the nonelectromagnetic part of the neutral current, J_3^μ, involve only the left-chiral projection of the quark and lepton fields,

$P_L=(1-\gamma^5)/2$. The right-handed fields enter only in the neutral current through the part of it proportional to the electromagnetic current $J^{\mu}_{\rm em}$. The amount of electromagnetic current in the neutral current is determined by the weak-interaction parameter $\sin^2\theta_W$. The current experimental value for this parameter of the standard model is $\sin^2\theta_W=0.228\pm0.0044$.

In Eq. (2.2) K is the unitary Cabibbo-Kobayashi-Maskawa quark mixing matrix. It arises because the quarks are massive and the quark mass eigenstates are not the same as the weak-interaction eigenstates. For massless neutrinos the weak-interaction eigenstates can be identified also as the mass eigenstates. Any unitary transformation on the degenerate mass eigenstates is unmeasurable, and so one can define each charged lepton to have only one neutrino associated with it. A conserved quantum number can be defined for each generation—electron number, muon number, and tau number.

Adding neutrino masses to the standard model involves only minimal changes in the model. There are no fundamental symmetries that prevent the neutrino from having a mass. Whether or not the neutrino has a mass is a question that must be answered experimentally. The current experimental limits on the neutrino masses are given in Sec. I.C. These mass limits are far below the masses of the charged leptons.

If the neutrinos have mass, then in general the mass eigenstates will not be the same as the weak-interaction eigenstates. Separate electron, muon, and tau numbers will not be conserved; however, the sum of the three, the lepton number, will be conserved just as the baryon number is conserved in the quark sector. The leptonic charged current will possess a unitary matrix U, analogous to the Cabibbo-Kobayashi-Maskawa quark mixing matrix K,

$$\begin{pmatrix}\nu_e\\ \nu_\mu\\ \nu_\tau\end{pmatrix}=U\begin{pmatrix}\nu_1\\ \nu_2\\ \nu_3\end{pmatrix}, \tag{2.4}$$

where U transforms between the weak-interaction (flavor) eigenstates (ν_α) and the mass eigenstates (ν_i). Besides a very small Higgs-neutrino interaction term, this change in the charged current [Eq. (2.2)] will be the only modification of the weak-interaction Hamiltonian due to the addition of a neutrino mass. The neutral-current interactions are unaffected, since they are flavor conserving. For antineutrinos, there is an equation analgous to Eq. (2.4) with the replacements $\nu\rightarrow\bar{\nu}$ and $U\rightarrow U^*$.

The neutrino masses, if they exist, are much smaller than the charged-fermion masses. Because of this, neutrino propagation can have properties that are very different from typical charged-fermion propagation. When a neutrino is produced via the electroweak interactions, it is in an interaction eigenstate. After production, it propagates in its mass eigenstates. Because these bases are not generally the same, the neutrino flavor will not be conserved by propagation. For quarks, too, the interaction and mass bases are not identical; however, because the neutrino masses are small, this change in flavor can occur over a correspondingly large distance scale. That this distance scale might be macroscopic and observable was first suggested independently by Pontecorvo (1958, 1968) and Maki *et al.* (1962).

2. The neutrino wave equation

Neutrinos may have either a Dirac or a Majorana mass, but for propagation of ultrarelativistic neutrinos the full spin structure is not probed. The weak interactions couple only to the left-handed component of the neutrino field. For ultrarelativistic particles, chirality conservation, which is exact for massless particles, is good to order (m/E). Thus, for neutrino with $E\gg m$, it is only the propagation of the left-handed component that is relevant. Eliminating the spin structure from the propagation equation yields the Klein-Gordon equation, whether the neutrino is a Dirac or a Majorana particle. It follows that, in either case, neutrino propagation (or neutrino oscillations) in the mass eigenstate basis is given by

$$\left[\frac{d^2}{dx^2}+m^2\right]|\nu\rangle=\frac{d^2}{dt^2}|\nu\rangle\ . \tag{2.5}$$

This equation describes the propagation of an ultrarelativistic neutrino. For n flavors of neutrinos, $|\nu\rangle$ is an n-dimensional vector and m^2 an $n\times n$ diagonal matrix.

In general, we want to solve Eq. (2.5) for the propagation of a neutrino state that is a linear combination of several different mass eigenstates. We start by assuming that all of the neutrino mass eigenstates have the same three-momentum. This is clearly an approximation; in general, one would expect the momentum and energy eigenstates both to be nondiagonal. However, this approximation is accurate up to small corrections for ultrarelativistic neutrinos. To see this, one can repeat the following analysis with the assumption that the energy is diagonal; the results will be the same.

Assuming that all the neutrino eigenstates have the same three-momentum, then the d^2/dx^2 in the Klein-Gordon equation is just proportional to the identity matrix. This term will give an identical phase factor of all of the mass eigenstates. Since overall phase factors of a wave function are unobservable, we can drop this term from Eq. (2.5).

Equation (2.5) can be simplified further. The Klein-Gordon equation has two solutions corresponding to waves traveling in opposite directions. However, once we specify a neutrino's direction, the reflected solution will not be relevant. Thus we can throw away the reflected solution to get a first-order equation. Substituting in $|\nu(t)\rangle=\exp(-iEt)|\nu\rangle\approx\exp(-ipt)|\nu\rangle$ yields

$$\frac{m^2}{p}|\nu\rangle=i\frac{d}{dt}|\nu\rangle\ . \tag{2.6}$$

The term ip from the d^2/dx^2 has been deleted from the left-hand side of Eq. (2.6).

3. Solutions to the wave equation

The equation describing neutrino propagation, Eq. (2.6), now resembles the Schrödinger equation. The solution for the neutrino wave function can be written for two neutrino species as

$$\begin{bmatrix} |\nu_1(t)\rangle \\ |\nu_2(t)\rangle \end{bmatrix} = \begin{bmatrix} e^{-iE_1 t} & 0 \\ 0 & e^{-iE_2 t} \end{bmatrix} \begin{bmatrix} |\nu_1(0)\rangle \\ |\nu_2(0)\rangle \end{bmatrix}, \tag{2.7}$$

where $E_i=(p^2+m_i^2)^{1/2}$ and m_i is the mass eigenvalue of m^2. As the mass eigenstates propagate, they each acquire a different phase. However, as mentioned before, mass eigenstates are not, in general, the states that are produced or detected. Neutrinos are produced or detected via the weak interactions; so the physical quantity that one observes is the flavor at the production and detection positions. Equation (2.4) describes the mixing between these two bases; choosing a parametrization,

$$U=\begin{bmatrix} C_\theta & S_\theta \\ -S_\theta & C_\theta \end{bmatrix}, \tag{2.8}$$

we can write the solution for the neutrino wave function that describes a neutrino's production and detection. If we produce an electron neutrino, the probability of detecting this neutrino as an electron neutrino after a time t, $P(\nu_e\to\nu_e)=|\langle\nu_e(t)|\nu_e(0)\rangle|^2$, can be written as

$$\begin{aligned} P(\nu_e\to\nu_e) &= \left| [1\ \ 0] \begin{bmatrix} C_\theta & S_\theta \\ -S_\theta & C_\theta \end{bmatrix} \begin{bmatrix} e^{-iE_1 t} & 0 \\ 0 & e^{-iE_2 t} \end{bmatrix} \right. \\ &\quad \left. \times \begin{bmatrix} C_\theta & -S_\theta \\ S_\theta & C_\theta \end{bmatrix} \begin{bmatrix} 1 \\ 0 \end{bmatrix} \right|^2 \\ &= 1-\tfrac{1}{2}\sin^2 2\theta[1-\cos(E_2-E_1)t] . \end{aligned} \tag{2.9}$$

The last term in Eq. (2.9) describes flavor oscillations. We can define a wavelength for the oscillations,

$$\begin{aligned} E_2-E_1 &= (m_2^2+p^2)^{1/2}-(m_1^2+p^2)^{1/2} \\ &\approx (m_2^2-m_1^2)/2p \equiv 2\pi/\lambda . \end{aligned} \tag{2.10}$$

For small neutrino masses the oscillation scale is macroscopic. For $m_2^2-m_1^2\approx 1\ \text{eV}^2$ and $p\approx 10$ MeV, $\lambda\approx 25m$.

4. The classical probability

The oscillation wavelength is the scale on which quantum interference occurs. Experimental searches for the oscillation of neutrino flavor can probe small neutrino mass differences where the oscillation wavelength is macroscopic. However, it is all too easy to miss these interference effects. For instance, if the production or detection positions extend over a distance much larger than the wavelength, the phase information will be averaged out. Or, for nonmonochromatic neutrino sources, if the neutrino propagates for a distance L much greater than λ, one may lose phase information by binning neutrino events with too large of an energy width, $\delta E/E>\lambda/L$.

Phase information can also be lost in more subtle ways. The previous examples assumed that the neutrino wave was coherent. But the length over which the neutrino wave is coherent will depend on the neutrino production process. For example, as discussed by Nussinov (1976), solar neutrino wave packets have a relatively short coherence length of about $d=10^{-6}$ cm. This is because solar neutrinos are produced in the core of the sun where the nuclei that emit them are undergoing rapid collisions. The neutrino mass eigenstates will then be incoherent after traveling a distance $L=d/(\delta\beta)=d(p\lambda)$, where $\delta\beta$ is the difference in velocity between the mass eigenstates.

If the phase information is lost, then the probability is just the classical probability. The classical probability can be calculated without using the equation for neutrino propagation, Eq. (2.6). One need only know the mixing matrix U between the two bases. The phase acquired during neutrino propagation is averaged out; so we can sum incoherently over the propagation eigenstates, the mass eigenstates:

$$\begin{aligned} P(\nu_e\to\nu_e) &= \sum_i P(\nu_e\to\nu_i)P(\nu_i\to\nu_e) \\ &= [1\ \ 0] \begin{bmatrix} C_\theta^2 & S_\theta^2 \\ S_\theta^2 & C_\theta^2 \end{bmatrix} \begin{bmatrix} 1 & 0 \\ 0 & 1 \end{bmatrix} \begin{bmatrix} C_\theta^2 & S_\theta^2 \\ S_\theta^2 & C_\theta^2 \end{bmatrix} \begin{bmatrix} 1 \\ 0 \end{bmatrix} \\ &= 1-\tfrac{1}{2}\sin^2 2\theta . \end{aligned} \tag{2.11}$$

The classical probability is the product of the magnitudes squared instead of the magnitude squared of the product. Equation (2.11) is similar to Eq. (2.9), but the oscillating term has been averaged out.

The explicit formulas in Eqs. (2.7)–(2.11) have assumed that there were only two neutrino flavors. However, it is known that there are at least three generations of fermions. The generalization to more flavors is straightforward. A useful parametrization of the mixing matrix for three flavors is (this is similar to Maiani's $V=\Gamma^* U, \delta\to\delta/2$)

$$\begin{aligned} U &= \exp(i\psi\lambda_7)\Gamma\exp(i\varphi\lambda_5)\exp(i\omega\lambda_2) \\ &= \begin{bmatrix} 1 & 0 & 0 \\ 0 & C_\psi & S_\psi \\ 0 & -S_\psi & C_\psi \end{bmatrix} \begin{bmatrix} 1 & 0 & 0 \\ 0 & e^{i\delta} & 0 \\ 0 & 0 & e^{-i\delta} \end{bmatrix} \\ &\quad \times \begin{bmatrix} C_\varphi & 0 & S_\varphi \\ 0 & 1 & 0 \\ -S_\varphi & 0 & C_\varphi \end{bmatrix} \begin{bmatrix} C_\omega & S_\omega & 0 \\ -S_\omega & C_\omega & 0 \\ 0 & 0 & 1 \end{bmatrix}, \end{aligned} \tag{2.12}$$

where the λ's are the Gell-Mann matrices that correspond to the spin-one matrices of SO(3). This type of parametrization is useful for discussing neutrino oscilla-

tions because, for small angles, each angle corresponds to mixing between two neutrino species.

One can write a general solution for the probability without choosing a parametrization,

$$P(\nu_\alpha \to \nu_\beta) = \left| \sum_i U_{\beta i} \exp(-iE_i t) U^*_{\alpha i} \right|^2$$
$$= \sum_i |U_{\beta i}|^2 |U_{\alpha i}|^2 + \mathrm{Re} \sum_{i \neq j} U_{\beta i} U^*_{\beta j} U^*_{\alpha i} U_{\alpha j} \times \exp[-it(m_i^2 - m_j^2)/2p] \ . \quad (2.13)$$

The first term is just the classical probability; all of the phase information is in the last term. If we average out the phase, the last term vanishes.

5. Unitarity constraints

Equation (2.13) satisfies the general constraints

$$\sum_\alpha P(\nu_\alpha \to \nu_\beta) = 1 \quad (2.14)$$

and

$$\sum_\beta P(\nu_\alpha \to \nu_\beta) = 1 \ , \quad (2.15)$$

and similar relations for antineutrinos. These just follow from unitarity (and are also valid for neutrino oscillations in matter). Other relations can be deduced from symmetries of the theory. Invariance under the combination of discrete symmetries *CPT* yields the relation

$$P(\nu_\alpha \to \nu_\beta) = P(\bar{\nu}_\beta \to \bar{\nu}_\alpha) \ . \quad (2.16)$$

If the mixing matrix is time reversal T invariant, then U is real and

$$P(\nu_\alpha \to \nu_\beta) = P(\nu_\beta \to \nu_\alpha) \quad (2.17)$$

[since normal matter is typically not *CP* symmetric or T symmetric, Eqs. (2.16) and (2.17) do not typically hold for neutrino oscillations in matter]. If Eq. (2.17) is valid, then the two unitary relations (2.14) and (2.15) are redundant. Since T violations just introduce an extra phase, (2.17) is also true for the vacuum oscillation probabilities when the phase information is averaged out—the classical probabilities. For two flavors there can be no T violations in the mixing matrix, so the unitarity relations give

$$P(\nu_e \to \nu_e) = 1 - P(\nu_e \to \nu_\mu) = 1 - P(\nu_\mu - \nu_e) = P(\nu_\mu \to \nu_\mu) \ . \quad (2.18)$$

B. Neutrino wave equation in matter

When neutrinos propagate through matter, the forward scattering of neutrinos off the background matter will induce an index of refraction for the neutrinos. This is exactly analogous to the index of refraction of light traveling through matter. However, the neutrino index of refraction will depend generally on the flavor—electron and muon neutrinos will have different indices of refraction because the background matter contains different amounts of electrons and muons. If the neutrinos are massive, then neutrino flavors will mix during propagation. An index of refraction is similar to a mass, and flavor-dependent indices of refraction can enhance neutrino flavor mixing during propagation.

1. The induced neutrino mass

Using the standard model description of neutrino interactions with matter, Eqs. (2.1)–(2.3), neutrinos will scatter off background matter via the charged current and the neutral current. For normal matter, only the charged current will alter the neutrino flavor content during propagation. The neutral current is flavor conserving and influences all neutrino flavors equally. But the background electrons in normal matter will interact via the charged current with electron neutrinos only. From Eqs. (2.1) and (2.2),

$$H = \frac{G_F}{\sqrt{2}} \bar{e} \gamma^\mu (1-\gamma^5) \nu_e \bar{\nu}_e \gamma_\mu (1-\gamma^5) e \ ; \quad (2.19)$$

Fierz rearranging of the spinors yields

$$H = \frac{G_F}{\sqrt{2}} \bar{\nu}_e \gamma^\mu (1-\gamma^5) \nu_e \bar{e} \gamma_\mu (1-\gamma^5) e \ . \quad (2.20)$$

For forward scattering of neutrinos off electrons, the electron momentum is unchanged. In the rest frame of normal matter the electrons are typically unpolarized at rest; so only the γ^0 component of the electron density can contribute. The $\gamma^0\gamma^5$ mixes "small" and "large" components of the electron spinor, so it does not contribute; γ^0 is just 1 for the "large" component, so $\bar{e}\gamma_\mu(1-\gamma^5)e = \delta_{\mu 0} N_e$. N_e is the number density of electrons. For neutrino forward scattering, the interaction term resembles an external potential for the left-handed field, $V = G_F \sqrt{2} N_e$. The potential is positive, indicating that the force is repulsive (Langacker *et al.*, 1983). Besides this real part of the forward scattering, the optical theorem tells us that there is also an imaginary term that is proportional to the total cross section. Since this is of order G_F^2, it is typically negligible compared to the real part.

Assuming a Dirac neutrino mass, the neutrino propagation equation takes the form

$$(i\partial_\mu \gamma^\mu - V\gamma^0)\nu_L - m\nu_R = 0 \ , \quad i\partial_\mu \gamma^\mu \nu_R - m\nu_L = 0 \ , \quad (2.21)$$

where $\nu_{R,L} = \frac{1}{2}(1 \pm \gamma^5)\nu$. We now proceed to derive a simple propagation equation for the left-handed fields analogous to the vacuum case discussed in Sec. II.A. If the variations of the electron density are small on

the scale of the neutrino de Broglie wavelength, $(1/VE)(dV/dt) \ll 1$, we can take $i\partial^\mu V \approx Vi\partial^\mu$. For relativistic neutrinos and a small potential we can use

$$\partial_\mu \gamma^\mu \gamma^0 \nu_L = \gamma^0(\partial^0\gamma^0 + \partial^i\gamma^i)\nu_L \approx \gamma^0(2\partial^0\gamma^0)\nu_L = 2\partial^0\nu_L \ .$$

Then the propagation equation for the relativistic left-handed states resembles the Klein-Gordon equation with a small potential

$$(\partial_\mu\partial^\mu + 2iV\partial^0 + m^2)\nu_L = 0 \tag{2.22}$$

(the equation for relativistic right-handed states is the free Klein-Gordon equation). The remaining discussion is identical to the vacuum case. Assuming a common three-momentum for the neutrino mass eigenstates, we can effectively just drop the $\partial^i\partial^i$ term. Neglecting any reflected solutions we use $\nu_L \approx \exp(-ipt)\nu_L$ to reduce the differential equation from second order to first order in time. The neutrino propagation equation now has a form analogous to Eq. (2.6), but within an added potential term. In the flavor basis, where the potential is diagonal, the propagation equation for two flavors is

$$\begin{aligned} -i\frac{d}{dt}|\nu_\alpha\rangle &= \frac{1}{2p}M^2|\nu_\alpha\rangle \ , \\ M^2 &= \left[U \begin{bmatrix} m_1^2 & 0 \\ 0 & m_2^2 \end{bmatrix} U^\dagger + \begin{bmatrix} A & 0 \\ 0 & 0 \end{bmatrix} \right] ; \end{aligned} \tag{2.23}$$

U is the unitary transformation between the flavor and mass bases, and $A = 2Vp = 2\sqrt{2}G_F N_e p$ (for antineutrinos, $A \to -A$ and $U \to U^*$). Equation (2.23) was first derived by Wolfenstein (1978a); for more recent derivations, see Bethe (1986), Halprin (1986), Chang and Zia (1988), and Mannheim (1988).

A acts like an induced mass (squared) for the electron neutrino from the propagation through a background of electrons. Evaluating the expression, $A \approx (10^{-2}\ \text{eV})^2$ for matter densities of 100 g/cm^3 and neutrino energies of 10 MeV.

Equation (2.23) was derived assuming that the neutrinos had a Dirac mass. For a Majorana neutrino mass, the derivation can be repeated to obtain Eq. (2.23). This equation is covariant under the transformation $U \to SUS'$, where S and S' are diagonal matrices of phases. Thus, as in the vacuum case, the extra phases that a Majorana neutrino has in its mixing matrix are not observable. It is not possible to distinguish between Majorana and Dirac neutrinos by their flavor mixing during propagation.

Equation (2.23) is a familiar equation in physics. Because it is first order in time, as is the Schrödinger equation, there are many quantum-mechanical problems that are described by this same equation. The equation can be interpreted as describing spin precession in a magnetic field (Mikheyev and Smirnov, 1986b; Kim *et al.*, 1988). One of the most common occurrences of Eq. (2.23) is for describing level-crossing phenomena. In this context, Eq. (2.23) was solved by Landau (1932), Stueckelberg (1932), and Zener (1932).

2. Corrections to the induced neutrino mass

The left-handed electron-neutrino potential $\sqrt{2}G_F N_e$, which comes from charged-current interactions with electrons, is the only relevant potential for neutrinos propagating through typical matter, the Earth, or the sun. However, for nontypical matter, during the early universe or in the core of a supernova, other potentials may be relevant.

Table II gives neutrino potentials from charged- and neutral-current tree-level interactions with background electrons, neutrons, protons, and also neutrinos (Notzold and Raffelt, 1988). The top sign refers to neutrinos and the bottom sign to antineutrinos. The terms in Table II that are of order G_F/M^2 come from expanding the gauge boson propagator. For charged-current scattering from electrons at rest,

$$\frac{-1}{k^2 - M_W^2} \approx \frac{1}{M_W^2} + \frac{k^2}{M_W^4} \approx \frac{1}{M_W^2} \pm \frac{2E_\nu m_e}{M_W^4} \ . \tag{2.24}$$

The top sign refers to positions, where $k = P_\nu + P_{\bar{e}}$, and the bottom sign to electrons, where $k = P_\nu - P_e$. This

TABLE II. Potentials induced for a neutrino traveling through background matter. The upper sign refers to neutrinos, the lower sign to antineutrinos. N_f is the number density of fermion f in the background matter. For nonrelativistic background electrons, $\langle E_e \rangle \to \frac{3}{4}m_e$.

Neutrino flavor	Background flavor	Potential V
ν_e	e	$\pm G_F(4\sin^2\theta_W + 1)(N_e - N_{\bar{e}})/\sqrt{2} - \frac{8\sqrt{2}G_F E_\nu}{3M_W^2}(\langle E_e \rangle N_e + \langle E_{\bar{e}} \rangle N_{\bar{e}})$
ν_μ, ν_τ	e	$\pm G_F(4\sin^2\theta_W - 1)(N_e - N_{\bar{e}})/\sqrt{2}$
ν_e, ν_μ, ν_τ	n	$\pm G_F(N_{\bar{n}} - N_n)/\sqrt{2}$
ν_e, ν_μ, ν_τ	p	$\pm G_F(1 - 4\sin^2\theta_W)(N_p - N_{\bar{p}})/\sqrt{2}$
ν_e	ν_e	$\pm 2\sqrt{2}G_F(N_\nu^L - N_{\bar{\nu}}^L) - \frac{8\sqrt{2}G_F E_\nu}{3M_Z^2}(\langle E_\nu \rangle N_\nu^L + \langle E_{\bar{\nu}} \rangle N_{\bar{\nu}}^L)$
ν_μ, ν_τ	ν_e	$\pm\sqrt{2}G_F(N_\nu^L - N_{\bar{\nu}}^L)$

sign difference cancels with the leading-order sign change between electrons and positrons. These small terms would be relevant if the first-order terms all vanished—as in a *CP* symmetric plasma that is similar to the conditions of the early universe.

At tree level in the weak interactions, the muon- and tau-neutrino flavors acquire identical potentials in typical matter. However, at the one-loop level, differences in the charged-fermion masses induce different potentials for these neutrinos. The difference was calculated by Botella *et al.* (1987) to be

$$V(\nu_\mu)-V(\nu_\tau)=\pm\frac{3G_F^2 m_\tau^2}{2\pi^2}\left[(N_p+N_n)\ln\left[\frac{m_\tau^2}{M_W^2}\right]+N_p+\tfrac{2}{3}N_n\right]. \quad (2.25)$$

The upper sign is for neutrinos; the lower sign is for antineutrinos. Evaluating the expression, $2p[V(\nu_\mu)-V(\nu_\tau)]\approx-(3\times10^{-5}\text{ eV})^2$ for matter densities of 100 g/cm^3 and neutrino energies of 10 MeV.

The derivation of Eq. (2.23) assumed that the background electrons were unpolarized. It is easy to relax this assumption. Defining $j_e^\mu=\bar{e}\gamma^\mu(1-\gamma^5)e$, then for electrons at rest $j_e^\mu=N_e(1,-2\mathbf{S}_e)$, where $\mathbf{S}_e$ is the average spin of the electrons normalized to $\frac{1}{2}$. The induced electron-neutrino mass A is then multiplied by the factor $(1+2\mathbf{S}_e\cdot\mathbf{n}_\nu)$, where $\mathbf{n}_\nu$ is a unit vector in the direction of neutrino propagation. For positrons, $j_{\bar{e}}^\mu=N_{\bar{e}}(-1,-2\mathbf{S}_{\bar{e}})$. It is interesting to note that a magnetic field in a *CP* symmetric plasma of electrons and positrons will not induce a net contribution to A from the polarization. For electrons the spin is parallel to the magnetic moment, while for positrons the spin is antiparallel. Thus an external magnetic field will cause the spins to align antiparallel with no net contribution to A.

One particle that is common to background matter but is not contained in Table II is the photon. For hot media, specifically *CP* symmetric media similar to the early universe, it has been speculated that neutrino forward scattering off photons could contribute significantly to the neutrino potential. However, a recent analysis by Nieves (1987), using gauge invariance and chirality, finds that the photon contribution to the neutrino potential is less than or of order, $V_\nu\approx O(\alpha G_F T^4 p/M_W^2)$ where T is the photon temperature. This is smaller by a power of α than the order G_F/M^2 contributions already calculated in Table II; so the neutrino-photon interactions are not important in the early universe.

3. Numerical integration of the wave equation

The wave equation (2.23), with the correct expression for the induced mass A, fully describes the flavor content of a neutrino as it propagates through matter. However, this equation can be difficult to solve when the induced mass A varies as a function of the propagation distance. Sections II.C and II.D concentrate on analytical techniques for solving this equation. It turns out that the wave equation can be accurately described analytically for a constant density (Sec. II.C.1); a long, slow density change (Sec. II.C.2); a long, smooth, monotonic, quick density change; and a step-function density (Secs. II.C.3 and II.C.4). This is a fairly comprehensive set of solutions; however, there are always conditions for which they are not satisfactory. One example of such a situation is for neutrino propagation through the Earth. There the density has some smoothly varying sections, between abrupt density changes, with all of this structure occurring on the same scale as the desired neutrino wavelength. Then one is forced to fall back on direct numerical integration of the wave equation.

The wave equation can be written in different, equivalent forms. Equation (2.23) is not necessarily in the best form for numerical integration. Typically, in numerical solving of differential equations, a specific application [i.e., a specific $A(x)$, $m_2^2-m_1^2$, θ, and E] will have a specific, optimal form for the differential equation. The degree to which the programmer must optimize the form of the wave equation depends on the desired accuracy of the result. We shall not discuss such matters here. Instead we present the wave equation in a form that has fewer degrees of freedom and hence is faster to integrate numerically.

For two flavors, Eq. (2.23) has four quantities that must be carried along on each increment—a real part and an imaginary part for each flavor. However, not all of these degrees of freedom are physical. There is a unitarity constraint (see Sec. III.A.5) on the wave functions; so we know that we can eliminate one degree of freedom. The wave equation can be written in the form of three real, coupled, first-order differential equations or, equivalently, as a single, real, third-order differential equation (Mikheyev and Smirnov, 1986b),

$$\begin{aligned}&\alpha\dddot{P}-\dot{\alpha}\ddot{P}-4\alpha(\alpha^2+\beta^2)\dot{P}-4\dot{\alpha}\beta^2(P-\tfrac{1}{2})=0\ ,\\ &\alpha\equiv[A-(m_2^2-m_1^2)\cos2\theta]/4E\ ,\\ &\beta\equiv(m_2^2-m_1^2)\sin2\theta/4E\ .\end{aligned} \quad (2.26)$$

Here $P=P(\nu_e\to\nu_e)\equiv|\nu_e(t)|^2$; the proper initial conditions for producing an electron neutrino are

$$P(0)=1,\quad \dot{P}(0)=0,\quad \ddot{P}(0)=-2\beta^2\ . \quad (2.27)$$

Equation (2.26) has fewer degrees of freedom and should be slightly faster and more accurate to iterate than Eq. (2.23). However, it may or may not be better to use, depending on the situation. The original equation has an advantage that depends on the unnecessary degree of freedom. The unitarity condition provides a useful check on the accuracy of the numerical integration. This check can often save the programmer time and effort. For three neutrino flavors, there is a single, real, fifth-order differential equation for P analogous to Eq. (2.26). However, this equation is definitely worse to use than the

three-flavor form of Eq. (2.23), because it is too long and complicated to be practical.

C. Two-flavor solutions to the wave equation

As a first approximation we try to solve the neutrino wave equation assuming that there are only two neutrino flavors (Wolfenstein, 1978a; Bethe, 1986; Mikheyev and Smirnov, 1986a). This problem is simpler to solve than the case of three neutrino flavors, and it provides a useful illustration of the kind of effects that matter can have on neutrino oscillations. In particular, one can get an almost total depletion of the average electron-neutrino flux with matter-enhanced oscillations and only two neutrino flavors. This is in sharp contrast to vacuum oscillations where, with two neutrino flavors, the maximum reduction achievable was only $\frac{1}{2}$. Thus two flavors are sufficient to explain the solar neutrino problem. Solutions to the neutrino wave equation with three flavors will be discussed in Sec. II.D.

1. Eigenvalues and eigenfunctions for fixed density

The effect of matter on neutrino propagation is contained in the parameter A, given by

$$A \equiv 2\sqrt{2}G_F N_e E = 2\sqrt{2}G_F(Y_e/m_n)\rho E \ , \tag{2.28}$$

where G_F is the Fermi constant, ρ the density, Y_e the number of electrons per nucleon, and m_n the nucleon mass. A is the induced mass squared of the electron neutrino that arises from propagation through a background of electrons. The neutrino propagation equation [Eq. (2.23)], with $c=1$ and $t \rightarrow x$, can be rewritten as

$$\begin{aligned} i\frac{d}{dx}\begin{bmatrix}\nu_e \\ \nu_\mu\end{bmatrix} &= \frac{1}{2E}M^2\begin{bmatrix}\nu_e \\ \nu_\mu\end{bmatrix} = \frac{1}{2E}\left[U\begin{bmatrix}m_1^2 & 0 \\ 0 & m_2^2\end{bmatrix}U^\dagger + \begin{bmatrix}A & 0 \\ 0 & 0\end{bmatrix}\right]\begin{bmatrix}\mu_e \\ \nu_\mu\end{bmatrix} \\ &= \frac{1}{4E}\left[(\Sigma + A) + \begin{bmatrix}A - \Delta C_{2\theta} & \Delta S_{2\theta} \\ \Delta S_{2\theta} & -A + \Delta C_{2\theta}\end{bmatrix}\right]\begin{bmatrix}\nu_e \\ \nu_\mu\end{bmatrix} , \end{aligned} \tag{2.29}$$

where $\Sigma = m_2^2 + m_1^2$, $\Delta = m_2^2 - m_1^2$, and $C_{2\theta} = \cos 2\theta$, $S_{2\theta} = \sin 2\theta$. The part of the mass matrix M^2 that is proportional to the identity matrix has been pulled out.

M^2 can be diagonalized to find the instantaneous eigenvalues and eigenstates. Defining U_m and $M_{2,1}^2$ by

$$U_m^\dagger M^2 U_m \equiv \begin{bmatrix}M_1^2 & 0 \\ 0 & M_2^2\end{bmatrix} ,$$

the eigenvalues of the mass matrix M^2 are

$$M_{2,1}^2 = \{(\Sigma + A) \pm [(A - \Delta C_{2\theta})^2 + (\Delta S_{2\theta})^2]^{1/2}\}/2 \ . \tag{2.30}$$

The mixing matrix in the medium, U_m, can be parametrized analogous to the vacuum mixing parametrization given in Eqs. (2.4) and (2.8),

$$\begin{aligned} \begin{bmatrix}\nu_1^m \\ \nu_2^m\end{bmatrix} &= \begin{bmatrix}\cos\theta_m & -\sin\theta_m \\ \sin\theta_m & \cos\theta_m\end{bmatrix}\begin{bmatrix}\nu_e \\ \nu_\mu\end{bmatrix} \\ &\equiv U^{m\dagger}\begin{bmatrix}\nu_e \\ \nu_\mu\end{bmatrix} . \end{aligned} \tag{2.31}$$

The mass eigenstates in the medium are $\nu_{2,1}^m$. Here θ_m is the neutrino mixing angle in matter and is given by

$$\tan 2\theta_m = \Delta \sin 2\theta/(-A + \Delta\cos 2\theta) \ , \tag{2.32}$$

or, equivalently,

$$\sin^2 2\theta_m = (\Delta \sin 2\theta)^2/[(A - \Delta\cos 2\theta)^2 + (\Delta \sin 2\theta)^2] \ . \tag{2.33}$$

The mixing angle is modified substantially by the coherent scattering of a medium. When $A \rightarrow 0$, $\theta_m \rightarrow \theta$ and the mixing matrix is just the vacuum expression. When $A \gg \Delta$, $\theta_m \rightarrow \pi/2$. However, the most interesting feature of θ_m is its resonance behavior as a function of A. This is exhibited in Fig. 2. The resonance occurs when

$$A = \Delta\cos 2\theta \ , \tag{2.34}$$

for which $\sin 2\theta_m = 1$ and neutrino mixing is a maximum. The half-width of the resonance is given by

$$|\delta A| = \Delta \sin 2\theta \ . \tag{2.35}$$

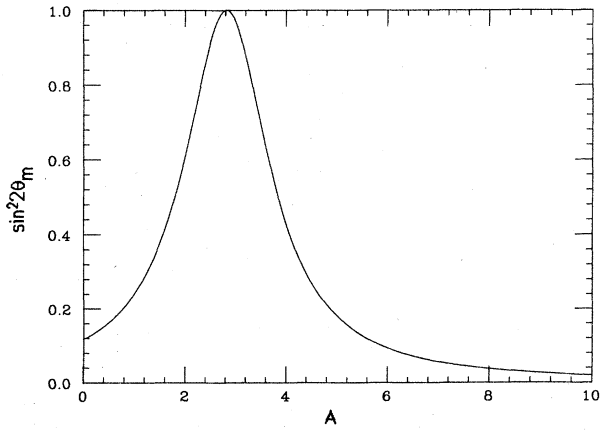

FIG. 2. Plot of $\sin^2 2\theta_m$, where θ_m is the effective neutrino mixing angle in matter, as a function of A, the induced electron-neutrino mass. Here we take $m_2^2 - m_1^2 = 3.0$ and $\sin^2\theta = 0.03$.

Thus, given the right conditions, coherent scattering off a background can enhance neutrino oscillations maximally.

It should be emphasized that the resonance occurs whether or not the mixing angle is small. The resonance would not occur if $\theta > \pi/4$—the heavier mass eigenstate coupled dominantly to the electron neutrino. In that case the resonance would occur for antineutrinos, since for antineutrinos the above formulas are changed by the substitution $A \rightarrow -A$ (see Sec. II.B). However, it is generally expected that θ is small, since this is what is observed in the hadronic sector. The seesaw model of neutrino masses does not substantially modify this expectation (see Sec. I.B). Thus we shall often make the tacit assumption that the resonance occurs for neutrinos.

Let us now examine the experimentally observable quantity $P(\nu_e \rightarrow \nu_e)$, which is the probability for a produced ν_e to remain a ν_e after propagation. For a constant-density medium the effective mass matrix is a constant, independent of x; the instantaneous eigenvalues and eigenstates are identical then for all x. This situation is similar to the vacuum case, and so solving the wave equation for a constant-density medium proceeds analogously to the discussion in Sec. II.A for the vacuum case. The vacuum solutions can be converted to the solution in a medium by replacing the vacuum quantities with their corresponding medium quantities: the vacuum masses are replaced by the mass eigenstates of the effective mass matrix in a medium, Eq. (2.30), and the vacuum mixing angle is replaced by the effective mixing angle in matter, Eqs. (2.32) and (2.33).

For example, the neutrino wavelength in matter follows from the neutrino wavelength in vacuum given by Eq. (2.10), $\lambda = 4\pi E/\Delta$. The induced mass A can be converted to a characteristic length scale for the medium

$$\lambda_0 \equiv 4\pi E/A = \sqrt{2}\pi/(G_F N_e) . \tag{2.36}$$

For a medium with $\rho = 1$ g/cm^3 and $Y_e = \frac{1}{2}$, $\lambda_0 = 2\times 10^9$ cm. The neutrino wavelength in matter is given in terms of the difference in the mass eigenstates in matter,

$$\begin{aligned}\lambda_m &= 4\pi E/(M_2^2 - M_1^2) \\ &= \lambda/[S_{2\theta}^2 + (A/\Delta - C_{2\theta})^2]^{1/2} \\ &= \lambda/[S_{2\theta}^2 + (\lambda/\lambda_0 - C_{2\theta})^2]^{1/2} ,\end{aligned} \tag{2.37}$$

where $M_2^2 - M_1^2$ was given in Eq. (2.30). We may now deduce $P(\nu_e \rightarrow \nu_e)$ for a medium with a constant density from the vacuum equations (2.9) and (2.10). Making the appropriate replacements, $\theta \rightarrow \theta_m$ and $\Delta \rightarrow (M_2^2 - M_1^2)$ (or, equivalently, $\lambda \rightarrow \lambda_m$), the probability is given by

$$P(\nu_e \rightarrow \nu_e) = 1 - \tfrac{1}{2}\sin^2 2\theta_m (1 - \cos 2\pi x/\lambda_m) . \tag{2.38}$$

The expression $P(\nu_e \rightarrow \nu_e)$ exhibits the typical form of a mixing phenomenon as a function of x; it oscillates between its extrema with a period of λ_m. As in the case of vacuum oscillations, one often averages out the phase information, thereby arriving at the classical probability

$$P(\nu_e \rightarrow \nu_e) = 1 - \tfrac{1}{2}\sin^2 2\theta_m . \tag{2.39}$$

This is the generalization of Eq. (2.11) with the replacement $\theta \rightarrow \theta_m$.

2. Medium with slowly varying density—adiabatic approximation

In the previous section we have seen that both the mass eigenvalues and the mixing angles become functions of ρ. This has very interesting implications for neutrino propagation in a medium with varying density. In actual physical situations, the neutrino often moves from one density to another. For instance, solar neutrinos and neutrinos from collapsing stars are produced at high densities and detected essentially in vacuum, after they have traversed the star. For a medium with varying density, however, the mass eigenstates we obtained are no longer eigenstates of the Hamiltonian. Indeed, we may write the neutrino propagation equation (2.29) in the form

$$i\frac{d}{dx}\begin{bmatrix}\nu_e \\ \nu_\mu\end{bmatrix} = \frac{1}{2E} U^m \begin{bmatrix} M_1^2 & 0 \\ 0 & M_2^2 \end{bmatrix} \begin{bmatrix}\nu_1 \\ \nu_2\end{bmatrix} . \tag{2.40}$$

Here we have used the definitions in Eqs. (2.30) and (2.31). Keeping in mind that U^m is now x dependent, we may rewrite Eq. (2.40) as

$$i\frac{d}{dx}\begin{bmatrix}\nu_1 \\ \nu_2\end{bmatrix} = \left[\frac{1}{2E}\begin{bmatrix} M_1^2 & 0 \\ 0 & M_2^2 \end{bmatrix} - U^{m\dagger} i\frac{d}{dx} U^m\right]\begin{bmatrix}\nu_1 \\ \nu_2\end{bmatrix} \tag{2.41}$$

$$= \begin{bmatrix} M_1^2/2E & -i\,d\theta_m/dx \\ i\,d\theta_m/dx & M_2^2/2E \end{bmatrix}\begin{bmatrix}\nu_1 \\ \nu_2\end{bmatrix} . \tag{2.42}$$

This last equation follows directly from the substitution of the explicit matrix U^m, as defined in Eq. (2.31), into the second term in Eq. (2.41).

Note that neutrino oscillations depend only on the parameters $d\theta_m/dx$ and $(M_2^2 - M_1^2)/4E$. The reason is that we can always take out a common diagonal phase factor $\exp[i(M_2^2 + M_1^2)x/4E]$ from ν_1 and ν_2, resulting in the equation

$$i\frac{d}{dx}\begin{bmatrix}\nu_1' \\ \nu_2'\end{bmatrix} = \begin{bmatrix} -(M_2^2 - M_1^2)/4E & -i\,d\theta_m/dx \\ i\,d\theta_m/dx & (M_2^2 - M_1^2)/4E \end{bmatrix}\begin{bmatrix}\nu_1' \\ \nu_2'\end{bmatrix} . \tag{2.43}$$

Here

$$\nu_1' = \exp[-i(M_1^2 + M_2^2)x/4E]\nu_1$$

and

$$\nu_2' = \exp[-i(M_1^2 + M_2^2)x/4E]\nu_2$$

are equivalent to ν_1 and ν_2, as far as oscillations are concerned. Similarly, a diagonal phase factor from the neutrino's three-momentum was dropped during the derivation of the wave equation.

From Eqs. (2.30) and (2.32), we have

$$(M_2^2-M_1^2)=[(A-\Delta C_{2\theta})^2+(\Delta S_{2\theta})^2]^{1/2}\ , \tag{2.44}$$

$$\frac{d\theta_m}{dx}=\frac{1}{2}\frac{\Delta\sin 2\theta}{(A-\Delta C_{2\theta})^2+(\Delta S_{2\theta})^2}\frac{dA}{dx}\ . \tag{2.45}$$

The off-diagonal term in Eqs. (2.42) and (2.43) causes the mixing of the states ν_1 and ν_2. Thus, as stated previously, the states ν_1 and ν_2, which are instantaneous mass eigenstates, cease to be eigenstates of the Hamiltonian when $dA/dx\neq 0$, or, equivalently, $d\rho/dx\neq 0$.

Let us now consider the case in which $\rho(x)$ is a slowly varying function, so that $d\theta_m/dx$ is small. More precisely, we assume that $|d\theta_m/dx| \ll |M_2^2-M_1^2|/4E=\pi/\lambda_m$, which, in terms of the density, translates to

$$\left|\frac{1}{N_e}\frac{dN_e}{dx}\right| \ll \frac{1}{S_{2\theta}}\frac{2\pi}{\lambda_m}\left[\frac{\lambda\lambda_0}{\lambda_m^2}\right]\ . \tag{2.46}$$

Thus if the density is slowly changing, on a distance scale of roughly the wavelength in matter, we may neglect the off-diagonal term $d\theta_m/dx$ completely, and ν_1 and ν_2 become eigenstates of the Hamiltonian. This is the adiabatic approximation.

Adiabatic propagation through a medium with varying density can have profound effects. For example, let us consider an electron neutrino produced in the center of the sun or in a collapsing star, where the density is high enough to satisfy $A \gg \Delta$. At production the neutrino is almost a pure mass eigenstate independent of the size of the mixing angle [Eq. (2.33)]. As this neutrino moves outward, A will decrease as the density decreases, and the neutrino will eventually go through the resonance region, where $A=\Delta\cos 2\theta$, and proceed out into the vacuum. If the density changes slowly enough so that the propagation is adiabatic, the neutrino state will remain the same mass eigenstate. However, as can be seen from Fig. 3, the mass eigenstate that is dominantly a ν_e at the high densities above the resonance is not dominantly a ν_e below the resonance. The mass eigenstate that is dominantly ν_e varies linearly with A, the induced mass of the electron neutrino; so above the resonance this is the upper mass eigenstate, but below the resonance it is the lower mass eigenstate. For the electron neutrino produced in the star and propagating adiabatically, it remains on the upper mass eigenstate, so that below the resonance this same mass eigenstate is essentially independent of A and corresponds dominantly to a ν_μ. The dominant flavor of the neutrino has been changed as it propagates through matter of decreasing density. This is known as the MSW effect, after Mikheyev and Smirnov (1985, 1986a, 1986b) and Wolfenstein (1978a, 1978b, 1979). See also Bethe (1986).

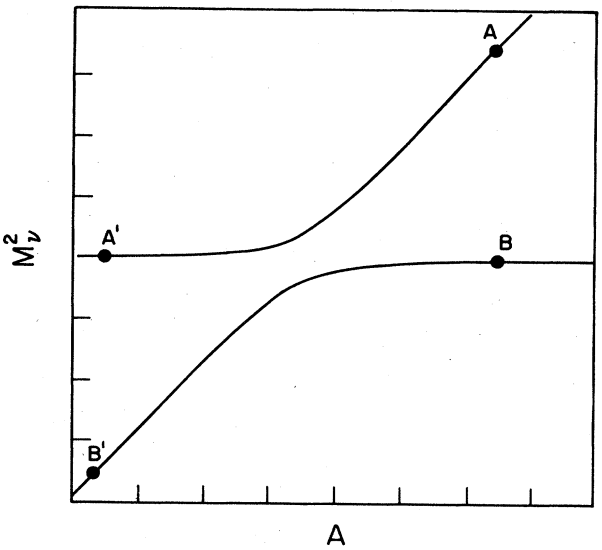

FIG. 3. Masses of two flavors of neutrinos as a function of A, the matter-induced electron-neutrino mass. Here we take $m_2^2=25m_1^2$, $\sin^2\theta=1\times10^{-2}$.

In the adiabatic limit it is easy to quantitatively describe the MSW effect. The condition (2.46) implies that the neutrino is propagating for many oscillation wavelengths. The phase information is then effectively lost and the adiabatic neutrino probabilities are the classical probabilities, similar to those of Eqs. (2.11) and (2.39). Consider the evolution of a ν_e that is produced at some density ρ, with the mixing angle θ_m. The probabilities of ν_e to be either ν_1 or ν_2 are given by $\sin^2\theta_m$ and $\cos^2\theta_m$, respectively. Figure 3 shows the two states labeled as A and B. Let us assume that, after production, a ν_e propagates adiabatically until reaching a location for which $\rho=0$ and the mixing angle is the vacuum angle. This means that A (B) will simply propagate to the states A' (B'). There the probability of ν_1 or ν_2 to be a ν_e is given by $\sin^2\theta$ and $\cos^2\theta$, respectively. In analogy to the vacuum case, Eq. (2.11), it follows that the propagation probability is, in the adiabatic approximation,

$$P(\nu_e\to\nu_e)=\sum_i P_m(\nu_e\to\nu_i)P(\nu_i\to\nu_e)$$

$$=[1\ 0]\begin{bmatrix}\cos^2\theta & \sin^2\theta\\ \sin^2\theta & \cos^2\theta\end{bmatrix}\begin{bmatrix}1 & 0\\ 0 & 1\end{bmatrix}\begin{bmatrix}\cos^2\theta_m & \sin^2\theta_m\\ \sin^2\theta_m & \cos^2\theta_m\end{bmatrix}\begin{bmatrix}1\\ 0\end{bmatrix}$$

$$=\sin^2\theta\sin^2\theta_m+\cos^2\theta\cos^2\theta_m=\tfrac{1}{2}(1+\cos 2\theta\cos 2\theta_m)\ . \tag{2.47}$$

In Fig. 3 the points A (B) and A' (B') are above and below the resonance, respectively. However, it should be emphasized that the derivation of Eq. (2.47) is valid for situations other than this. It does not matter whether a resonance has been crossed or not. In general, if an electron neutrino propagates adiabatically from one region, with mixing angle θ_1, to another region, with mixing angle θ_2, then

$$P(\nu_e \to \nu_e) = \tfrac{1}{2}(1+\cos 2\theta_1 \cos 2\theta_2) \ . \tag{2.48}$$

For other discussions on adiabatic propagation, see Wolfenstein (1978b), Barger *et al.* (1986), Messiah (1986), and Balantekin *et al.* (1988).

3. Corrections to the adiabatic approximation

Equation (2.47) is a simple, analytic equation for the survival probability of an electron neutrino propagating through matter. It describes quantitatively the MSW effect. However, it is only valid when the matter density is slowly changing, so that the adiabatic approximation is valid. When this approximation breaks down, one must go back and solve the wave equation. For a few specific density distributions there exist exact solutions of the wave equation, but in general the wave equation is not solvable algebraically However, it is still possible to derive for the survival probability a simple, analytic equation that is accurate when nonadiabatic effects are important (Parke, 1986).

For a neutrino going through monotonically decreasing density, like neutrinos coming from the sun, the adiabatic approximation will break down when Eq. (2.46) approaches an equality. This equation follows from Eq. (2.43) when $|d\theta/dx|$ becomes of the order of $(M_2^2 - M_1^2)/4E$. Equation (2.45) shows that for a smoothly varying density, $|d\theta/dx|$ has a sharply peaked maximum at the resonance, $\Delta C_{2\theta} \equiv A(x_0)$. At the same time, according to Eq. (2.44), $|M_2^2 - M_1^2|$ is a minimum. Therefore the condition for adiabatic transition, Eq. (2.46), is most stringent at the resonance. Since $\lambda_m \to \lambda/S_{2\theta}$ for $A = \Delta C_{2\theta}$, we may rewrite Eq. (2.46) in the form

$$1 \ll \gamma \equiv \frac{\Delta S_{2\theta}^2}{2EC_{2\theta}|dN_e/N_e dx|_0} \ . \tag{2.49}$$

The subscript 0 denotes that this quantity should be evaluated at the resonance; γ is the adiabaticity parameter.

If $\gamma \approx 1$, there will be considerable corrections to the probabilities obtained using the adiabatic approximation, Eqs. (2.47) and (2.48). Such corrections will typically occur only in a small region around the resonance density, because the resonance is very narrow. Propagation outside this region will be adiabatic and hence describable by Eq. (2.48). If the nonadiabatic effects in this narrow region can be described simply, we can still patch together a simple equation for the total probability.

In Eq. (2.43), γ of order 1 corresponds with the off-diagonal elements becoming of order the diagonal elements. Thus the corrections take the form of "level crossing," where the state ν_1 can cross over to ν_2 and vice versa. This is analogous to a quantum tunneling effect. Let us denote by P_c the crossing probability from ν_1 to ν_2:

$$P_c \equiv |\langle \nu_2(x_+)|\nu_1(x_-)\rangle|^2 \ . \tag{2.50}$$

Here, $x_\pm$ refer to two faraway points on either side of the resonance position, points where the adiabatic approximation is still valid. Unitarity for two neutrino flavors tells us that P_c is also the probability of crossing from ν_2 to ν_1 and that $1-P_c$ is the probability for ν_1 or ν_2 to stay in the same mass eigenstate.

Using P_c, we can write a simple equation for $P(\nu_e \to \nu_e)$ analogous to Eq. (2.47). Referring again to Fig. (3), we see there is now a probability P_c for state A (B) to propagate to B' (A'). Thus we have

$$\begin{aligned} P(\nu_e \to \nu_e) &= [1\ 0] \begin{bmatrix} \cos^2\theta & \sin^2\theta \\ \sin^2\theta & \cos^2\theta \end{bmatrix} \begin{bmatrix} (1-P_c) & P_c \\ P_c & (1-P_c) \end{bmatrix} \begin{bmatrix} \cos^2\theta_m & \sin^2\theta_m \\ \sin^2\theta_m & \cos^2\theta_m \end{bmatrix} \begin{bmatrix} 1 \\ 0 \end{bmatrix} \\ &= \tfrac{1}{2} + (\tfrac{1}{2} - P_c)\cos 2\theta \cos 2\theta_m \ . \end{aligned} \tag{2.51}$$

The correction to the adiabatic approximation is totally embodied in the function P_c. In the next section we shall present some formulas for P_c in terms of the neutrino parameters.

4. The probability for level crossing P_c

Neutrino propagation is governed by the wave equation, (2.29). To obtain P_c, we must solve this set of coupled equations under appropriate boundary conditions. Unfortunately, these solutions must, in general, be obtained numerically, unless we approximate the density $N_e(x)$ by a simple function. However, because nonadiabatic effects are typically relevant only for a narrow range of x around the resonance point, as discussed in the last section, it may not be a bad approximation to use a simple density distribution over this small range.

Such a solution was first worked out independently by Landau (1932) and Zener (1932), after whom it is named, and by Stueckelberg (1932). They were working on the level-crossing problem in connection with atomic collisions. Applying their results to neutrinos (Haxton, 1986; Parke, 1986; see also Dar *et al.*, 1987; Petcov,

1987; and Toshev, 1988a, 1988b), we see that their solution is appropriate for a linear density change. This is a natural first choice, since it corresponds to the first term in a Taylor-series expansion about the resonance point. In this case the solution of the wave equation (2.29) is proportional to a Weber function. Imposing the proper boundary conditions, expanding the Weber functions about the production and detection positions far from the resonance, and dropping oscillating terms, we obtain the solution for $P(\nu_e \rightarrow \nu_e)$. Up to small corrections, $P(\nu_e \rightarrow \nu_e)$ has precisely the standard form given in Eq. (2.51), with P_c given by

$$P_c = \exp\left[-\frac{\pi}{2}\gamma\right]; \tag{2.52}$$

γ is exactly the adiabaticity parameter defined in Eq. (2.49). Thus when $\gamma \gg 1$, $P_c = 0$, and we go back to the adiabatic approximation. The exponential form for P_c is familiar from other quantum tunneling probabilities. The small corrections to the standard form, Eq. (2.51), first occur in the asymptotic expansion of the Weber function at order (θ^6/γ^2). These corrections are singular in the extreme nonadiabatic limit, $\gamma \rightarrow 0$. But since the probability is bounded between 0 and 1, they must cancel with oscillating terms that have been dropped. It is to be expected that the phase-dependent terms become very important in the extreme nonadiabatic limit, since this is comparable to the wavelength becoming large. These phase effects are discussed in the next section.

The Landau-Zener equation for P_c, Eq. (2.52), is simple and effectively accounts for nonadiabatic effects in arbitrary monotonically varying density distributions. It allows easy numerical calculations and has been used by most groups that calculate neutrino resonance effects. However, the accuracy of the LZ equation depends on the presumed adequacy of the linear density approximation throughout the resonance layer, which is proportional to $\sin 2\theta$, as defined in Eq (2.35). For large θ, Eq. (2.52) is thus expected to receive corrections for a general density function.

For a medium with an arbitrary density profile, one can generalize Eq. (2.52) in the form of a contour integral due to Landau (1932; see also Landau and Lifshitz, 1977),

$$\ln P_c = -\frac{1}{E}\,\mathrm{Im}\int_{A=\Delta C_{2\theta}}^{A=\Delta e^{\pm i2\theta}} [(A-\Delta C_{2\theta})^2 + (\Delta S_{2\theta})^2]^{1/2} dx\ . \tag{2.53}$$

The $+$ $(-)$ sign is to be used for $dA/dx < 0$ (>0); it simply determines the overall sign of Eq. (2.53) to be always negative. We may now write the crossing probability P_c for an arbitrary density profile in the form

$$P_c = \exp\left[-\frac{\pi}{2}\gamma F\right], \tag{2.54}$$

where the function F, which reduces to unity for an exactly linear density, can be calculated according to Eq. (2.53). We give the function F in Table III for a variety

TABLE III. Level-crossing probability P_c for various electron-density distributions, as calculated by Landau's method, Eq. (2.53) (Kuo and Pantaleone, 1988). The right-hand column is the natural logarithm of P_C divided by $-\pi/2$ and γ, the adiabaticity parameter. $A_0^{(n)} \equiv 2\sqrt{2}G_F E N_0^{(n)}$ denotes the nth derivative of A with respect to x evaluated at the resonance position $A = \Delta\cos 2\theta$. The coefficient of $(\tan 2\theta)^{2m}$ in the series expression for the power-law density is the product of two binomial coefficients.

Density distribution	$\left[\frac{\ln(P_{c;\mathrm{Landau}})}{-\gamma(\pi/2)}\right]$
$A \propto \exp(-r)$	$1-\tan^2\theta$
$A \propto r$	1
$A \propto 1/r$	$(1-\tan^2\theta)^2/(1+\tan^2\theta)$
$A \propto r^n$	$2\sum_{m=0}^{\infty}\begin{bmatrix}(1/n)-1\\ 2m\end{bmatrix}\begin{bmatrix}\frac{1}{2}\\ m+1\end{bmatrix}(\tan 2\theta)^{2m}$
	or, for small $1/n$
	$(1-\tan^2\theta)(1-(1/n)\{\ln(1-\tan^2\theta)+1-[(1+\tan^2\theta)/\tan^2\theta]\ln(1+\tan^2\theta)\}+\cdots)$
	or, for small $(1+1/n)$
	$[(1-\tan^2\theta)^2/(1+\tan^2\theta)](1-(1+1/n)\{\ln(1-\tan^2\theta)-1+[(1-\tan^2\theta)/\tan^2\theta]\ln(1+\tan^2\theta)]\}+\cdots)$
	or, for small $(-1+1/n)$
	$\{1-(-1+1/n)[-\frac{1}{2}\tan^2\theta-\ln(1-\tan^2\theta)]+\cdots\}$
$A=\Delta[a\tanh(x/l)+b]$	$(b+a-C_{2\theta})[C_{2\theta}-(b-a)]/(aS_{2\theta}^2)\{[(b-a-C_{2\theta})^2+S_{2\theta}^2]^{1/2}+[(b+a-C_{2\theta})^2+S_{2\theta}^2]^{1/2}-2a\}$
$A=\Delta C_{2\theta}+A_0^{(1)}x+\frac{1}{2}A_0^{(2)}x^2+\frac{1}{6}A_0^{(3)}x^3$ $+\frac{1}{24}A_0^{(4)}x^4+\frac{1}{120}A_0^{(5)}x^5+\cdots$	$1-\frac{1}{8}\left[\frac{-A_0^{(3)}}{A_0^{(1)}}+3\frac{(A_0^{(2)})^2}{(A_0^{(1)})^2}\right]\left[\frac{\Delta S_{2\theta}}{A_0^{(1)}}\right]^2$ $+\frac{1}{192}\left[\frac{-A_0^{(5)}}{A_0^{(1)}}+15\frac{A_0^{(4)}A_0^{(2)}}{(A_0^{(1)})^2}+10\frac{(A_0^{(3)})^2}{(A_0^{(1)})^2}-105\frac{A_0^{(3)}(A_0^{(2)})^2}{(A_0^{(1)})^3}+105\frac{(A_0^{(2)})^4}{(A_0^{(1)})^4}\right]\left[\frac{\Delta S_{2\theta}}{A_0^{(1)}}\right]^4+\cdots$

of medium-density profiles. The adiabaticity factor γ, defined in Eq. (2.49), is different for distinct density distributions. Furthermore, F can be given in closed form only for a few specific density functions: $A(x)$ proportional to x, $1/x$, $\exp(-x/l)$ (Pizzochero, 1987), and $\tanh(x/l)$. However, an expansion in powers of $\sin^2 2\theta$ can be made for arbitrary $A(x)$. It corresponds to an expansion of dx/dA around the resonance point, $A=\Delta\cos 2\theta$. One drawback of the expansion in $\sin^2 2\theta$ is that it converges slowly for large angles. In this case there is another expansion scheme, applicable when the density distribution is of the form $A(x)\propto x^N$. For arbitrary $\sin^2 2\theta$ one can expand F as a power series in $1/N$, $(1+1/N)$, or $(-1+1/N)$. These expansions are also given in Table III. The $1/N$ expansion is particularly useful for the calculation of crossing probability in stars. It can be used for the case of the supernova neutrinos where $A(x)\propto 1/x^3$ approximately. It can also be used for the sun to calculate corrections due to density deviations from $A(x)\propto\exp(-x/l)$, which corresponds to $N\to\infty$. For details of this calculation see Kuo and Pantaleone (1989).

We now turn to another problem with Eqs. (2.52) and (2.54). They are the leading exponentials in a semiclassical expansion and, as such, are only valid if $P_c \ll 1$, or $\gamma F \gg 1$. In the extreme nonadiabatic limit, $\gamma\to 0$, there are corrections to these formulas. To understand these corrections we first calculate P_c in the extreme nonadiabatic limit. In this limit, corresponding to an abrupt density change, it is the flavor eigenstates that are continuous across the boundary. Let $\theta^{(1)}$ and $\theta^{(2)}$ be the mixing angles in matter before and after the sudden density change. The amplitude for going from one mass eigenstate to another is

$$\mathrm{Amp}(\nu_i^{(1)}\to\nu_j^{(2)})=\begin{bmatrix}\cos\theta^{(2)} & -\sin\theta^{(2)}\\ \sin\theta^{(2)} & \cos\theta^{(2)}\end{bmatrix}\begin{bmatrix}\cos\theta^{(1)} & \sin\theta^{(1)}\\ -\sin\theta^{(1)} & \cos\theta^{(1)}\end{bmatrix}$$

$$=\begin{bmatrix}\cos(\theta^{(1)}-\theta^{(2)}) & \sin(\theta^{(1)}-\theta^{(2)})\\ -\sin(\theta^{(1)}-\theta^{(2)}) & \cos(\theta^{(1)}-\theta^{(2)})\end{bmatrix}. \tag{2.55}$$

This corresponds to an equation for P_c of

$$P_c=\sin^2(\theta^{(1)}-\theta^{(2)}) . \tag{2.56}$$

For a continuous, monotonic, quickly varying density (such as occurs in a star), the nonadiabatic region enlarges to extend far above and below the resonance as we approach the extreme nonadiabatic limit, $\gamma\to 0$. In this case, $\theta^{(1)}\to\pi/2$ and $\theta^{(2)}\to\theta$ [quantitatively, for $A(x)\propto x^N$, these limits are smoothly approached in the extreme nonadiabatic limit for $N<-\frac{1}{2}$ or $1<N$, as can be derived from Eq. (2.46)]. Thus

$$P_c=\cos^2\theta . \tag{2.57}$$

When this value is substituted in Eq. (2.51), one has $P(\nu_e\to\nu_e)=1-\frac{1}{2}\sin^2 2\theta$, which is just the vacuum oscillation equation given in Eq. (2.11). This is expected, since the extreme nonadiabatic limit, $\gamma\to 0$, corresponds to the neutrino vacuum oscillation wavelength growing larger than the dimension of the star; matter effects should then be negligible.

It is now clear what is wrong with Eqs. (2.52) and (2.54). In the limit $\gamma\to 0$, $P_c\to 1$, in contrast to $P_c\to\cos^2\theta$, according to Eq. (2.57). This deviation becomes substantial when the mixing angle θ is large. To remedy this, we may resort to solving the neutrino wave equation directly. This can be done for density functions $A(x)$ proportional to $\exp(-x/l)$ (Kaneko, 1987; Toshev, 1987b; Ito *et al.*, 1988; Krastev and Petcov, 1988b; Petcov, 1988a), $\tanh(x/l)$ (Notzold, 1987a), $1/x$ (Kuo and Pantaleone, 1989), and, of course, x. For a linear density function the change in density is never fast enough for the extreme nonadiabatic limit, Eq. (2.57), to apply [see comments before Eq. (2.57)]. For the other three cases, the solutions can all be cast in the following form for the crossing probability:

$$P_c=\frac{\exp\left[-\frac{\pi}{2}\gamma F\right]-\exp\left[-\frac{\pi}{2}\gamma\left[\frac{F}{S_\theta^2}\right]\right]}{1-\exp\left[-\frac{\pi}{2}\gamma\left[\frac{F}{S_\theta^2}\right]\right]} . \tag{2.58}$$

Here, the function F can be read from Table III. Equation (2.58) reduces to Eq. (2.54) for $\gamma F\gg 1$. In the limit $\gamma\to 0$, it reduces to Eq. (2.57). It is free of the inadequacies of Eq. (2.52) or (2.54) and is suitable for general use. Indeed, Eq. (2.58), with the function F given in Table III has been suggested as an ansatz for an arbitrary density distribution (Kuo and Pantaleone, 1989).

In practice the difference between using Eq. (2.52), (2.54), or (2.58) may not be very important for actual applications. Consider the neutrinos from the sun. It may be that the neutrino parameters fall in regions where the differences of the equations are never significant. Furthermore, the experimental measurements must be folded in with uncertainties in the neutrino spectra, the cross section, and the detector efficiencies. All of these can have uncertainties larger than the differences discussed above. Thus for numerical calculations the choice among the various equations may be dictated more by ease of use than by accuracy.

5. Phase effects

One problem with using an average probability like Eq. (2.51) occurs when the distance between the resonance position and the source (or detector) becomes small. For solar neutrinos this occurs as the resonance density approaches the central neutrino production region. The phase generated during the propagation between the source and the resonance can be important if the propagation through the resonance is nonadiabatic. Equation (2.51) was derived assuming that this phase was large and hence effectively irrelevant. As the phase becomes small and the neutrino production point approaches and moves through the resonance point, P_c changes drastically. For a neutrino produced well below the resonance region, level crossing cannot occur and neutrino propagation will again be adiabatic; $P_c=0$. Thus the equations for P_c discussed in the previous section must be modified to account for this situation.

One possible solution to this problem is to fall back on numerical integration of the wave equation [or the confluent hypergeometric functions (Haxton, 1987a)] when phase effects are relevant. However, this method requires much more effort than is called for at this time. For solar neutrinos, nonadiabatic propagation near the solar core occurs only when the vacuum mixing angle is very small, $\sin\theta\approx 10^{-3}$. Hence the errors in Eq. (2.51), because of phase effects, are relevant for only a small region of parameter space, since the resonance region is typically relatively narrow. A crude but reasonably effective way to account for the neutrino production point moving though the resonance region is to modify P_c by multiplying by a theta function,

$$P_c\rightarrow\overline{P_c}=\Theta(A-\Delta C_{2\theta})P_c\ , \tag{2.59}$$

so that $\bar{P}_c$ is zero if the neutrino is produced below the resonance point. Here $\Theta(x)$ is 0 for $x<0$ and 1 for $x>0$. Above the resonance point the simple equations discussed in the previous section that ignore phase effects are used for P_c.

For other discussions of these phase effects see Kuo and Pantaleone (1987a), Mikheyev and Smirnov (1987b), and Krastev and Petcov (1988a). For a discussion of phase effects due to density fluctuations see Schafer and Koonin (1987).

6. Properties of the average probability $P(\nu_e\rightarrow\nu_e)$

The function $P(\nu_e\rightarrow\nu_e)$ is the single most important quantity in a neutrino oscillation analysis. It is used to relate directly the experimental data with the neutrino parameters. In the previous sections we obtained an algebraic formula for the average probability $P(\nu_e\rightarrow\nu_e)$. For a neutrino produced in the sun, at a density where the mixing angle is θ_m, and detected in vacuum where the mixing angle is θ,

$$P(\nu_e\rightarrow\nu_e)=\tfrac{1}{2}+[\tfrac{1}{2}-\Theta(A-\Delta C_{2\theta})P_c]\cos2\theta\cos2\theta_m\ . \tag{2.60}$$

In a physical measurement, $P(\nu_e\rightarrow\nu_e)$ is folded in with the flux and the cross section by integration over the neutrino energy. In this section we shall discuss in detail the behavior of $P(\nu_e\rightarrow\nu_e)$ as a function of the neutrino parameters $m_2^2-m_1^2$ and θ and especially as a function of the neutrino energy E.

We first examine the energy dependence of $\cos2\theta_m$, the cosine of twice the mixing angle at the production point. This function enters in the adiabatic formula Eq. (2.47) as well as the corrected equations (2.51) and (2.60). The mixing angle in matter is given by Eqs. (2.32) and (2.33). All of the energy dependence in these equations enters through A [Eq. (2.28)] in the combination

$$\begin{aligned}(A-\Delta C_{2\theta})&=(2\sqrt{2}G_F N_e|_P E-\Delta C_{2\theta})\\ &\equiv 2\sqrt{2}G_F N_e|_P(E-E_A)\ ,\end{aligned} \tag{2.61}$$

$$E_A=\frac{\Delta\cos2\theta}{2\sqrt{2}G_F N_e|_P}\ .$$

Here $N_e|_P$ is the density at the production point, and E_A is defined to be the energy at which $(A-\Delta C_{2\theta})=0$. At this energy, the neutrino is produced exactly at the center of the resonance, $\theta_m=\pi/4$, so that $\cos2\theta_m=0$. For $E<E_A$, the neutrino does not go through the resonance but is produced below it. Then $\theta_m\rightarrow\theta$ away from the resonance, and the oscillation probability approaches its vacuum value, $P(\nu_e\rightarrow\nu_e)=1-\frac{1}{2}\sin^2 2\theta$. For $E>E_A$, the neutrino does go through the resonance and the MSW effect can operate. Then $\theta_m\rightarrow\pi/2$ away from the resonance, and the adiabatic oscillation probability ($P_c=0$) approaches $P(\nu_e\rightarrow\nu_e)=\sin^2\theta$. Thus E_A is the energy that is on the threshold between no matter effects and adiabatic resonant conversion (the MSW effect). Hence E_A denotes the adiabatic threshold energy.

This transition between no matter effects and resonant conversion, which is described by the adiabatic approximation, is a very abrupt function of energy. For small angles, the resonance is very narrow and neutrino production can quickly move through it. The threshold energy E_A is directly proportional to the vacuum mass difference Δ. It is relatively insensitive to the vacuum mixing angle, since $\cos2\theta$ is approximately 1 for small angles.

Now we examine the energy dependence of the nonadiabatic correction P_c. Whether one uses the LZ equation (2.52) or the exponential equation (2.58), all of the energy dependence is contained in the adiabaticity parameter γ; γ has an explicit factor of the energy in the denominator, but $|dN_e/N_e dr|_0$ is also, in general, E dependent. This is because $|dN_e/N_e dr|_0$ is evaluated at the resonance, and the resonance location is energy dependent, since it is determined by the condition $A(x)=\Delta\cos2\theta$. However, for N_e an exponential function, as is approximately valid

with the sun, $dN_e/N_e dr$ is a constant, independent of x. In this case the dependence of P_c on E is simply given by

$$\frac{\pi}{2}\gamma \equiv \frac{E_{\rm NA}}{E} ,$$
$$E_{\rm NA} = \frac{\pi\Delta \sin^2 2\theta}{4\cos 2\theta |dN_e/N_e dr|_0} . \tag{2.62}$$

The nonadiabatic correction P_c depends on $E_{\rm NA}$ only, where NA denotes "nonadiabatic." For $E \ll E_{\rm NA}$, $P_c \to 0$ and we recover the adiabatic limit. In the extreme nonadiabatic limit, $E \gg E_{\rm NA}$, the survival probability $P(\nu_e \to \nu_e)$ approaches the vacuum equation, as discussed previously. Thus $E_{\rm NA}$ is the energy scale for the transition between the adiabatic and the nonadiabatic regions.

The nonadiabatic transition in $P(\nu_e \to \nu_e)$ at E_A is different from the adiabatic transition at E_A. The width in energy of the nonadiabatic transition is controlled by the exponential function, not by the width of the resonance. Moreover, $E_{\rm NA}$ is much more sensitive to the vacuum mixing angle than is E_A. For small angles, $E_{\rm NA}$ varies as θ^2, while E_A is a constant.

The survival probability $P(\nu_e \to \nu_e)$ is plotted in Fig. 4 for neutrinos produced in the sun for typical choices of Δ and θ. The range of neutrino energies for which conversion from one flavor to another occurs is

$$E_A < E < E_{\rm NA} . \tag{2.63}$$

Outside this region, $P(\nu_e \to \nu_e)$ approaches the vacuum oscillation expression, $1 - \frac{1}{2}\sin^2 2\theta$. Inside, $P(\nu_e \to \nu_e)$ has a flat region with

$$P(\nu_e \to \nu_e) \to \sin^2\theta . \tag{2.64}$$

D. Three-flavor solutions to the wave equation

The previous section concentrated on neutrino oscillations with only two flavors. Since it is known that at least three flavors of neutrinos exist, this analysis can only be valid if the "third" neutrino decouples or if the three-flavor solution can always be reduced to an "equivalent" two-flavor solution. However, this need not occur. The three-flavor problem can be qualitatively different from the two-flavor problem. We shall explicitly solve the three-flavor problem; then we shall examine the differences between two- and three-flavor oscillations in matter and the conditions under which the "third" neutrino decouples so that the two-flavor solution indeed suffices. For further discussion of the three-neutrino problem, see Kuo and Pantaleone (1986, 1987a, 1987b); Baldini and Giudice (1987); Kim *et al.* (1987a); Petcov and Toshev (1987); Toshev (1987a); Zaglauer and Schwarzer (1987, 1988); Mikheyev and Smirnov (1988); Petcov (1988d).

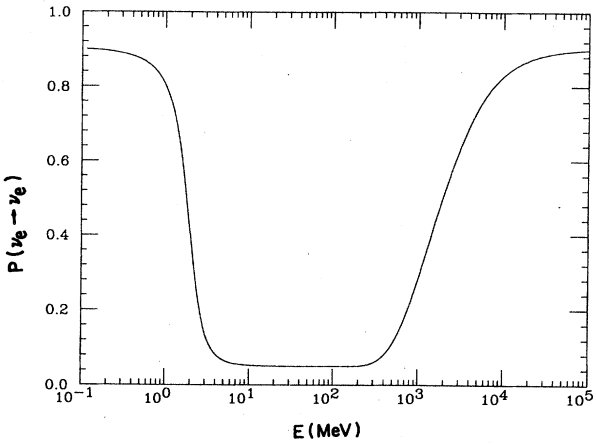

FIG. 4. Probability of a ν_e, produced at the center of the sun, reaching the Earth as a function of energy. We used Eqs. (2.51) and (2.58) with $F = 1 - \tan^2\theta$ and the values $\Delta = 3\times 10^{-5}$ eV^2 and $\sin^2\theta = 0.05$.

1. General formalism

Let us begin by writing the neutrino propagation equation for three flavors, which is a straightforward generalization of Eq. (2.29),

$$i\frac{d}{dx}\begin{bmatrix}\nu_e\\ \nu_\mu\\ \nu_\tau\end{bmatrix} = \frac{1}{2E}M^2\begin{bmatrix}\nu_e\\ \nu_\mu\\ \nu_\tau\end{bmatrix} = \frac{1}{2E}\left\{U\begin{bmatrix}m_1^2 & 0 & 0\\ 0 & m_2^2 & 0\\ 0 & 0 & m_3^2\end{bmatrix}U^\dagger + \begin{bmatrix}A & 0 & 0\\ 0 & 0 & 0\\ 0 & 0 & 0\end{bmatrix}\right\}\begin{bmatrix}\nu_e\\ \nu_\mu\\ \nu_\tau\end{bmatrix} . \tag{2.65}$$

Without loss of generality, we assume $m_3^2 > m_2^2 > m_1^2$. The 3×3 mixing matrix U was defined in Eq. (2.12),

$$U = \exp(i\psi\lambda_7)\Gamma\exp(i\varphi\lambda_5)\exp(i\omega\lambda_2) = \begin{bmatrix} C_\varphi C_\omega & C_\varphi S_\omega & S_\varphi \\ -C_\psi S_\omega e^{i\delta} - S_\psi S_\varphi C_\omega e^{-i\delta} & C_\psi C_\omega e^{i\delta} - S_\psi S_\varphi S_\omega e^{-i\delta} & S_\psi C_\varphi e^{-i\delta} \\ S_\psi S_\omega e^{i\delta} - C_\psi S_\varphi C_\omega e^{-i\delta} & -S_\psi C_\omega e^{i\delta} - C_\psi S_\varphi S_\omega e^{-i\delta} & C_\psi C_\varphi e^{-i\delta} \end{bmatrix} . \tag{2.66}$$

This parametrization is convenient for two reasons. First, the angles ψ, φ, and ω can be associated with oscillations of the 2-3, 3-1, and 1-2 neutrino states. In addition, the order of the product submatrices is important. It is chosen so that we can rotate away the angles ψ and the phase δ without affecting A, the induced mass of the electron neutrino. Thus the effects of a medium only enter the propagation through the remaining two mixing angles: ω and φ. These two mixing angles are the parameters that determine the mixing between the electron neutrino and the mass eigenstates. If the electron neutrino is the component that is produced and detected, as for solar neutrinos, then these two mixing angles are the only ones that are relevant.

2. Eigenvalues and eigenfunctions for fixed density

The exact eigenfunctions and eigenvalues of M^2 can be obtained analytically (Barger *et al.*, 1980; Zaglauer and Schwarzer, 1988). Since the characteristic equation is cubic, however, the physical implications are far from transparent (and nonadiabatic effects are not easily incorporated). For this reason we shall develop approximate solutions whose physical meanings are easy to decipher. One can gain some idea of the solution by referring to Fig. 5, where the mass eigenstates are plotted as a function of A. In this plot small mixings and a hierarchy of vacuum mass values are assumed. We see that there are two regions where the levels almost cross. Thus there are two resonances. They occur when A, the induced electron-neutrino mass, approaches one of the heavier neutrino masses. The lower resonance is at $A \approx m_2^2$, while the higher resonance occurs when $A \approx m_3^2$.

We now turn to the mass matrix M^2 and develop approximate solutions near the resonances (Kuo and Pantaleone, 1986). To study the lower resonance we rotate the flavor basis by $\exp(-i\varphi\lambda_5)\Gamma^\dagger \exp(-i\psi\lambda_7)$ to obtain the transformed mass matrix

$$\tilde{M}^2 \equiv \exp(-i\varphi\lambda_5)\Gamma^\dagger \exp(-i\psi\lambda_7) M^2 \exp(i\psi\lambda_7)\Gamma \times \exp(i\varphi\lambda_5) = \frac{1}{2}\begin{bmatrix} \Sigma - \Delta C_{2\omega} + 2AC_\varphi^2 & \Delta S_{2\omega} & AS_{2\varphi} \\ \Delta S_{2\omega} & \Sigma + \Delta C_{2\omega} & 0 \\ AS_{2\varphi} & 0 & 2(m_3^2 + AS_\varphi^2) \end{bmatrix} . \tag{2.67}$$

Here $\Sigma = m_2^2 + m_1^2$, $\Delta \equiv m_2^2 - m_1^2$, $C_{2\omega} \equiv \cos 2\omega$, etc. Near the lower resonance, $A \approx \Delta$. The term $AS_{2\varphi}$ can be treated as a perturbation if it is small compared to $m_3^2 - \Sigma$. In this case the matrix $\tilde{M}^2$ breaks apart into a decoupled neutrino and a 2×2 submatrix of the form of Eq. (2.29). To zeroth order in $AS_{2\varphi}/2m_3^2$, we find the eigenvalues

$$\lambda_\pm = \{(\Sigma + AC_\varphi^2) \pm [(AC_\varphi^2 - \Delta C_{2\omega})^2 + (\Delta S_{2\omega})^2]^{1/2}\}/2 , \qquad \lambda_3 = m_3^2 + AS_\varphi^2 , \tag{2.68}$$

and the mixing angle

$$\sin 2\omega_m = \Delta S_{2\omega}/[(AC_\varphi^2 - \Delta C_{2\omega})^2 + (\Delta S_{2\omega})^2]^{1/2} . \tag{2.69}$$

Comparing this with Eq. (2.67), we see that the flavor eigenstates are related to the mass eigenstates in matter by

$$\nu_\alpha = U_{\alpha i}^m \nu_i^m , \quad i = +, -, 3 , \tag{2.70}$$

with

$$U^m = \exp(i\psi\lambda_7)\Gamma \exp(i\varphi\lambda_5)\exp(i\omega_m\lambda_2) . \tag{2.71}$$

Thus, while ψ and φ maintain their vacuum values, the angle ω_m rotates ($\approx \pi/2$) as in the case of the two-neutrino resonance. The position of the resonance is at

$$AC_\varphi^2 = \Delta C_{2\omega} . \tag{2.72}$$

We now turn to the higher resonance with $A \approx m_3^2$. In this case it is more convenient to rotate the flavor basis by $\Gamma^\dagger \exp(-i\psi\lambda_7)$,

$$\bar{M}^2 \equiv \Gamma^\dagger \exp(-i\psi\lambda_7) M^2 \exp(i\psi\lambda_7)\Gamma = \frac{1}{2}\begin{bmatrix} \Lambda C_\varphi^2 + 2m_3^2 S_\varphi^2 + 2A & \Delta S_{2\omega} C_\varphi & (m_3^2 - \Lambda/2)S_{2\varphi} \\ \Delta S_{2\omega} C_\varphi & \Sigma + \Delta C_{2\omega} & -\Delta S_{2\omega} S_\varphi \\ (m_3^2 - \Lambda/2)S_{2\varphi} & -\Delta S_{2\omega} S_\varphi & \Lambda S_\varphi^2 + 2m_3^2 C_\varphi^2 \end{bmatrix} , \tag{2.73}$$

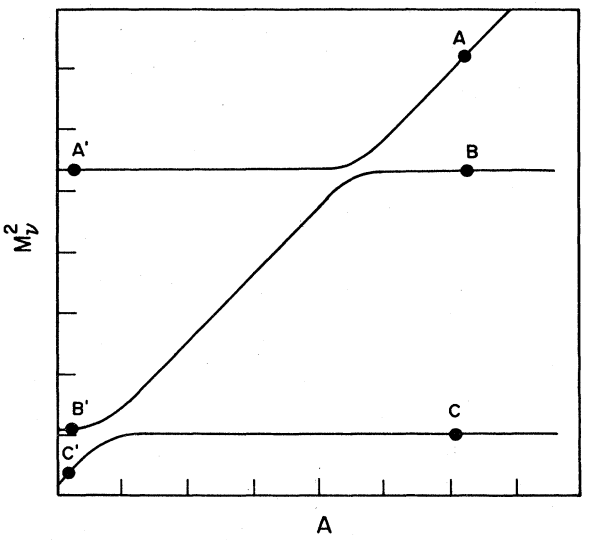

FIG. 5. Masses of three flavors of neutrinos as a function of A, the matter-induced electron-neutrino mass. Here we take $m_3^2 = 5m_2^2 = 25m_1^2$, $|U_{e2}|^2 = 5\times 10^{-2}$, and $|U_{e3}|^2 = 5\times 10^{-4}$.

where $\Lambda \equiv (\Sigma - \Delta C_{2\omega})$. We may now treat $\Delta S_{2\omega}$ as a perturbation. To zeroth order in $\Delta S_{2\omega}/2m_3^2$, $\overline{M}^2$ again takes the form of a decoupled neutrino and a two-neutrino mass matrix. The eigenvalues are

$$\begin{aligned}\lambda_{\pm} &= ((m_3^2 + \Lambda/2 + A) \\ &\quad \pm \{[A - C_{2\varphi}(m_3^2 - \Lambda/2)]^2 \\ &\quad + [(m_3^2 - \Lambda/2) S_{2\varphi}]^2\}^{1/2})/2 , \\ \lambda_2 &= (\Sigma + \Delta C_{2\omega})/2 ,\end{aligned} \tag{2.74}$$

while the mixing angle is

$$\begin{aligned}\sin 2\varphi_m = (m_3^2 - \Lambda/2) S_{2\varphi} / \{[A - C_{2\varphi}(m_3^2 - \Lambda/2)]^2 \\ + [(m_3^2 - \Lambda/2) S_{2\varphi}]^2\}^{1/2} .\end{aligned} \tag{2.75}$$

Thus the mass eigenstates are now related to the flavor states by

$$\nu_\alpha = W_{\alpha j} \nu_j^m , \quad j = -, 2, + \tag{2.76}$$

with

$$W = \exp(i\psi\lambda_7)\Gamma \exp(i\varphi_m \lambda_5) . \tag{2.77}$$

The angle φ_m goes through the resonance at

$$A = C_{2\varphi}(m_3^2 - \Lambda/2) . \tag{2.78}$$

Corrections to the solutions for Eqs. (2.68)–(2.72) and (2.74)–(2.76) can be obtained easily by using perturbation theory; this is discussed in Kuo and Pantaleone (1987a). The corrections vanish when the mass scales separate and the mixing angle between ν_e and the nonresonant neutrino vanishes.

The above analysis shows that, for many natural choices of masses and mixing angles, three-neutrino oscillations in matter separate into two resonances, each resembling a two-flavor resonance. The resonances occur when the induced mass of the electron neutrino, A, becomes degenerate with a heavier mass state. Then a small vacuum mixing between the electron neutrino and the heavier mass eigenstate can become very important. This is true for more than three flavors, and the approximate analysis can easily be generalized. For three neutrinos, with small vacuum mixing, the resonances are an e-2 (or, approximately, e-μ) resonance when $A \approx m_2^2$ and an e-3 (or, approximately, e-τ) resonance when $A \approx m_3^2$. We shall refer to these as the lower (l) and higher (h) resonances, respectively.

This approximate formalism assumes that there are two separate resonances and calculates the masses and mixing angles in matter near each resonance as a function of A. The validity of this assumption depends on the vacuum mass and mixing angles, since they determine the location and width of the resonances. The matter effects enter only through A; so the resonances are well separated when

$$A^l + \delta A^l < A^h - \delta A^h , \tag{2.79}$$

where $A^{l(h)}$ is the value of A at the lower (higher) resonance and $\delta A^{l(h)}$ is the width of that resonance. These quantities can be found from the approximate equations near each resonance,

$$\begin{aligned}A^l &= \Delta C_{2\omega}/C_{\varphi}^2 , \quad \delta A^l = \Delta S_{2\omega}/C_{\varphi}^2 , \\ A^h &= (m_3^2 - \Lambda/2) C_{2\varphi} , \quad \delta A^h = (m_3^2 - \Lambda/2) S_{2\varphi} .\end{aligned} \tag{2.80}$$

For small angles, Eq. (2.79) takes the form

$$\frac{m_2^2 - m_1^2}{m_3^2 - m_1^2} < 1 + O(\theta, \varphi) . \tag{2.81}$$

For $m_3^2 \gg m_2^2 \gg m_1^2$, Eq. (2.79) takes the form

$$\varphi < \frac{\pi}{8} + O\left[\frac{m_2^2}{m_3^2}, \frac{m_1^2}{m_3^2}\right] ; \tag{2.82}$$

φ is the angle associated with the e-3 mixing. Equation (2.82) depends on our definition of the width of the resonance but, to leading order, Eqs. (2.81)–(2.82) are both independent of the small parameters. The two equations are similar in that once we have small mass ratios or small mixing angles, the constraint on the other parameters is rather weak.

The approximate equations are easy to use. For two well-separated resonances we combine the leading-order expressions from each resonance to get a general formula. The mixing matrix that relates the mass and flavor eigenstates can be obtained by combining Eqs. (2.71) and (2.77) to get

$$U^m \approx \exp(i\psi\lambda_7)\Gamma \exp(i\varphi_m \lambda_5) \exp(i\omega_m \lambda_2) ; \tag{2.83}$$

ω_m and φ_m are the mixing angles in matter given by Eqs. (2.69) and (2.75), respectively. Away from the resonances ω_m, φ_m and U^m take on simple asymptotic values (see Table IV). These and other results are easy to read from the simple, approximate formalism.

3. Medium with varying density

The solutions presented in the previous section give the mass eigenstates in matter for a particular fixed A. For neutrinos propagating through matter with changing density, A depends on x, and the neutrino propagation equation (2.65) is difficult to solve. If we denote the eigenvalues of the mass matrix M^2 by Λ_1, Λ_2, and Λ_3, then, in complete analogy with Eq (2.41), we have

TABLE IV. Elements of the mixing matrix in matter as a function of $A = 2\sqrt{2} G_F N_e E$. A^h (A^l) is the value of A at the e-τ (e-μ) resonance.

Matrix elements in matter	$A \to 0$	$A^l \ll A \ll A^h$	$A \to \infty$
$\lvert U_{e1}^m \rvert^2$	$\lvert U_{e1} \rvert^2$	0	0
$\lvert U_{e2}^m \rvert^2$	$\lvert U_{e2} \rvert^2$	$\lvert U_{e1} \rvert^2 + \lvert U_{e2} \rvert^2$	0
$\lvert U_{e3}^m \rvert^2$	$\lvert U_{e3} \rvert^2$	$\lvert U_{e3} \rvert^2$	1

$$i\frac{d}{dx}\begin{bmatrix}\nu_1\\ \nu_2\\ \nu_3\end{bmatrix}=\left[\frac{1}{2E}\begin{bmatrix}\Lambda_1 & 0 & 0\\ 0 & \Lambda_2 & 0\\ 0 & 0 & \Lambda_3\end{bmatrix}-(U^m)^\dagger i\frac{d}{dx}U^m\right]\begin{bmatrix}\nu_1\\ \nu_2\\ \nu_3\end{bmatrix} \tag{2.84}$$

$$=\begin{bmatrix}\Lambda_1/2E & -i(d\omega_m/dx) & -i\cos\omega_m(d\varphi_m/dx)\\ i(d\omega_m/dx) & \Lambda_2/2E & i\sin\omega_m(d\varphi_m/dx)\\ i\cos\omega_m(d\varphi_m/dx) & -i\sin\omega_m(d\varphi_m/dx) & \Lambda_3/2E\end{bmatrix}\begin{bmatrix}\nu_1\\ \nu_2\\ \nu_3\end{bmatrix}. \tag{2.85}$$

Thus, as in the case of the two-flavor problem, the adiabatic approximation consists in completely ignoring the term $(U^m)^\dagger(dU^m/dx)$.

The adiabatic approximation receives corrections near the resonances. At the lower resonance, $(d\omega_m/dx)$ is sharply peaked; crossing may occur between levels 1 and 2. At the upper resonance, $\omega_m\approx\pi/2$ and $(d\varphi_m/dx)$ is sharply peaked; so any crossing occurs between levels 2 and 3. For the average probability $P(\nu_e\to\nu_e)$ in a medium with a monotonically decreasing density, we may again use the arguments leading to Eq. (2.51). Figure 5 shows that the probabilities for the state at production positions A, B, and C to be ν_e's are $|U_{e3}^m|^2$, $|U_{e2}^m|^2$, and $|U_{e1}^m|^2$, respectively. Similarly, at detection positions A', B', and C', the probabilities of these states to be ν_e's are given by the vacuum values $|U_{e3}|^2$, $|U_{e2}|^2$, and $|U_{e1}|^2$. The propagation of the states will be along the mass eigenvalue curves, except near the crossing points. If we denote by P_c^h and P_c^l the crossing probabilities at the higher and lower resonances, respectively, then, for instance, the probability of state A going to B' is $P_c^h(1-P_c^l)$. Following the propagations of each of the states, we obtain

$$P(\nu_e\to\nu_e)=[|U_{e1}|^2|U_{e2}|^2|U_{e3}|^2]X^lX^h\begin{bmatrix}|U_{e1}^m|^2\\ |U_{e2}^m|^2\\ |U_{e3}^m|^2\end{bmatrix},$$

$$X^l=\begin{bmatrix}1-\bar{P}_c^{\,l} & \bar{P}_c^{\,l} & 0\\ \bar{P}_c^{\,l} & 1-\bar{P}_c^{\,l} & 0\\ 0 & 0 & 1\end{bmatrix}, \tag{2.86}$$

$$X^h=\begin{bmatrix}1 & 0 & 0\\ 0 & 1-\bar{P}_c^{\,h} & \bar{P}_c^{\,h}\\ 0 & \bar{P}_c^{\,h} & 1-\bar{P}_c^{\,h}\end{bmatrix},$$

where $\bar{P}_c^{\,l}=\Theta(AC_\varphi^2-\Delta C_{2\omega})P_c^l$ and $\bar{P}_c^{\,h}=\Theta[A-(m_3^2-\Lambda/2)C_{2\varphi}]P_c^h$, analogous to the two-flavor expression in Eq (2.60).

The quantities in the above formula can easily be extracted from the expressions in Sec. II.D.2. An approximate expression for the mixing matrix in matter has already been given in Eq. (2.69) with (2.75) and (2.83). From these latter two equations come definitions of the energy scales E_A^l and E_A^h for the lower and higher adiabatic threshold energies

$$E_A^l=\frac{\Delta C_{2\omega}/C_\varphi^2}{2\sqrt{2}G_FN_e|_P},\qquad E_A^h=\frac{(m_3^2-\Lambda/2)C_{2\varphi}}{2\sqrt{2}G_FN_e|_P}, \tag{2.87}$$

analogous to the two-flavor definitions in Eq. (2.61). The superscript l (h) denotes the lower e-μ (higher, e-τ) resonance. These are the energy scales where each of the two resonances occurs at the neutrino production position.

Expressions for the crossing probabilities P_c^h and P_c^l also follow from analogy with the two-flavor derivation. An adiabaticity parameter can be defined at each resonance from Eq. (2.85). Evaluating them at their respective resonances gives

$$\frac{\pi}{2}\gamma^l\equiv\frac{E_{\rm NA}^l}{E},\qquad E_{\rm NA}^l\equiv\frac{\pi}{4}\frac{\Delta}{|dN_e/N_edx|_0}\frac{S_{2\omega}^2}{C_{2\omega}},$$
$$\frac{\pi}{2}\gamma^h\equiv\frac{E_{\rm NA}^h}{E},\qquad E_{\rm NA}^h\equiv\frac{\pi}{4}\frac{(m_3^2-\Lambda/2)}{|dN_e/N_edx|_0}\frac{S_{2\varphi}^2}{C_{2\varphi}}. \tag{2.88}$$

The masses and mixing angles are as defined in Sec. II.D.2. These nonadiabatic parameters can be used with either the LZ expression for the crossing probability, Eq. (2.52), or the ansatz density equation (2.58). If the latter equation is used for the crossing probabilities, then the vacuum mixing angle that occurs in the exponents of Eq. (2.58), outside the adiabaticity parameter, is given by the corresponding three-flavor vacuum angle. For the lower (upper) resonance the mixing angle ω (φ) is used. With this natural prescription the survival probability $P(\nu_e\to\nu_e)$ goes to the vacuum oscillation probability in the extreme nonadiabatic limits.

The survival probability given in Eq. (2.86) is plotted for solar neutrinos in Fig. 6 for a typical choice of the neutrino parameters. Comparing with the corresponding probability function for two flavors, as in Fig. 4, we see that they are different. For three neutrino species, conversion of one flavor to another (the MSW effect) occurs over two different energy ranges,

$$E_A^l<E<E_{\rm NA}^l,\quad E_A^h<E<E_{\rm NA}^h, \tag{2.89}$$

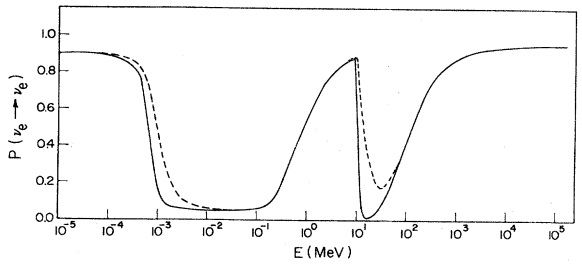

FIG. 6. Probability of a ν_e, produced in the sun, reaching the Earth as a function of energy, Eqs. (2.54) and (2.86). Here we take three flavors and $m_3=1.2\times10^{-2}$ eV, $m_2=1\times10^{-4}$ eV, $m_1=0$, $|U_{e2}|^2=5\times10^{-2}$, and $|U_{e3}|^2=5\times10^{-4}$. The solid line is for a neutrino produced at the center of the sun; the dashed line is for neutrinos produced with the p-p distribution predicted by the standard solar model.

one for each resonance. The flat minima of $P(\nu_e\to\nu_e)$ in these two regions correspond to adiabatic propagation through the higher and lower resonances, respectively. Substituting in Eq. (2.86) the values of φ and ω inferred from Table IV, we find

$$\begin{aligned} &P(\nu_e\to\nu_e)\to|U_{e3}|^2, \quad E_A^h<E\ll E_{\rm NA}^h , \\ &P(\nu_e\to\nu_e)\to|U_{e2}|^2(|U_{e1}|^2+|U_{e2}|^2)+|U_{e3}|^4 , \\ &\qquad\qquad E_A^l<E\ll E_{\rm NA}^l . \end{aligned} \tag{2.90}$$

This should be compared to the case of two-flavor oscillations, for which $P(\nu_e\to\nu_e)\to\sin^2\theta$, according to Eq. (2.64).

Outside the regions defined by Eq. (2.89), the survival probability approaches the vacuum oscillation equation

$$\begin{aligned} P(\nu_e\to\nu_e)&=\sum_1|U_{ei}|^4 \\ &=1-2(|U_{e2}|^2+|U_{e3}|^2-|U_{e2}|^4 \\ &\quad -|U_{e2}|^2|U_{e3}|^2-|U_{e3}|^4) . \end{aligned} \tag{2.91}$$

It should be noted that, in the limit of small mixing angles, Eq. (2.86) can be shown to reduce to the intuitive result [Kuo and Pantaleone, 1987a, Eq. (3.35); Mikheyev and Smirnov, 1988]

$$P(\nu_e\to\nu_e)=P^h(\nu_e\to\nu_e)P^l(\nu_e\to\nu_e)+O(|U_{ei}|^2) . \tag{2.92}$$

4. Three flavors versus two flavors

Comparing the two-flavor and three-flavor electron-neutrino survival probabilities, we see that they appear quite different. However, for the realistic situation in which the experimental information on the neutrino flux is quite limited, it is often sufficient to represent the survival probability by the slightly simpler two-flavor description. We shall describe the conditions under which this is appropriate.

A simplification in the description of neutrino oscillations occurs for neutrinos from astrophysical sources like the sun or a supernova. The emitted neutrinos are typically of low energy—tens of MeV or less. A neutrino with energies less than 106 MeV has insufficient energy to produce a muon in a collision with a proton or neutron, so that it is impossible to differentiate between a ν_μ or ν_τ. The measured neutrino flux can then only be discriminated into the electron and the sum of the nonelectron neutrino fluxes. Furthermore, because astrophysical sources of neutrinos are at low energies, any μ or τ neutrino flavors are produced equally via the neutral current. Using these two observations we can simplify the expressions for the effect of neutrino oscillations on the astrophysical neutrino fluxes. The neutrino flux of species α at the Earth, F_α, can be expressed in terms of the initially produced neutrino flux of species β, F_β^0, as

$$F_\alpha=\sum_\beta P(\nu_\beta\to\nu_\alpha)F_\beta^0 , \tag{2.93}$$

where $P(\nu_\beta\to\nu_\alpha)$ is the probability that if species β is produced in the astrophysical object, then species α is observed on the Earth. Both the P's and F^0's are, in principle, functions of time and energy, and the P's include matter and vacuum oscillation effects. However, all the P's for neutrino oscillations are constrained by the unitarity conditions given by Eqs. (2.14)–(2.18). When we combine these constraints with the two observations that followed from the neutral-current interaction of neutrinos, that $F_\mu^0=F_\tau^0\equiv F_x^0$ and that the only detectable flux is $F_\mu+F_\tau$, we get

$$\begin{aligned} &F_e=F_e^0-[1-P(\nu_e\to\nu_e)](F_e^0-F_x^0) , \\ &F_\mu+F_\nu=2F_x^0+[1-P(\nu_e\to\nu_e)](F_e^0-F_x^0) . \end{aligned} \tag{2.94}$$

We see that the only relevant oscillation probability for solar or supernova neutrinos is $P(\nu_e\to\nu_e)$, even for three neutrino flavors.

The above argument is equally valid for antineutrinos, and the relations between the produced and the detected fluxes are identical to the above expressions, with the neutrinos replaced everywhere by antineutrinos. For antineutrinos the only relevant probability is $P(\bar\nu_e\to\bar\nu_e)$. These two probabilities, $P(\nu_e\to\nu_e)$ and $P(\bar\nu_e\to\bar\nu_e)$, are thus the only quantities that must be specified to determine how neutrino oscillations mix the fluxes.

For experiments with a limited energy resolution, $P(\nu_e\to\nu_e)$ can sometimes be represented as an "effective" two-flavor expression. For instance, if an experiment only measures a constant $P(\nu_e\to\nu_e)$, this can easily be described by a constant region of a two-flavor probability formula like Eq. (2.51) with an appropriately chosen vacuum mixing parameter. Observing a change in $P(\nu_e\to\nu_e)$ with energy would allow the fixing of a mass scale in a two-flavor analysis and would possibly even show the effects of more than two flavors. At an energy threshold in $P(\nu_e\to\nu_e)$, there are deviations from

the two-flavor description that depend on the mixing between the electron neutrino and the nonresonant mass eigenstate.

For example, let us define R to be the ratio of $P(\nu_e \to \nu_e)$ inside the energy range of resonant conversion (the MSW probability) to $P(\nu_e \to \nu_e)$ outside that range (the vacuum oscillation probability). For two neutrino species, the ratio is, using Eqs. (2.64) and (2.11),

$$R_2 = \frac{\sin^2\theta}{1-\sin^2 2\theta/2} = \frac{\sin^2\theta}{1-2\sin^2\theta(1-\sin^2\theta)} . \quad (2.95)$$

However, for three flavors we have two different expressions, one for each resonance. For the higher resonance, $\sin^2\theta$ corresponds to $\sin^2\varphi = |U_{e3}|^2$ [see Eqs. (2.66) and (2.77)]; using Eqs. (2.90) and (2.91) results in a ratio having the form

$$R_3^h = \frac{|U_{e3}|^2}{1-2(|U_{e2}|^2+|U_{e3}|^2-|U_{e2}|^4-|U_{e3}|^4-|U_{e2}|^2|U_{e3}|^2)} ,$$
$$R_3^h \approx \frac{|U_{e3}|^2}{1-2|U_{e3}|^2(1-|U_{e3}|^2)}(1+2|U_{e2}|^2+\cdots) . \quad (2.96)$$

In the last expression we have expanded in terms of off-diagonal mixing matrix elements in order to write the expression as an effective two-flavor quantity times a correction term. For the lower resonance, $\sin^2\theta$ corresponds to $\sin^2\omega = |U_{e2}|^2/(1-|U_{e3}|^2)$ [see Eqs. (2.66) and (2.71)]; using Eqs. (2.90) and (2.91) results in a ratio of the form

$$R_3^l = \frac{|U_{e2}|^2(1-|U_{e3}|^2)+|U_{e3}|^4}{1-2(|U_{e2}|^2+|U_{e3}|^2-|U_{e2}|^4-|U_{e3}|^4-|U_{e2}|^2|U_{e3}|^2)} ,$$
$$R_3^l \approx \frac{|U_{e2}|^2/(1-|U_{e3}|^2)}{1-2[|U_{e2}|^2/(1-|U_{e3}|^2)][1-|U_{e2}|^2/(1-|U_{e3}|^2)]}\left[1+\frac{|U_{e3}|^4}{|U_{e2}|^2}+\cdots\right] . \quad (2.97)$$

For both resonances, the correction term vanishes when the mixing matrix element between the electron neutrino and the nonresonant neutrino vanishes. Thus a careful measurement of a single energy threshold could show the effects of three flavors if the electron neutrino coupling to the nonresonant neutrino is large.

A straightforward way to see the effects of three flavors would be to observe two resonant energy regions for neutrino conversion. For instance, if one observed a $P(\nu_e \to \nu_e)$ that was peaked at some energy, that would require a description in terms of more than two flavors. Such a case is shown in Fig. 6. For typical neutrino parameters, the two energy ranges where flavor conversion occurs may be very close to each other, even overlapping. The assumption of a hierarchy of masses does not imply a relation between $E^l_{\rm NA}$ and E^h_A. These two energy scales depend on different properties of the medium: the former on the rate of density change and the latter on the maximum density. If parts of both of these flavor conversion energy ranges lie in the range of experimental sensitivity, then it will not be possible to reproduce three-flavor oscillations by an equivalent two-flavor oscillation.

III. APPLICATIONS

A. The sun

The standard solar model goes back 50 years to Bethe's (1939) detailed formulation of the nuclear reaction cycles involved in the stellar transformation of hydrogen into helium. These cycles still form the basis for the present solar model, which quantitatively describes all aspects of the sun: radius, luminosity, temperature, density distributions, etc. There are, however, few significant tests of the model. Most solar observations are sensitive only to surface conditions—it takes millions of years for a photon to diffuse from the core of the sun to the surface. To test the solar core, where the nuclear reactions occur, one must measure the flux of particles produced in the core that do not diffuse out of the sun but instead pass through the sun without scattering—neutrinos. The neutrino spectrum given by the standard solar model is shown in Fig. 7 and Table V. For a recent review of the standard solar model see Bahcall and Ulrich (1988).

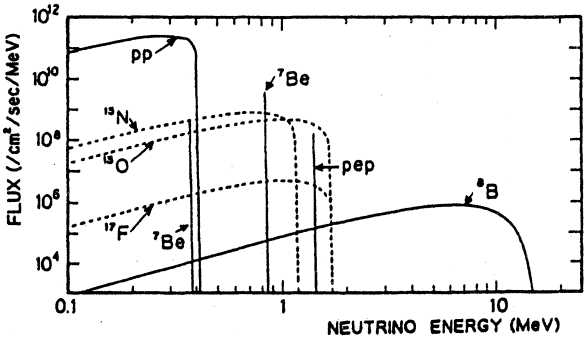

FIG. 7. Solar neutrino spectra predicted by the standard solar model (Bahcall and Ulrich, 1988). The neutrino fluxes from continuum sources are given in units of number per cm^2 per second per MeV, and the line fluxes are given in number per cm^2 per second, both at a distance of 1 AU.

TABLE V. Solar neutrino reactions, fluxes, and 3σ uncertainties (Bahcall and Ulrich, 1988).

Solar reaction	$E_{\nu,\max}$ (MeV)	Flux (10^{10} cm^{-2}s^{-1})	^{37}Cl (SNU)
$p+p\rightarrow{}^2\mathrm{H}+e^++\nu$	0.420	$6.0(1\pm0.02)$	0.0
${}^8\mathrm{B}\rightarrow{}^8\mathrm{Be}^*+e^++\nu$	14.02	$5.8\times10^{-4}(1\pm0.37)$	6.1
${}^{13}\mathrm{N}\rightarrow{}^{13}\mathrm{C}+e^++\nu$	1.199	$6.1\times10^{-2}(1\pm0.50)$	0.1
${}^{15}\mathrm{O}\rightarrow{}^{15}\mathrm{N}+e^++\nu$	1.732	$5.2\times10^{-2}(1\pm0.58)$	0.3
$p+e^-+p\rightarrow{}^2\mathrm{H}+\nu$	1.442	$1.4\times10^{-2}(1\pm0.05)$	0.2
${}^7\mathrm{Be}+e^-\rightarrow{}^7\mathrm{Li}+\nu$	0.862 89.6% 0.384 10.4%	$4.7\times10^{-1}(1\pm0.15)$	1.1
Total		$6.6(1\pm0.02)$	$7.9(1\pm0.33)$

This was the central motivation behind the ^{37}Cl solar neutrino experiment, which began operation in 1967 (Davis *et al.*, 1968). In this experiment, electron neutrinos are captured by the ^{37}Cl atoms in a tank filled with perchloroethylene (C_2Cl_4), and ^{37}Ar is produced at a rate of about one atom every three days. About once a month the ^{37}Ar atoms are extracted from the tank and "counted" by observing their decay. However, for the past 20 years (Davis, 1988) this experiment has yielded a result that is 2.1 ± 0.3 SNU (solar neutrino units, 1 SNU$=10^{-36}$/(target atom) sec, which averages about $\frac{1}{4}$ of the expected capture rate given in Table V. This is the so-called solar neutrino problem.

Neutrino mixing can easily explain the solar neutrino problem. The neutrinos produced by the sun are all one flavor, ν_e. The ^{37}Cl experiment is only sensitive to one flavor, ν_e. Neutrino mixing will cause the ν_e to leak into other flavors that cannot be detected by the experiment; hence the measured flux will be less than the total neutrino flux. Considering only vacuum effects, the amount of mixing with other flavors is expected to be small, since the analogous hadronic mixings are small (Sec. I.B). However, Mikheyev and Smirnov (1986a) first suggested that matter effects, which can enhance neutrino mixing and also give resonant conversion between neutrino flavors, provide a natural solution to the solar neutrino problem. The solar neutrinos that are observed on Earth come from near the center of the sun. The solar density falls off smoothly from the center (approximately as an exponential); so the probability for a ν_e produced in the sun to reach the Earth, $P(\nu_e\rightarrow\nu_e)$, has large energy ranges where resonant conversion of neutrino flavor can occur, as described in Sec. II.

1. Calculating the solar neutrino capture rate

With neutrino mixing, the capture rate observed in a terrestrial neutrino absorption experiment, like the ^{37}Cl experiment, is given by

$$\text{capture rate}=\sum_i\int_0^\infty dE_\nu\langle P(E)\rangle\sigma(E)\varphi_i(E)\ ; \tag{3.1}$$

$\sigma(E)$ is the cross section for neutrino capture and $\varphi_i(E)$ the neutrino flux spectrum (Fig. 7). $\langle P(E)\rangle$ is the neutrino conversion probability averaged over the distribution of neutrino production in the sun, $\Phi_i(\mathbf{x})$,

$$\langle P(E)\rangle=\int d^3x\ P(\nu_e\rightarrow\nu_e)(E,\mathbf{x})\Phi_i(\mathbf{x})\ . \tag{3.2}$$

The phase-averaged probabilities derived in Sec. II are quite appropriate for describing $P(\nu_e\rightarrow\nu_e)$ through the sun. This is because there are typically many oscillations between neutrino production and a resonance, and again between the resonance and detection. Hence the phase information from before and after resonance is easily lost [as assumed for Eq. (2.51)]. In particular, propagation after a neutrino resonance in the sun is always many oscillation wavelengths because the Earth-sun distance is many times the solar radius; the solar radius is roughly the maximum-size neutrino vacuum wavelength for which resonant conversion in the sun can occur. This observation is important for adiabatic resonant transitions. For those cases there is no level crossing, so the phase associated with the production-to-resonance propagation is added directly to the phase associated with resonance to detection. This total phase is always large, because of the large sun-Earth separation, and hence unobservable. The only time any phases might be observable is for propagation between the production and a nonadiabatic resonance. This does not occur frequently, since the neutrino wavelength at the solar core is about $10^{-3}R_{\text{solar}}\times[(100\ \text{g/cm}^3)/\rho]$, much less than typical solar scales. The rare case in which the production point is not many oscillations from a nonadiabatic resonance point is discussed explicitly in Sec. II.C.5.

To use the phase-averaged probability for $P(\nu_e\rightarrow\nu_e)$, Eq. (2.60), to describe neutrino propagation through the sun, a crossing probability must be specified. For $0.75>x=R/R_{\text{solar}}>0.25$, the electron-density distribution in the sun is given approximately by (Bahcall and Ulrich, 1988)

$$\log(n_e/N_A)=2.32-4.17x-0.000\,125/[x^2+(0.5)^2]\ , \tag{3.3}$$

where N_A is Avogadro's number per cm^3 and the logarithm is base 10. The last term is quite small; so the density decrease is approximately exponential, and Eq. (2.58) is the appropriate choice for the crossing probability P_c.

The averaging over the production position, Eq. (3.2), produces relatively minor changes in the survival probability. This is because neutrino production occurs dominantly in a small region at the center of the sun. The standard solar model (Bahcall and Ulrich, 1988), gives the distance scales for neutrino production, $\Phi_i(\mathbf{x})$, ranging from about $0.05R_{\text{solar}}$ for ^{8}B neutrinos to $0.1R_{\text{solar}}$ for *pp* neutrinos. Referring to Eq. (2.60) for the probability, we see that $P(\nu_e \rightarrow \nu_e)$ depends on $\mathbf{x}$, the production position, in two different ways. The mixing angle at the production point depends on the density there and hence on position through $\rho(r)$. The theta function in Eq. (2.60) also depends on the production position. Furthermore, Eqs. (2.51) and (2.60) are modified if a neutrino is produced on the far side of the sun and travels inward through two resonances before emerging from the production zone. Then the matrix representing the level-crossing probability is effectively doubled,

$$\begin{bmatrix} (1-P_c) & P_c \\ P_c & (1-P_c) \end{bmatrix} \begin{bmatrix} (1-P_c) & P_c \\ P_c & (1-P_c) \end{bmatrix} = \begin{bmatrix} [1-2P_c(1-P_c)] & 2P_c(1-P_c) \\ 2P_c(1-P_c) & [1-2P_c(1-P_c)] \end{bmatrix} . \quad (3.4)$$

The net effect on the equation for $P(\nu_e \rightarrow \nu_e)$ is to replace P_c, the probability of level crossing at the resonance, by $2P_c(1-P_c)$. The results of averaging over the production region can be seen from Fig. 6, where they have been plotted on the same graph as the case $\Phi_i(\mathbf{x})=\delta^3(\mathbf{x})$. The adiabatic threshold is modified slightly, since the resonance then occurs near the production position. The largest finite production size effects occur for the *pp* spectrum.

The cross sections for neutrino absorption as a function of energy, $\sigma(E)$, are difficult to determine accurately. They are evaluated by a combination of nuclear model calculations and laboratory-measured transition rates. Extensive laboratory measurement of the relevant nuclear transition rates have been performed for the ^{37}Cl experiment's cross section. This cross section has been checked by exposing the ^{37}Cl detector to a radioactive source. However, the cross sections for most of the other proposed neutrino detectors are much more uncertain. For example, the absorption cross section for the geochemical ^{98}Mo experiment, which may soon yield results (Cowan and Haxton, 1982; Wolfsberg *et al.*, 1985), is uncertain by about a factor of 2. The estimated event rates and their uncertainties for many experiments are shown in Table VI. The energy dependence of the absorption cross sections for the present and for many of the proposed solar neutrino experiments can be found in Bahcall and Ulrich's (1988) Table IX [see also Mathews *et al.* (1985), Grotz *et al.* (1986), and Parke and Walker (1986)].

Neutrino-electron scattering experiments, such as Kamiokande II, are different from neutrino absorption experiments. They have the advantages of detecting neutrinos with some information on their time, direction, and energy. The electron energy spectrum of $\nu e \rightarrow \nu e$ elastic scattering is given by

$$\sum_i \int_{E_{\nu,\min}}^{\infty} dE_\nu \varphi_i(E) \left[\langle P(E) \rangle \frac{d\sigma(\nu_e e)}{dE_e} + [1-\langle P(E) \rangle] \frac{d\sigma(\nu_n e)}{dE_e} \right] , \quad (3.5)$$

where $d\sigma/dE_e$ is the differential cross section of ν-e scattering, and E_e is the electron kinetic energy. This differential cross section is easily calculated from the standard weak-interaction model given in Eqs. (2.1)–(2.3) and is free of the nuclear model uncertainties associated with the absorption cross sections.

$$\frac{d\sigma}{dE_e} = \frac{\sigma_0}{m_e} \left[g_L^2 + g_R^2 \left[1 - \frac{E_e}{E_\nu} \right]^2 - g_L g_R \left[\frac{m_e E_e}{E_\nu^2} \right] \right] ,$$

$$\sigma_0 = 88 \times 10^{-46} \text{ cm}^2 , \quad (3.6)$$

$$g_L = (\pm \tfrac{1}{2} + \sin^2\theta_W), \quad g_R = \sin^2\theta_W .$$

The upper sign applies to ν_e-e scattering, the lower sign

TABLE VI. Properties of proposed solar neutrino experiments. E_{thr} is the threshold energy.

Experiment	Type	Event rate (SNU)	E_{thr} (MeV)	Main source
^{37}Cl(ν,e)^{37}Ar	radiochemical	7.9±2.6	0.814	^{8}B
^{71}Ga(ν,e)^{71}Ge	radiochemical	132±20	0.236	*pp*, ^{7}Be
^{81}Br(ν,e)^{81}Kr	radiochemical	27.8±17	0.459	^{7}Be, ^{8}B
^{98}Mo(ν,e)^{98}Tc	geochemical	17.4±18	1.74	^{8}B
^{205}Tl(ν,e)^{205}Pb	geochemical	263	0.043	*pp*
^{115}In(ν,e)^{115}Sn	direct counting	639^{+639}_{-320}	0.12	*pp*, ^{7}Be
^{2}H(ν,e)*pp*	direct counting	6.0±2.1	1.44	^{8}B
			(6.44)[a]	
^{2}H(ν,ν)*np*	direct counting	3.0	2.2	^{8}B
^{40}Ar(ν,e)^{40}K*	direct counting	1.7±0.6	5.885	^{8}B
ν-e scattering	direct counting	0.35[b]		^{8}B

[a]Assumed threshold for calculation of event rate.
[b]This value is only from ^{8}B neutrinos.

to ν_n-e scattering (here ν_n represents either the μ or τ neutrino); for $\bar{\nu}$-e scattering, g_L and g_R are interchanged. The cross section for ν_n-e scattering is approximately $\frac{1}{6}-\frac{1}{7}$ smaller than that of ν_e-e scattering. Thus neutrino-electron scattering experiments are primarily sensitive to electron neutrinos, as is the ^{37}Cl experiment. In fact, the electron recoil spectra for ν_n-e scattering is so similar to that of ν_e-e scattering that the two are indistinguishable in a solar neutrino experiment (Bahcall, 1987; Bahcall *et al.*, 1987). A ν_n flux from the sun cannot be distinguished from a small ν_e flux by neutrino-electron scattering.

The spectra for the neutrino fluxes from the sun are shown in Fig. 7. The solar reactions that produce the neutrinos are shown in Table V along with the maximum energy of the reaction. The electron-absorbing reactions produce neutrinos with discrete energies. The spectra for a positron-emitting reaction is

$$\varphi(E_\nu)\propto E_\nu^2 w_e(w_e^2-1)^{1/2}F(-Z_{\text{emitter}},w_e)\ . \tag{3.7}$$

Here $w_e\equiv[1+(E_{\nu,\max}-E_\nu)/m_e]$ is the positron energy; F is the Fermi function (Bahcall, 1978; Bahcall *et al.*, 1982), usually only a small correction. For the neutrinos from the ^{8}B reaction there is an additional correction due to the broad character of the ^{8}Be state (Bahcall and Holstein, 1986).

2. Iso-SNU contour plots

It is fashionable to evaluate Eq. (3.1) numerically and to make a contour plot of the result. The plots usually assume two neutrino flavors and show the percent reduction in the capture rate, as a function of neutrino parameters, $m_2^2-m_1^2$ vs $\sin^2 2\theta$. In order to "understand" such plots, we shall derive approximate analytic expressions for the contours that solve the solar neutrino problem, the neutrino parameters that reduce the ^{37}Cl capture rate by $\frac{1}{4}$. These approximations should give results accurate to about 10–20 %.

The ^{37}Cl detector is sensitive to neutrino energies in the range

$$E_{\min}=0.81<E<14\ \text{MeV}=E_{\max}\ . \tag{3.8}$$

Introducing $x=E/E_{\max}$, $x_{\min}=E_{\min}/E_{\max}$, we have

$$x_{\min}<x<1\ . \tag{3.9}$$

The neutrino flux of a continuous spectrum is given approximately by $x^2(1-x)^2$. The detection cross section for the ^{8}B neutrinos is given roughly by $\sigma\propto x^{2.8}$ for $x<0.5$, and by $\sigma\propto x^{3.5}$ for $x>0.5$. Neglecting finite production size effects, we see that the total capture rate is given by

$$I=\int_{x_{\min}}^{I} dx\ P(x)x^N(1-x)^2\ , \tag{3.10}$$

with $N=4.8$ or 5.5 for $x<0.5$ or $x>0.5$; $P(x)$ is given by Eq. (2.60) and for small angles takes the form

$$P(\nu_e\to\nu_e)\approx\Theta(E_A-E)+\Theta(E-E_A)\exp(-E_{\text{NA}}/E)\ , \tag{3.11}$$

where Θ is the theta function and E_A and E_{NA} are given by Eqs. (2.61) and (2.62). The first term describes the adiabatic threshold and the second term describes the nonadiabatic threshold.

For two flavors and small angles, we see from Eq. (3.11) that there are two solutions to the solar neutrino problem (Bethe, 1986; Mikheyev and Smirnov, 1986a; Rosen and Gelb, 1986). The first one corresponds to having the energy range ($E_{\min}<E<E_{\max}$) straddle the adiabatic transition region with $\exp(-E_{\text{NA}}/E)\ll 1$. Then all neutrinos with $E>E_A$ are converted. The rate from the ^{37}Cl experiment then determines one parameter, E_A. As was shown by Bethe (1986), one may use Table V and Eq. (3.10) to find

$$E_A\approx 6\ \text{MeV},\quad \Delta\approx 1.0\times10^{-4}\ \text{eV}^2\ . \tag{3.12}$$

We have used Eq. (2.61) and $N_e|_P=99\ \text{g/cm}^3$.

With two flavors there is a second solution (Mikheyev and Smirnov, 1985; Kolb *et al.*; 1986, Rosen and Gelb, 1986); when the energy range ($E_{\min}<E<E_{\max}$) overlaps the nonadiabatic region near E_{NA}, so that $P(x)\approx\exp(-x_{\text{NA}}/x)$, $x_{\text{NA}}=E_{\text{NA}}/E_{\max}$. Here it is mainly the neutrinos of lower energy that are converted. For the ^{37}Cl experiment, this means that the detected neutrinos almost all come from the ^{8}B source. Since the ^{8}B contributes 6.1 SNU, the experimental result of 2.1 SNU is obtained by demanding that

$$\frac{\int_{x_{\min}}^{1} dx\ x^N(1-x)^2\exp(-x_{\text{NA}}/x)}{\int_{x_{\min}}^{1} dx\ x^N(1-x)^2}\approx\exp(-x_{\text{NA}}/x_M)=\frac{2.1}{6.1}\ . \tag{3.13}$$

Here we have used the fact that the function $x^N(1-x)^2$ is sharply peaked at $x_M=N/(N+2)$. Taking $N\approx 5.5$, we find that $x_{\text{NA}}\approx 0.5$ or, using Eq. (2.62) and $(dN/N\,dr)_0=3\times10^{-15}$ eV,

$$E_{\text{NA}}\approx 10\ \text{MeV}\ ,\qquad \Delta\sin^2 2\theta\approx 4\times10^{-8}\ \text{eV}^2\ . \tag{3.14}$$

These values agree with the numerical calculations.

We have thus seen that each of the above small-angle solutions determines only one parameter—E_A in the adiabatic solution and E_{NA} in the nonadiabatic solution. For large angles, there is a third solution. This corresponds to having $E_A<E_{\min}<E<E_{\max}\ll E_{\text{NA}}$. Here $P_c\to 0$, $P(\nu_e\to\nu_e)\approx\sin^2\theta$ [see Eq. (2.64)]. Thus, for the ^{37}Cl experiment, one has $\sin^2\theta\approx\frac{1}{4}$, and neutrinos of all energies are depleted equally.

These three solutions are obtained by analytic methods and are useful in understanding the problem and the numerical calculations. Similar analyses can be carried out for the other experiments. However, for experiments

with thresholds much lower than the ^{37}Cl experiment, the neutrino spectra become complex and the results of analytic analyses are not very accurate. The above analysis can also be extended to the more general problem with three neutrino flavors (Kuo and Pantaleone, 1987a).

Figure 8 shows contour plots for the ^{37}Cl and ^{71}Ga experiments, assuming only two neutrino species. The contours approximately form triangles with each side of the triangle corresponding to one of the approximate analytic solutions derived above: the upper contour corresponds to the adiabatic solution, the lower left contour corresponds to the nonadiabatic solution, and the right-hand contour corresponds to the large-angle solution. Where two different types of solutions intersect, there are often extra corrections that must be taken into account. The corner of the triangle where the nonadiabatic and large-angle solutions intersect is the parameter region where the corrections to P_c given in Table III and Eq. (2.58) are important. The corner of the triangle where the adiabatic and nonadiabatic solutions intersect is the parameter region where the phase effects discussed in Sec. II.C.5 are important.

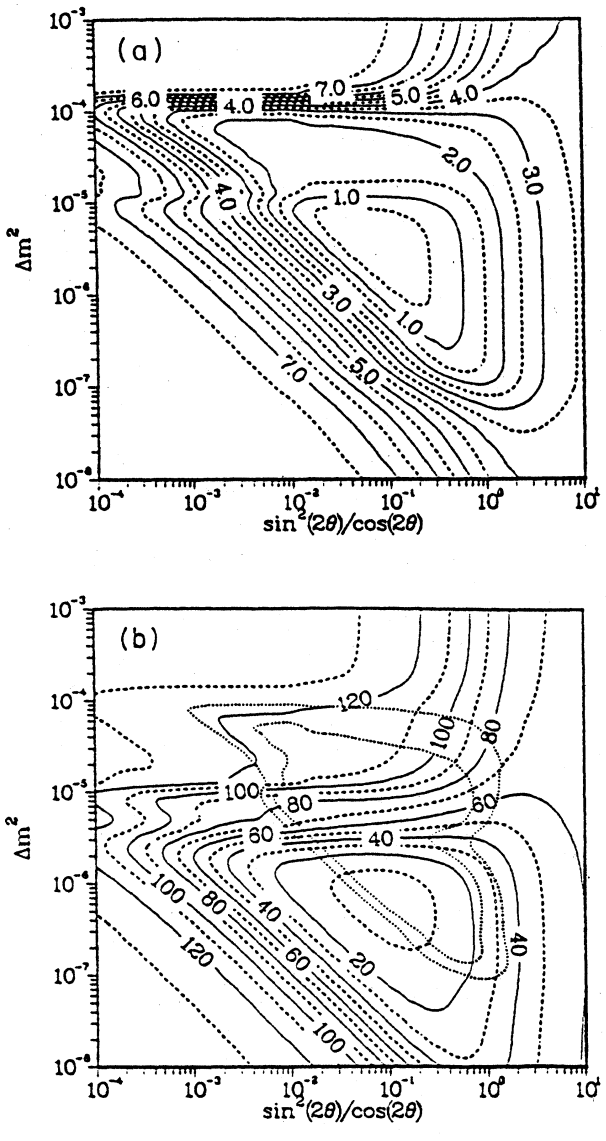

FIG. 8. Iso-SNU contours for the (a) ^{37}Cl, and (b) ^{71}Ga experiments (Baltz and Weneser, 1988b). It is assumed that there are only two flavors.

Comparing different contour plots, we see that the ^{71}Ga contours are shifted down with respect to the ^{37}Cl contours, because the ^{71}Ga experiment has a lower threshold and hence is sensitive to lower energy scales. A contour plot for the total reduction of a H_2O experiment would almost exactly overlap those of the ^{37}Cl experiment, because the two are sensitive to neutrinos in approximately the same energy range. For other contour plots see Bouchez *et al.* (1986), Mikheyev and Smirnov (1986a), Parke and Walker (1986), and Dar *et al.* (1987).

Figure 9 shows contour plots for the ^{37}Cl experiment, assuming three neutrino species. For three neutrino species, $P(\nu_e \rightarrow \nu_e)$ depends on four parameters—two mixing parameters and two mass parameters. In order to make a two-dimensional plot, there must be two constraints among these four parameters. We have chosen both the mixing angle and the masses to be hierarchical, in accordance with theoretical expectations as discussed in Sec. I.B. For other three-flavor plots, see Kuo and Pantaleone (1986, 1987a), Baldini and Giudice (1987), Kim *et al.* (1987a, 1987b), Kim and Sze (1987), and Zaglauer and Schwarzer (1987, 1988).

3. New experiments

One must be cautious in accepting the MSW effect as the solution to the solar neutrino problem. The predicted solar neutrino flux is based on the intricate standard solar model, which could be inaccurate. Since the ^{8}B neutrino flux is very sensitive to the solar core temperature, a slight modification of the solar model can lead to dramatic changes in the predicted flux. Thus more experiments are needed to test whether neutrino mixing, and in particular the MSW effect, is the correct solution to the solar neutrino problem. We shall describe the different ways that matter-enhanced mixing of solar neutrinos could be observed experimentally.

The most straightforward test of flavor mixing, be it matter enhanced or just vacuum, is to look for ν_μ or ν_τ neutrinos in the solar neutrino flux. This would be unmistakable evidence for neutrino mixing. In principle, neutrino scattering off electrons is sensitive to all flavors, and a comparison between the flux measured by this method and the flux measured by a method sensitive only to ν_e, like the ^{37}Cl experiment, could test for new neutrino flavors. However, the ν_e has an electron-scattering cross section that is 7 times that of ν_μ or ν_τ. Thus statistical and systematic errors render it extremely difficult to confirm the presence of new flavors in the solar neutrino flux via electron scattering. However, future, more sensi-

tive detectors like Super Kamiokande (32 ktons; see Suzuki, 1987), Icarus (3 ktons; see Bahcall *et al.*, 1986), or LVD (2.8 ktons; see Alberini *et al.*, 1986) may be able to accomplish this. Another process sensitive to all neutrino flavors is the excitation of nuclear energy levels via neutral-current neutrino scattering. This cross section is equal for all neutrino species. This method could be implemented on deuterium in the planned Sudbury Neutrino Observatory (1 kton; Chen, 1985; Aardsma *et al.*, 1987), and it has also been discussed for a detector based on ^{11}B (Raghavan *et al.*, 1986; Raghavan and Pakvasa, 1988). Failure to find new neutrino flavors when studying the same energy range in which there is an alleged depletion of the ν_e flux would kill the MSW explanation of the solar neutrino problem.

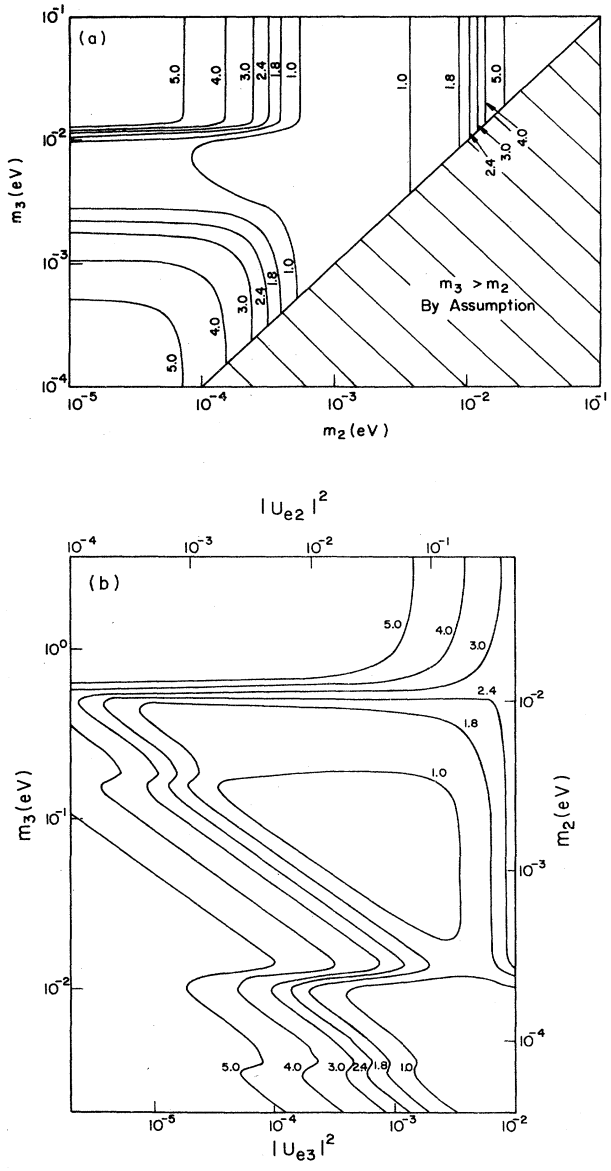

FIG. 9. Iso-SNU contours for the ^{37}Cl experiment (Kuo and Pantaleone, 1987a). Three flavors are assumed and typical constraints are taken on some of the parameters: (a) $|U_{e2}|^2=5\times10^{-2}$ and $|U_{e3}|^2=1\times10^{-3}$; (b) $(m_3/m_2)=(|U_{e2}|^2/|U_{e3}|^2)=50$.

Another way to test for flavor mixing in the solar neutrino flux is to observe solar neutrinos in a different energy range, one which is less sensitive to details of the standard solar model. This is the basis of ^{71}Ga radiochemical experiments, which are presently under construction [SAGE (60 tons), Barabanov *et al.*, 1985; GALLEX (30 tons), Kirsten, 1986]. These experiments are primarily sensitive to low-energy neutrinos, which come from the basic *pp* solar reaction. Most other experiments are sensitive to higher-energy neutrinos, which come from different solar reactions. If the ^{71}Ga experiments were to yield results different from the standard solar model predictions, it would indicate either neutrino flavor mixing or a radical departure from the standard solar model. However, if the ^{71}Ga experiments were to yield results consistent with the standard solar model, it would not eliminate the MSW solution of the solar neutrino problem, since resonant conversion is energy dependent. In particular, the ν_e flux would not be distorted in the energy range of the ^{71}Ga experiment if an adiabatic threshold occurred in the range of the ^{37}Cl experiment. Then lower-energy neutrinos like those detected by the ^{71}Ga experiment would be essentially unaffected. On the contour plots, this possibility corresponds to the top of contours of the ^{37}Cl "triangle" overlapping a region on the ^{71}Ga plot where there is very little reduction.

This indicates yet another way to test specifically for the MSW effect in solar neutrinos—by looking for unusual energy dependences in the solar neutrino flux. While the magnitudes of the fluxes predicted by the standard solar model are uncertain, the shapes of the energy distributions are very well known. Distortions in these energy distributions from the energy-dependent probability, $\varphi_i(E)\rightarrow\varphi_i(E)\langle P(E)\rangle$, would be unmistakable evidence for matter-enhanced mixing. The MSW effect can produce large energy thresholds in the electron-neutrino flux, which, in principle, are detectable. Unfortunately, this is experimentally difficult, since it requires very good energy resolution, which is typically sacrificed because of the low counting rate. Moreover, the MSW effect may solve the solar neutrino problem without a MSW energy threshold overlapping with the narrow range of energies to which a detector is sensitive.

Another way to test specifically for matter-enhanced mixing of solar neutrino flavors is to look for a temporal variation in the flux. A difference between the daytime and nighttime ν_e fluxes would unmistakably indicate that the neutrinos were undergoing matter-enhanced mixing during propagation through the Earth. Experimentally, the ^{37}Cl detector is incapable of measuring this difference, but with a minor upgrade it may be capable of measuring it in the future. Constant monitoring is a feature of the Kamiokande H_2O Cherenkov detector and is also a feature of most proposed experiments; so temporal effects should be well measured in the future. Un-

fortunately, matter-enhanced mixing in the Earth only occurs for a narrow range of neutrino parameters. This range is much smaller than the corresponding range of parameters for propagation through the sun, as will be discussed in the next section. A failure to observe a day-night effect would not eliminate the MSW solution of the solar neutrino problem.

There are other solar neutrino detectors under consideration besides the ones mentioned above. Two low-temperature detectors have been proposed: a crystalline silicon detector (Cabrera *et al.*, 1985) and a liquid-helium "roton-multiplier" detector (Lanou *et al.*, 1987). In addition, detectors based on neutrino capture by ^{81}Br and ^{115}In (Bellefon *et al.*, 1985; Booth, 1987) have been discussed. Table VI shows the capture rates for proposed solar neutrino detectors. For other discussions of future experiments, see Flaminio and Saitta (1987), Friedlander and Weneser (1987), or Bahcall, Davis, and Wolfenstein (1988).

B. Earth

1. Calculating neutrino propagation through the Earth

In Sec. II, approximate analytic solutions to the neutrino propagation equation were derived for matter that was slowly or smoothly changing in density. These solutions were applied to neutrinos propagating through the sun. Neutrinos propagating through the Earth may also undergo matter-enhanced neutrino mixing. However, the Earth's density does not always change smoothly. At the surface of the Earth, the average density changes abruptly from 0 to 3 g/cm^3. The interior of the Earth consists of two regions of slowly varying density—the core and the mantle—with an abrupt density change between them. The mantle is 3000 km thick and the density increases from 3 to 5.5 g/cm^3. The core has a radius of 3400 km and the density varies from 10 to 13 g/cm^3 (for a detailed distribution see Stacey, 1985).

The neutrino wavelength in matter is the relevant distance scale with which to decide whether or not the matter is slowly varying. This is given by Eq. (2.37). The largest matter effects on neutrino mixing occur near the resonance, and there the equation for the wavelength in matter takes a particularly simple form,

$$\lambda_m|_{\text{resonance}}=\frac{\lambda_0}{\sin 2\theta}\approx\frac{R_{\text{Earth}}}{\sin 2\theta}\left[\frac{5\ \text{g/cm}^3}{\rho}\right] . \tag{3.15}$$

The oscillation wavelength is at a maximum at resonance and, at resonance, the oscillation wavelength in the Earth is greater than or of the order of the radius of the Earth. Since the density jumps abruptly on this scale, the solutions to the neutrino propagation equation for slow, smooth density changes, which were derived in Sec. II, are not valid. Furthermore, because the total propagation distance for neutrinos in the Earth will typically be less than or of the order of the wavelength in the medium, the phase information will be very important. Classical probabilities will not be an accurate solution to the wave equation, even over those regions where the density is approximately constant. Thus for neutrinos propagating through the Earth, the only way to accurately solve the neutrino propagation equation (2.23) is via numerical methods, as discussed in Sec. II.B.3.

The range of neutrino parameters for which there is significant mixing enhancement during propagation through the Earth is easy to estimate. For significant flavor oscillations to develop, the propagation distance must be greater than about a quarter of a wavelength. This condition, with Eq. (3.15) for the wavelength, gives us a lower limit on the mixing angle. For the longest propagation distance possible through the Earth, $2R_{\text{Earth}}$, and the largest densities possible, 13 g/cm^3,

$$\theta>0.05 . \tag{3.16}$$

The limit is more severe for neutrinos propagating through the Earth on shorter trajectories, especially so for those paths that only go through the low-density mantle.

There is also an upper limit for the vacuum mixing angle. The mixing enhancement from matter vanishes for large vacuum angles. There is no enhancement when the electron neutrino is dominantly the heavier mass eigenstate, $\theta>\pi/4$.

The neutrino mass differences that can undergo significant mixing enhancement from matter can also be estimated. From the resonance condition $A\approx(m_2^2-m_1^2)\cos 2\theta$, Eq. (2.34), the range of densities in the Earth give rise to a range of neutrino masses where maximum mixing enhancement may occur,

$$\frac{0.3\times10^{-5}\ \text{eV}^2}{10\ \text{MeV}}<\frac{m_2^2-m_1^2}{E_\nu}<\frac{1\times10^{-5}\ \text{eV}^2}{10\ \text{MeV}} . \tag{3.17}$$

Here we have taken $\cos 2\theta\approx 1$.

This range of masses is much smaller than the corresponding one for the sun. Because of this, the effects of three flavors are less likely to be relevant for neutrino propagation through the Earth than they were for neutrino propagation through the sun. If neutrino vacuum mixing is as small as naively expected, then the effects of three flavors will only be important when the neutrino goes through both resonances. It is unlikely to have $m_3^2-m_1^2$ and $m_2^2-m_1^2$ lie in the range given by Eq. (3.17) (see Sec. I.B).

The above estimates will help the reader to "understand" the results of numerical calculations. Another feature of the numerical calculations can be understood with some simple observations. Neutrino propagation through the Earth is qualitatively different from propagation through the sun. The matter distribution encountered during propagation through the Earth is symmetric, first increasing then decreasing, while solar neutrinos encounter purely decreasing density in the sun. Thus we do not expect the type of flavor conversion that

occurs in the sun to occur in the Earth. This can be made quantitative with the following approximations. Since most of the numerical calculations involve some averaging over different neutrino trajectories and energies, we make the approximation that we can average over the neutrino phase at the midpoint in the symmetric matter distribution. The neutrino transmission probabilities then satisfy the Schwarz inequality, if we ignore time-reversal violating phases:

$$P(\nu_\alpha \to \nu_\beta)^2 \leq P(\nu_\alpha \to \nu_\alpha) P(\nu_\beta \to \nu_\beta) \ . \tag{3.18}$$

For two flavors this gives that the minimum of $P(\nu_e \to \nu_e)$ is $\frac{1}{2}$. This is also the minimum for vacuum oscillations.

2. Solar neutrinos

The range of parameters that give significant enhancement of neutrino mixing in the Earth, Eqs. (3.16) and (3.17), is much smaller than, and lies well within, the similar range of parameters for neutrinos in the sun. This is because the sun has a much larger radius and because the range of densities in the sun encompasses that of the Earth. Since the electron neutrinos may be converted by the solar medium into other flavors, these other neutrinos may also be converted back by propagation through the Earth. This effect has been discussed by several authors: Bouchez *et al.* (1986), Cribier *et al.* (1986, 1987), Ermilova *et al.* (1986), Baltz and Weneser (1987, 1988b), Dar and Mann (1987), and Hiroi *et al.* (1987a, 1987b).

The solutions for $P(\nu_e \to \nu_e)$ derived in Sec. II for neutrinos propagating through the sun can be modified to incorporate the effects of propagation through the Earth. For two flavors with only solar-medium effects, Eq. (2.51) describes $P(\nu_e \to \nu_e)$. Since passage through the Earth occurs only at the end of the neutrino's flight, only the last matrix in Eq. (2.51) need be altered. This last matrix converts from the incoherent mass eigenstates to the flavor eigenstates, at the detector position. (We remind the reader that, for the relevant range of neutrino mass differences, the Earth-sun separation is many oscillation wavelengths; it is a good approximation to take the neutrino mass eigenstates to be incoherent. See Sec. III.A.) To include propagation through the Earth in Eq. (2.51), we replace the last matrix with

$$\begin{bmatrix} (1-P_E) & P_E \\ P_E & (1-P_E) \end{bmatrix} . \tag{3.19}$$

Here P_E is the propagation probability for mass eigenstate ν_1 to travel through the Earth and to be observed as a muon neutrino. It must be obtained by numerical methods. Equation (3.19) uses the two-flavor unitarity relations: $P_E = P(\nu_2 \to \nu_e) = P(\nu_1 \to \nu_\mu) = [1 - P(\nu_1 \to \nu_e)] = [1 - P(\nu_2 \to \nu_\mu)]$, Sec. II.A. The new propagation probability, including the Earth effect, is

$$P(\nu_e \to \nu_e) = [1 \ \ 0] \begin{bmatrix} C_{\theta m}^2 & S_{\theta m}^2 \\ S_{\theta m}^2 & C_{\theta m}^2 \end{bmatrix} \begin{bmatrix} (1-P_S) & P_S \\ P_S & (1-P_S) \end{bmatrix} \begin{bmatrix} (1-P_E) & P_E \\ P_E & (1-P_E) \end{bmatrix} \begin{bmatrix} 1 \\ 0 \end{bmatrix}$$

$$= \tfrac{1}{2} + [\tfrac{1}{2} - (P_S + P_E - 2P_S P_E)] \cos 2\theta_m \ , \tag{3.20}$$

where $C_{\theta m}^2 = \cos^2\theta_m$, $S_{\theta m}^2 = \sin^2\theta_m$, and P_S is the probability for level crossing in the sun. The generalization of Eq. (3.20) to three flavors is straightforward.

The trajectory of a solar neutrino through the Earth is constantly changing, primarily because of the Earth's rotation, but also because of the orbit of the Earth around the sun. Thus P_E is not a static quantity, unlike all the other terms in Eq. (3.20). The nature of P_E's variations with time are precisely calculable, once given the Earth's density distribution. Thus this may provide a new experimental signal for ascertaining the solution to the solar neutrino problem. Timing capabilities could be an important part of a solar neutrino experiment if the neutrino parameters were such [Eqs. (3.16) and (3.17)] as to give rise to significant mixing enhancement in the Earth.

The classic ^{37}Cl experiment is almost a static experiment (Fig. 10). The ^{37}Ar atoms are flushed from the tank and counted only every couple of months. This procedure averages out any day-night changes, but not necessarily the seasonal variations in the data taken over the last 20 years. A calculation by Mikheyev and Smirnov (1987b) finds that the largest seasonal Earth effect possible has an amplitude of about 0.7 SNU. This is not too much larger than the error of the total average of the ^{37}Cl data, 2.1±0.3 SNU. Thus it is not possible to put significant limits on neutrino parameters by this method. An earlier calculation by Cribier *et al.* (1986, 1987) found a much larger seasonal variation.

These calculations are difficult, since the numerical integration through the Earth must in turn be averaged numerically over the diurnal variations. The calculations are also site specific, since the neutrino trajectories depend on the latitude of the solar neutrino detector. The farther the detector is from the equator, the more the trajectories miss the high-density core of the Earth. Trajectories through the core produce the largest mixing effects.

A diurnal variation of the electron-neutrino flux would be much larger than the corresponding seasonal variation. Experiments with continuous monitoring of the neutrino flux could hope to see this variation; however, radiochemical experiments can also test this possibility.

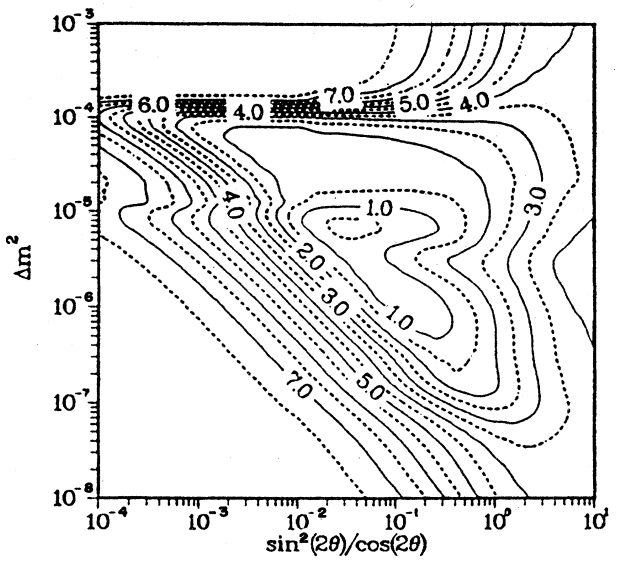

FIG. 10. Iso-SNU contours for the ^{37}Cl experiment, labeled by SNU values. Includes Earth effect averaged over the year (Baltz and Weneser, 1988b).

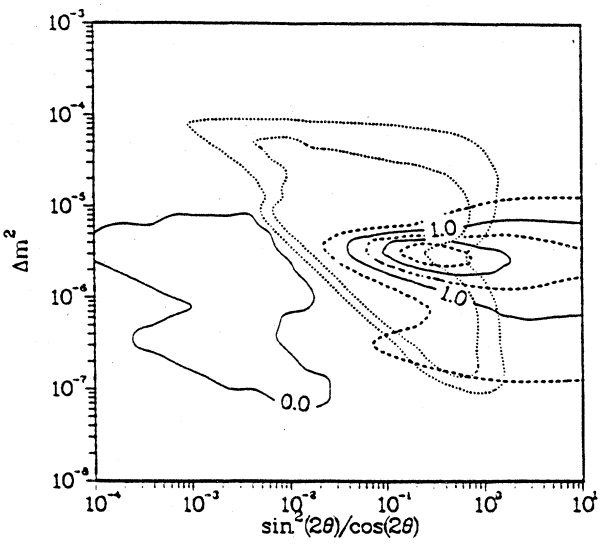

FIG. 12. Night minus day contours (solid) for the ^{37}Cl experiment, labeled by SNU values. The band between the dotted contours is the region consistent with the existing experimental result of 2.1±0.3 SNU (Baltz and Weneser, 1988b).

The ^{37}Cl experiment could be upgraded to allow separation of day- and night-captured ^{37}Ar atoms. Figure 11 shows a calculation for the diurnal variation in the ^{37}Cl capture rate. Figure 12 shows a numerical calculation of the range of neutrino parameters that give a diurnal effect. It agrees with our qualitative estimates from Eqs. (3.16) and (3.17), using the fact that the average neutrino energy to which the ^{37}Cl experiment is sensitive is about 10 MeV.

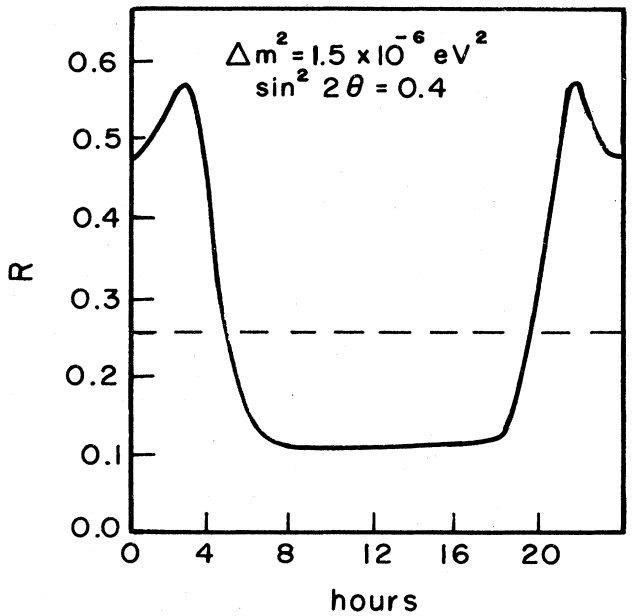

FIG. 11. Effect of the Earth on the ^{37}Cl capture rate for $(m_2^2-m_1^2)=1.5\times10^{-6}$ eV^2 and $\sin^2 2\theta=0.4$. R = ratio of measured capture rate to the standard-solar-model prediction; dashed line is the average. The time scale is the diurnal variations averaged over the year (Mikheyev and Smirnov, 1987b).

3. Atmospheric neutrinos

Primary cosmic rays interact in the atmosphere, producing a flux of neutrinos from the decay of pions, kaons, and muons. The flux is small, but it has been observed in large detectors where it is the primary background for proton-decay experiments. The neutrinos are produced all over the Earth's surface; by observing the angle of the neutrino one can infer the distance traveled since production and hence be sensitive to neutrino oscillations. Since these paths go through the Earth, one is, in fact, sensitive to neutrino mixing in matter. Matter effects on atmospheric neutrinos have been discussed by several authors [Carlson (1986), LoSecco (1986), LoSecco *et al.* (1987), and Auriemma *et al.* (1988)].

The atmospheric neutrino flux has been calculated by many groups; for some recent results see Volkova (1980), Bugaev *et al.* (1986), and Gaisser *et al.* (1988). The calculations are quite involved and often differ on the order of 30% or more in their predictions for the magnitude of the fluxes. The atmospheric neutrino flux peaks at about 50–100 MeV, with $F_\nu \approx 10^5$ (m^2 s sr GeV)$^{-1}$, and falls off at roughly E^{-3}. The flux varies in time with the solar wind; its angular dependence is different at each location (because of the Earth's magnetic field), and it contains a combination of ν_e, ν_μ, $\bar{\nu}_e$, and $\bar{\nu}_\mu$. These properties, plus low statistics, combine to make atmospheric neutrinos a difficult source to exploit for the study of neutrino properties.

However, it may be possible to reduce or avoid some of these uncertainties. The flux calculations tend to agree on their predictions for the ratio of neutrino flavors (Fig. 13). Naively one expects twice as many muon neutrinos as electron neutrinos, since the pions and kaons decay primarily to muons. However, at high energies not all of

the muons decay in flight, thus increasing the ratio; at low energies the neutrinos come mainly from muon decay, so the ratio approaches 1. By comparing this ratio for up-going and down-going neutrinos, many uncertainties cancel out and it may be possible to put some constraints on neutrino parameters.

In recent years there has been progress in the understanding of atmospheric neutrino fluxes. Table VII compares the number of atomspheric neutrino events predicted to occur in various proton-decay experiments with those actually observed. The agreement is surprising. But there is some recent disagreement between the atmospheric neutrino flux observed by Kamiokande and those predicted (Hirata *et al.*, 1988b). However, with the increasing amount of experimental feedback, it may soon be possible to have confidence in the magnitude of the atmospheric neutrino fluxes and their ratios.

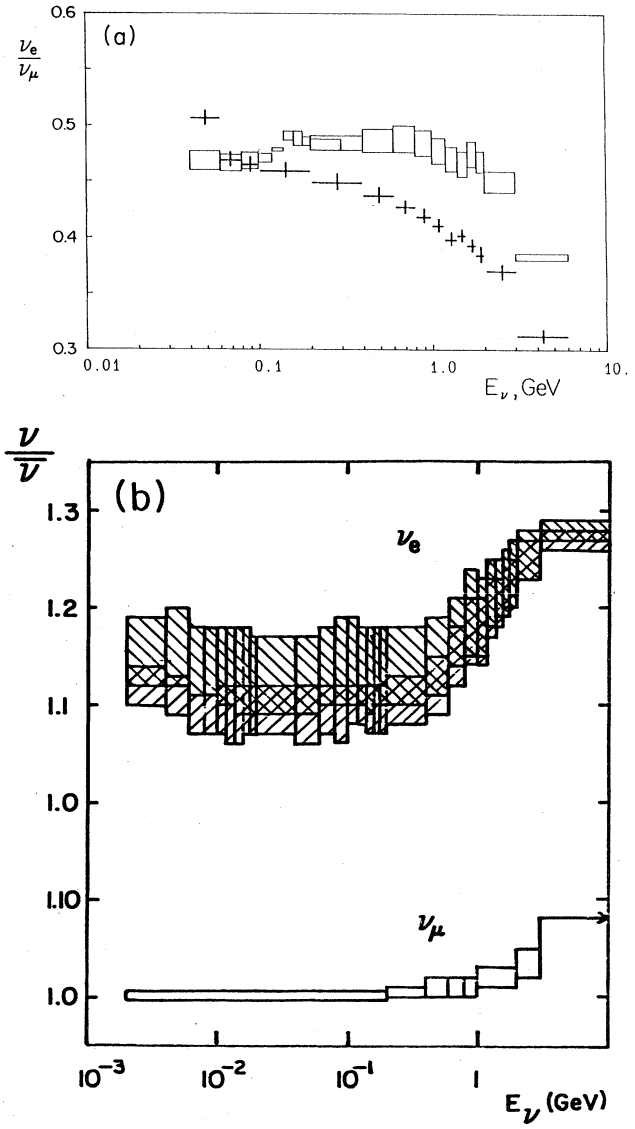

FIG. 13. Ratios (a) $(\nu_e+\bar{\nu}_e)/(\nu_\mu+\bar{\nu}_\mu)$ and (b) $\bar{\nu}_\alpha/\nu_\alpha$ for the atmospheric neutrino flux (Gaisser *et al.*, 1988). In (a) the crosses represent an earlier calculation. In (b) the electron-neutrino upper band is for solar minimum and the lower band is for solar maximum. The vertical size of each band reflects the differences among different locations. The top of each band is for Soudan and the bottom for Kamioka.

TABLE VII. Number of atmospheric neutrino interactions in various "proton decay" detectors.

Detector	Exposure (kT yr)	Measured	Calculated
KGF	0.28	23	17
NUSEX	0.41	37	37
Frejus	0.6	65	60
IMB	3.8	401	403
Kamiokande	1.5	181	170

There are two methods for detecting the atmospheric neutrino flux. One method is to observe the neutrino flux directly by requiring the neutrino interaction to be contained within the detector volume. Both electron and muon neutrinos are detected and can be resolved. Averaging the flux over a solid angle to improve statistics, one can compare the ratio of upward and downward neutrino fluxes, $(U_e/U_\mu)/(D_e/D_\mu)$, to search for neutrino oscillations. This method is sensitive to atmospheric neutrinos with energies of 0.2–1 GeV. There the increase in the neutrino flux at low energies $(dN/dE \propto E^{-2.7})$ balances with the threshold for producing muons. Tau neutrinos that may have been produced by oscillations are generally not detectable. The energy threshold for producing tau neutrinos lies above the sensitive energy range in a region where the neutrino flux is very small.

The atmospheric neutrino flux is unusual in that it is made up of an assortment of neutrinos: electron and muon flavors, particles, and antiparticles. Thus, unlike solar neutrinos, the flux may be sensitive to neutrino propagation probabilities other than $P(\nu_e \to \nu_e)$. The upward-going neutrino flux of flavor α, U_α, in terms of the downward-going neutrino flux of flavor β, D_β, is given by

$$\begin{aligned} U_e &= D_e P(\nu_e \to \nu_e) + D_\mu P(\nu_\mu \to \nu_e) , \\ U_\mu &= D_e P(\nu_e \to \nu_\mu) + D_\mu P(\nu_\mu \to \nu_\mu) , \\ U_\tau &= D_e P(\nu_e \to \nu_\tau) + D_\mu P(\nu_\mu \to \nu_\tau) . \end{aligned} \tag{3.21}$$

Unitarity will not reduce all the probabilities down to one unknown probability unless one ignores U_τ and assumes there are only two flavors. For antineutrinos, there is an analogous set of equations. We remind the reader that $P(\nu_\alpha \to \nu_\beta)$ and $P(\bar{\nu}_\alpha \to \bar{\nu}_\beta)$ are, in general, quite different; one is enhanced by matter effects and the other is suppressed.

A contour plot for direct detection of the atmospheric neutrino flux, assuming only two flavors, is shown in Fig. 14 (Carlson, 1986). The location of the contours agrees with the qualitative estimates of Eqs. (3.16) and (3.17) using the given energy range of sensitivity. If the detector

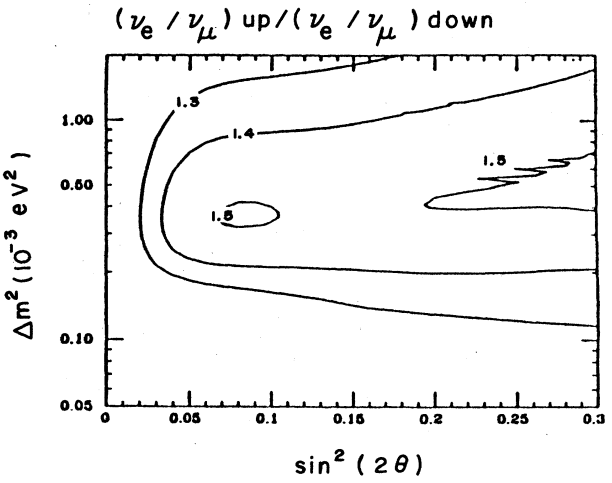

FIG. 14. Contours of constant $(\nu_e/\nu_\mu)_{\rm up}/(\nu_e/\nu_\mu)_{\rm down}$. Oscillations were averaged from 0 to 30 degrees (Carlson, 1986).

cannot resolve neutrinos from antineutrinos, and if $P(\bar{\nu}_e \rightarrow \bar{\nu}_e)=0$, then the values for the contour labels should be reduced by about 10%.

The other method for observing the atmospheric neutrino flux is to detect it indirectly by observing the muons produced in the rock surrounding the detector. This has been analyzed for the MACRO detector (Longo *et al.*, 1987) by Auriemma *et al.* (1988). This method should have a higher event rate because of the larger mass available for neutrino interactions, but only the muon-neutrino flux is observed. Thus an accurate knowledge of the magnitude of the atmospheric neutrino flux is crucial. This method is sensitive to higher-energy neutrinos than the first method because higher-energy muons travel farther and are more likely to be detected, muons with energies below 2 GeV are probably not detectable. For muons in the range 2–10 GeV, it may be possible to distinguish the charge of the muon, allowing separation of neutrino and antineutrino fluxes. Above 10 GeV the neutrino and antineutrino rates are probably not separable. Figure 15 compares the neutrino parameter limits achievable by this method with those achievable by other methods.

4. Accelerator neutrinos

There has been speculation in the past on constructing accelerators for shooting neutrino beams through the Earth (De Rújula *et al.*, 1983). In the study of matter-enhanced neutrino mixing, accelerator neutrinos would have several advantages over natural sources of neutrinos. The flavor and magnitude of the neutrino flux would be known accurately. The energy range of the neutrino flux could be made very narrow, $\Delta E/E \ll 1$, and the neutrino energy could be varied. The accelerator would be a static, point source of neutrinos. All of these features would be improvements over natural neutrino sources like the sun or cosmic rays.

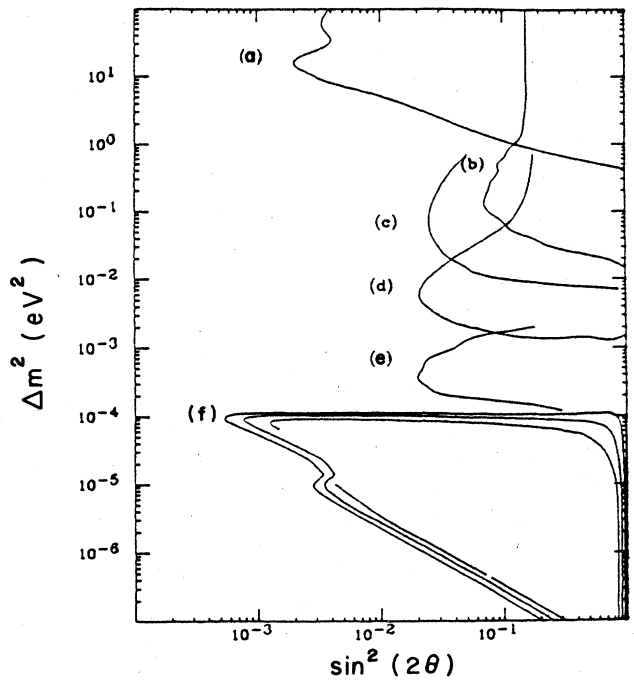

FIG. 15. Comparison of the limits on neutrino parameters achievable by (a) accelerators; by (b) reactors; and by atmospheric neutrinos with an underground detector for (c) high-energy muons (10 GeV $< E_\mu$), (d) low-energy muons ($2 < E_\mu < 10$ GeV), and (e) contained neutrino events. Curve (f) is the region of parameter space that solves the solar neutrino problem. From Auriemma *et al.* (1988).

Such a neutrino source could be used to study the density distribution of the Earth (Ermilova *et al.*, 1986; Nicolaidis, 1988). In the calculations above, a model for the density distribution was assumed, but there are large uncertainties in this model. The density could be inferred from matter-enhanced mixing effects. For a particular neutrino energy, the mixing is a moment of the density distribution. If neutrino mixing were observed for several energies, the moments could be used to reconstruct the density.

As argued previously, phase effects are especially important for the Earth and necessitate numerical solutions to the wave equation. All of the advantages of accelerator neutrinos over natural sources increase the importance and observability of neutrino phase effects. Averaging over the movement, distribution, energy, and variability of the neutrino source would be tremendously reduced or eliminated. If phase effects are resolvable, then it could be possible to observe directly a time-reversal (T) violating phase in the neutrino mass matrix. As shown by Kuo and Pantaleone (1987b) and by Krastev and Petcov (1988c), matter enhancement of mixing angles also enhances the effects of a T violating phase in the mixing matrix. If the neutrino parameters are such that both the "ν_e-ν_μ" and "ν_e-ν_τ" resonances occur in the Earth, then T violation effects are doubly enhanced. A T violating phase could only be isolated

from T violating matter effects for neutrinos going through a medium with a symmetric matter distribution, like the Earth.

C. Supernovae

The recent observations of neutrinos from a supernova (Bionta *et al.*, 1987, 1988; Hirata *et al.*, 1987, 1988a; see also Alekseev *et al.*, 1987 and Dadykin *et al.*, 1987) have implications for astrophysics and particle physics. They have confirmed the qualitative ideas on the dynamics of supernovae. One application of this is to place limits on exotic particle physics scenarios such as significant energy loss from axion emission during the collapse, large neutrino magnetic moments, a nonzero neutrino charge, different gravitational couplings for photons and neutrinos, and others. The recent observations also promise the possibility of future observations of supernova neutrino emission, thus opening a new area of astronomy.

The observations of neutrinos from a supernova are also sensitive to the somewhat less speculative idea of a nonzero neutrino mass. A relatively large electron-neutrino mass would affect the kinematics of neutrino propagation; however, this is ruled out because the time dependence of the observed signal agrees roughly with expectations, as described in Sec. I.C.1. Small neutrino masses, with their accompanying mixing of the different neutrino fluxes during propagation, could also have an effect on the neutrino signal. In order to interpret the observations, the uncertainties in supernova dynamics must, if possible, be disentangled from the effects of neutrino propagation.

Besides the possibility of matter-enhanced oscillations, all supernova neutrinos are sensitive to a new range of parameters associated with vacuum oscillations. For a supernova 100 000 light years from Earth, and neutrino energies of tens of MeV, the neutrinos will undergo vacuum oscillations if the mass difference is greater than $m_2^2 - m_1^2 > 10^{-20}$ eV^2. This is more than 10 orders of magnitude smaller than the analogous mass difference for solar neutrinos (and is well below the estimates of neutrino mass expected in grand unified theories). Thus detection of supernova neutrinos may ultimately provide the best possible limit on small neutrino masses, if no evidence for neutrino mass is found.

In Sec. III.C.1, we shall briefly review aspects of stellar collapse that are relevant for neutrino emission. In Sec. III.C.2 we shall illustrate how neutrino oscillations can mix the neutrino fluxes by calculating how this can change the expected number of neutrino events observed in a H_2O Cherenkov detector. In Sec. III.C.3 we shall compare these expectations with the neutrino detection of the supernova 1987A and see what conclusions can be drawn. In Sec. III.C.4 we shall briefly indicate how neutrino mixing could be relevant for supernova dynamics and vice versa.

1. Supernova models and the expected neutrino fluxes

We begin by summarizing some of the general features of stellar core collapse that are relevant to neutrino oscillations (see, e.g., Bethe, 1984; Mayle *et al.*, 1986; Wilson *et al.*, 1986; Schramm, 1987; Brown *et al.*, 1988; for an introduction to supernovae see Shapiro and Teukolsky, 1983). The source of energy for a supernova is the gravitational collapse of a 1–1.5 solar mass core, from one supported by electron degeneracy down to a mass supported by neutron degeneracy—a neutron star (or possibly down to a black hole). This releases about 3×10^{53} ergs, 99% of which is emitted from the supernova over a few seconds as neutrinos.

There are two mechanisms by which neutrinos are emitted from a supernova—neutronization and thermal emission. Neutronization occurs first and results from electron capture onto nuclei and free protons; hence it is responsible for a flux of ν_e. Since electron capture decreases the degeneracy support of the initial core, a large burst of ν_e is expected to occur during infall, which occurs on a time scale of 10^{-3} s. After infall, the densities are large enough to trap the neutrinos in the collapsed core. Any remaining trapped neutronization neutrinos slowly diffuse out while the newly produced hot neutron star thermally radiates more neutrinos. This thermal neutrino emission proceeds via the annihilation of real and virtual e^+e^- pairs, producing $\nu\bar{\nu}$ pairs of all flavors, and is expected to occur on a diffusion time scale of a few seconds. The relative importance of these two processes, thermal and neutronization, is not well known.

The relative magnitudes of the different fluxes in purely thermal emission are less uncertain. Since they are produced in pairs, the magnitude of the neutrino and antineutrino fluxes are equal for each flavor. Since $\bar{\nu}_\mu$ and $\bar{\nu}_\tau$ production and scattering only proceed via neutral-current processes, these fluxes are identical. Furthermore, the thermal electron-neutrino flux will be somewhat larger and have a smaller temperature than the others. This is because the production and scattering cross sections are larger for electron neutrinos than for the others; so more electron neutrinos are produced and they are in equilibrium out to a larger radius where the temperature is smaller.

We will take the fluxes, neutronization and thermal, to be given by static Fermi-Dirac distributions with zero chemical potential. This is an approximation since, in diffusing out of the star, the neutrinos can last scatter from a range of depths with a range of temperatures. But it should be a good first approximation for the thermally emitted neutrinos. For the neutronization neutrinos it will be a worse approximation, but it is probably better than taking a single typical energy. The initial temperatures T and the relative total luminosities of the initial thermal fluxes, L, are taken to be values typical of theoretical supernova models before the supernova detection (Mayle *et al.*, 1986),

$$\begin{aligned} &L_\alpha^t = L_{\bar{\alpha}}^t, \quad T_e^t = T_{\bar{e}}^t = 3 \text{ MeV}, \\ &L_\mu^t = L_\tau^t \equiv L_x^t, \quad T_x^t = T_{\bar{x}}^t = 6 \text{ MeV}, \\ &L_e^t = 2L_x^t, \quad T_e^n = 3 \text{ MeV}, \end{aligned} \tag{3.22}$$

where the superscripts t and n denote thermal and neutronization, and the subscripts e, x, and α denote the neutrino flavors electron, muon or tau, and any flavor, respectively. The present state of supernova modeling is such that the thermal temperatures in Eq. (3.22) are probably uncertain by about 50–100 %. The neutronization temperature is even more uncertain; it could be much larger. This uncertainty is partly because of the lack of supernovae close enough to observe, but also because of the difficult nature of the calculations.

In addition to the neutrino temperatures and luminosities, we also need the matter density distributions through which the neutrinos propagate, in order to calculate the effects of matter on neutrino flavor conversion. Immediately after the core of a supernova collapses, model calculations generally yield a density function in the core and mantle of the form

$$\rho(r)=C/r^3, \quad 10^{-5}<\rho<10^{12}\ \text{g/cm}^3 , \tag{3.23}$$

with C varying weakly with r over the range

$$1<C/10^{31}\ \text{g}<15$$

(for later numerical calculations, we will take C from Wilson *et al.*, 1986).

2. Neutrino mixing effects on H_2O Cherenkov detector results

The survival probabilities for supernova neutrinos are qualitatively similar to those of solar neutrinos. Neutrinos are in equilibrium at densities greater than about 3×10^{11} g/cm^3; so, as they leave this region, they travel through a gradually decreasing density and, as described in Sec. II and in Sec. III.A for the sun, the ν_e could undergo a resonant conversion. However, unlike the sun, supernova neutrino fluxes contain more than just ν_e. For $\bar{\nu}_e$, resonant oscillations are not expected to occur for typical neutrino parameters (as in Sec. I.B). Moreover, the $\bar{\nu}_\mu$ and $\bar{\nu}_\tau$ fluxes are expected to be equal, and so the possible resonant conversion due to radiative corrections, Eq. (2.25), will have no effect. Of course, oscillations in vacuum are relevant for all species of neutrinos and antineutrinos as they propagate from the supernova to the Earth. Thus we shall examine the effects of mixing on all of the neutrino flavors.

In order to make quantitative statements about oscillation effects on supernova neutrinos and what the relevant neutrino parameters are, we shall now work through some explicit examples. We calculate the total number of events expected in a water Cherenkov detector with and without oscillations and define ths ratio to be R,

$$R\equiv\frac{\text{No. of events in detector with oscillations}}{\text{No. of events in detector without oscillations}} . \tag{3.24}$$

This will be a measure of oscillation effects while many of the details of the supernova model will cancel out in this ratio. We choose a water Cherenkov detector in anticipation of Sec. III.C.3. We note that, as was discussed in Sec. II.D.4, only $P(\nu_e\to\nu_e)$ or $P(\bar{\nu}_e\to\bar{\nu}_e)$ is needed in this calculation.

There will be more than one type of R to calculate. In a water Cherenkov detector there are two kinds of neutrino events which can be distinguished from each other. One type of event is inverse beta decay, on the hydrogen nucleus in H_2O, where the positron is emitted almost isotropically,

$$\sigma(\bar{\nu}_e+p)\approx 89\times10^{-43}\ \text{cm}^2(E_\nu/10\ \text{MeV})^2 . \tag{3.25}$$

The other type of event is neutrino-electron scattering, which is extremely directional, as given in Eq. (3.6).

The cross section for inverse beta decay is about 2 orders of magnitude larger than the electron-scattering cross section. This is partially ameliorated by two facts: H_2O contains five times as many electrons as it does H nuclei, and electron scattering can occur for all flavors while inverse beta decay occurs for only electron antineutrinos. Inverse beta decay is still expected to be the dominant signal, but the electron-scattering signal is only down by about 1 order of magnitude.

These two classes of events, directional and isotropic, combined with the two supernova emission processes, give us three relevant R's to calculate. There are two R's for thermal emission, one for directional and one for isotropic events, and one R for the directional events from neutronization. We are assuming that the neutronization and thermal events are discernible by their timing, the neutronization events occurring predominately before the thermal. This should be an adequate first approximation.

Using the formulas for the fluxes, Eq. (2.94), the equation for the first ratio, the R for the directional events from neutronization, is

$$R_d^n=1+\frac{\int dE_\nu F_e^{0n}[1-P(\nu_e\to\nu_e)]\int\varepsilon[d\sigma(\nu_x+e)-d\sigma(\nu_e+e)]}{\int dE_\nu F_e^{0n}\int\varepsilon\, d\sigma(\nu_e+e)} . \tag{3.26}$$

Here $\int\varepsilon\, d\sigma$ denotes an integral over electron energies (from 0 to E_ν) of the differential cross section times ε, the detector efficiency, a known function of E_e; ν_x represents either ν_μ or ν_τ. To calculate how R_d^n depends on neutrino parameters, we must first specify some relevant quantities. We use the detector efficiency of Kamiokande (Hirata *et al.*, 1987). To fix the neutrino flux we use a static Fermi-Dirac distribution, as discussed in the previous section. For $P(\nu_e\to\nu_e)$ we use the three-flavor expression of Eq. (2.86) (the two-flavor approximation, as

will be made clear, is worse for supernova neutrinos than it was for solar neutrinos; see Fig. 16). This probability depends on four independent neutrino parameters; so, in order to make a two-dimensional plot, we constrain two of the four parameters consistent with the theoretical expectations of grand unified theories, as discussed in Sec. I.B. Using these, we get contour plots for R_d^n, as given in Fig. 17 (this graph is qualitatively similar to the graphs showing the effects of three-flavor neutrino oscillations on the solar neutrino flux).

The range of neutrino parameters for which oscillations can affect the supernova flux is amazingly large because of the large range of densities in the supernova. The central region has $R_d^n=0.14$, which is just the ratio of ν_x to ν_e cross sections. However, there is some uncertainty in the contours, especially in the extreme parts of the graph. The upper part of Fig. 17 depends on the densities of the supernova near the core, which are being produced during infall. The extreme bottom of Fig. 17 depends on the outermost layers of the supernova and may be sensitive to H_2 shell mass loss by the progenitor. In addition, we have neglected the effects of propagation through the Earth on the supernova neutrino mixing. As to the effect of three flavors, for most reasonably expected neutrino parameters the two energy ranges where flavor conversion occurs overlap, as shown in Fig. 16. To a good approximation, the top, horizontal contours of Fig. 17 are given by $E_A^l \approx$ constant, where E_A^l is the adiabatic threshold of the lower, e-μ resonance. Similarly, the lower, diagonal contours of Fig. 17 are given by $(E_{\rm NA}^u)^{2/3}+(E_{\rm NA}^l)^{2/3}\approx$ constant, where $E_{\rm NA}^{u(l)}$ is the nonadiabatic threshold energy of the upper, e-τ (lower, e-μ) resonance. A general expression for the nonadiabatic 50% contour is $m_2^{4/3}|U_{e2}|^2+m_3^{4/3}|U_{e3}|^2\approx 8\times 10^{-7}$ eV$^{4/3}$. This expression comes from the overlap of the Landau-Zener probability factors of the upper e-τ times the lower e-μ resonances [see Eq. (2.92)] and is applicable when $E>E_A^u|_{\max}$ or, equivalently, using typical core densities and neutrino energies, when $m_3<200$ eV.

Solar densities occur in the supernova models at solar distance scales. Thus there is some overlap of the nonadiabatic contours of the supernova with the nonadiabatic solutions to the solar neutrino problem. The amount of overlap depends on our assumed supernova parameters. The bottom part of the adiabatic contour is sensitive to H_2 shell mass loss by the progenitor; shell mass loss will raise the contours in this region. Furthermore, the nonadiabatic contours are sensitive to the assumed temperature of the neutronization flux; an increase of the temperature by a factor of 2 will raise the contours by a factor of about 2. In addition, the overlap occurs when the same resonance dominates for both the solar and the supernova resonances. This is most naturally the case when the resonance that occurs at solar densities is the heaviest possible resonance. Any heavier resonance would almost certainly occur in the higher densities of the supernova and would tend to dominate the situation because it would occur first and because it would be expected to satisfy more readily the adiabatic criterion. This is the situation in Fig. 17 where the e-τ nonadiabatic solar and supernova contours overlap, but the solar e-μ nonadiabatic contours lie inside those of the supernova contours. Only in the case of very small $|U_{e3}|$ when the e-τ resonance decouples, $m_2^2|U_{e2}|^3 \gg m_3^2|U_{e3}|^3$, can there be some overlap of the solar and the supernova e-μ nonadiabatic contours.

The calculation of R for the directional events from thermal emission, R_d^t, is similar to the previous case.

$$R_d^t=1+\frac{\int dE_\nu \left\{[1-P(\nu_e\to\nu_e)](F_e^{0t}-F_x^{0t})\int \varepsilon[d\sigma(\nu_x+e)-d\sigma(\nu_e+e)]+(\nu\to\bar{\nu})\right\}}{\int dE_\nu \left\{F_e^{0t}\int \varepsilon\, d\sigma(\nu_e+e)+2F_x^{0t}\int \varepsilon\, d\sigma(\nu_x+e)+(\nu\to\bar{\nu})\right\}} . \tag{3.27}$$

Now there is more than one flavor of initial flux present, and oscillations can either increase or decrease R_d^t. R_d^t is more sensitive to the details of the supernova model than is R_d^n, because we must specify the temperatures and the relative magnitudes of each produced flux [Eq. (3.22)]. Generally, it is found that oscillation effects are not large ($\approx$20%) for this type of event, and we will not detail the analysis here (Kuo and Pantaleone 1988).

The calculation of R for the isotropic events follows from

$$R_i^t=1+\frac{\int dE\ \varepsilon\sigma(\bar{\nu}_e+p)[1-P(\bar{\nu}_e\to\bar{\nu}_e)](F_{\bar{x}}^{0t}-F_{\bar{e}}^{0t})}{\int dE\ \varepsilon\sigma(\bar{\nu}_e+p)F_{\bar{e}}^{0t}} . \tag{3.28}$$

As in the previous case, more than one species is present; so the calculation of R_i^t will again depend on the temper-

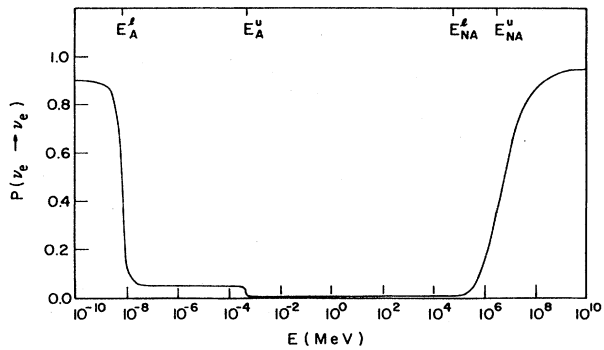

FIG. 16. Probability of a ν_e, produced in a supernova, reaching the Earth as a function of energy. Here we take three neutrino flavors and "typical" vacuum parameters, $m_2^2-m_1^2=10^{-4}$ eV^2, $m_3^2-m_1^2=6.3$ eV^2, $|U_{e2}|^2=5\times10^{-2}$, and $|U_{e3}|^2=5\times10^{-4}$. The adiabatic ($A$) and nonadiabatic (NA) energy thresholds for the e-τ, upper (u), and e-μ, lower (l), resonances are shown.

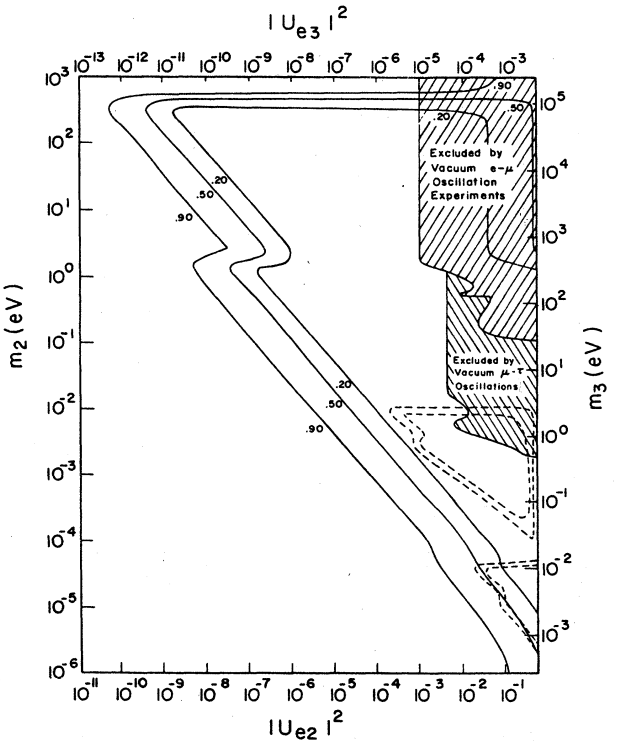

FIG. 17. Contour plot of R_d^n, ratio of the number of events with oscillations to those without for directional events from neutronization, for the Kamiokande detector. Here we use three flavors and "typical" constraints on the relevant neutrino vacuum parameters: $m_1=0$, $(m_3/m_2)=250$, and $(|U_{e2}|^2/|U_{e3}|^2)=100$. The dashed lines show the (3σ) solutions to the solar neutrino problem. The shaded regions are excluded by reactor oscillation experiments where we have taken $|U_{\mu 3}|^2 \approx |U_{e2}|^2$ (Sec. I.C.2).

atures and relative magnitude of the thermal fluxes. Here the probability $P(\bar{\nu}_e \rightarrow \bar{\nu}_e)$ is most likely insensitive to matter effects and only depends on vacuum oscillations, which are independent of energy. This assumption allows us to easily evaluate R_i^t. Taking the supernova parameters given, we find

$$R_i^t = 1 + [1 - P(\bar{\nu}_e \rightarrow \bar{\nu}_e)]\bar{B}_i^t ,$$
$$\bar{B}_i^t = 0.20 \quad \text{Kamiokande} , \qquad (3.29)$$
$$\bar{B}_i^t = 4.5 \quad \text{IMB} .$$

We note that $\bar{B}_i^t$ is always positive for the given supernova parameters. The isotropic cross section increases faster with energy than the directional cross section; so $\bar{B}_i^t$ is more sensitive to the small amount of a higher-temperature flux that oscillation adds. IMB's threshold is much larger than the temperature, so there the expected number of events is very sensitive to the temperature(s) of the flux.

Summarizing, Eqs. (3.26)–(3.29) illustrate how mixing can alter the total number of neutrino events in a detector. Equation (3.26) shows that mixing will always decrease the electron-scattering signal from the neutronization neutrino flux, up to a factor of about $\frac{1}{7}$ for resonant conversion in matter. The largest effect on the thermal neutrino events occurs in the neutrino absorption detection. For detectors with high thresholds, R_i^t can be sizable, as in Eq. (3.29). Unfortunately, one expects no resonant conversion for antineutrinos.

3. The neutrino observation of supernova 1987A

We turn now to a discussion of the recently detected neutrinos from the supernova 1987A and the implications there might be for neutrino mixing. The effects of matter-enhanced mixing on supernova neutrinos have been discussed by many authors (Bethe, 1986; Mikheyev and Smirnov, 1986b, 1987a; Arafune and Fukugita, 1987; Arafune *et al.*, 1987a, 1987b; Lagage *et al.*, 1987; Minakata *et al.*, 1987; Notzold, 1987b; Walker and Schramm, 1987; Wolfenstein, 1987; Kuo and Pantaleone, 1988; Minakata and Nunokawa, 1988; Rosen, 1988)

The observed neutrino signal consists of 11 events in the Kamiokande data (Hirata, 1987, 1988a) and eight events in the IMB data (Bionta *et al.*, 1987) [reports of supernova neutrinos in LSD (Dadykin in *et al.*, 1987) and Baksan (Alekseev *et al.*, 1987) will not be included in our discussion]. The first event in the Kamiokande data appears to be a directional event. Subsequent events are consistent with mostly isotropic events (originally it was thought that the second event was also directional, but subsequent analysis has shown it to be otherwise; see Hirata, 1988a). The angular distribution of the IMB data shows some limited directionality (Bratton *et al.*, 1988); however, the events can be interpreted as isotropic.

It is tempting to attribute the first event in Kamiokande to ν_e emitted during neutronization. However, this interpretation is uncertain. There is a probability of roughly $[(20\pi/180)^2/4] \approx 0.03$ that an isotropic event will lie in the forward 20 degrees and look like a directional event. The expected number of neutronization events in Kamiokande is highly model dependent; estimates lie in the range 0.01 to $O(1)$ (Arnett, 1987; Sato and Suzuki, 1987; Cooperstein in Brown, 1988). With neutrino resonant conversion, Eq. (3.26) indicates that the expected event rate becomes even smaller, reduced by a factor of $\frac{1}{7}$. Thus neutrino parameters that yield maximal suppression are disfavored, but by an amount that is at most this factor, $\frac{1}{7}$.

The disfavored range of neutrino masses and mixings is quite large. In particular, the reduction is near maximal for most of the parameter region that solves the solar neutrino problem. For Fig. 17 this includes all of the e-μ resonance solution (adiabatic, nonadiabatic, large angle, and Earth effect) and the e-τ adiabatic solution; however, this situation is more general than Fig. 17. As long as there is a hierarchy of masses and mixing angles (as expected from grand-unification-theory seesaw mecha-

nisms), and $|U_{e3}|$ does not vanish, then only the e-τ nonadiabatic solution to the solar neutrino problem is not completely disfavored (Kuo and Pantaleone, 1988; Rosen, 1988). This solution is partially suppressed, but we note that the supernova contours in this region depend sensitively on the amount of H_2 shell mass loss (Minakata and Nunokawa, 1988) and the temperature of the neutronization flux. Thus they are especially dependent on supernova models and so cannot be excluded. If we relax the assumption of a hierarchy of masses and mixing angles, there is another region of neutrino parameters for which the supernova neutronization flux is not substantially suppressed. For these parameters, neutrino conversion does occur in the supernova, but there is a reconversion during propagation through the Earth (Arafune *et al.*, 1987a, 1987b; Lagage *et al.*, 1987; Minakata *et al.*, 1987; Notzold, 1987b). Since the supernova energies are about twice as large as the solar neutrino energies, this parameter region is similar to the solar-Earth-effect region, but with the contours shifted up by a factor of 2. However, for this solution to be viable, an unexpected arrangement of the neutrino parameters is required and the flavors with which the ν_e resonates in the supernova and in the earth must be the same. While this is not a bad assumption for solar neutrinos, it is a worse assumption for supernova neutrinos. Because of the higher densities in a supernova (the induced mass at trapping densities is about 200 eV), the heaviest neutrino will always dominate the flux, since it will be the first to undergo resonant conversion; that resonant conversion is likely to be adiabatic (Fig. 17). Furthermore, one naively expects that the heaviest neutrino also has the smallest coupling to the electron neutrino (Sec. I.B). However, the reconversion in the Earth requires a large mixing angle, $\sin^2 2\theta > 0.2$ for less than 50% suppression. Thus the reconversion of the supernova effect by the Earth is possible, but it requires an unusual neutrino parameter arrangement.

We now consider events that may have originated from the thermal phase. They appear to make up the majority of the data sample. As far as the directional events in Kamiokande are concerned, from Eq. (3.27), oscillation does not have any major impact on them. The $\bar{\nu}_e$ (isotropic, thermal) events can, however, be enhanced substantially by mixing. Large changes in the number of events are possible if the vacuum angles are large or if there are unusual neutrino parameter arrangements where resonant conversion could occur for $\bar{\nu}_e$. To resolve purely experimentally the mixing of $\bar{\nu}$ from uncertainties in $T_{\bar{e}}^t$, one must fit the isotropic spectrum with the flux described in Eq. (2.94). There are at least four parameters to be extracted—the temperatures and the magnitudes of the $\bar{\nu}_e$ and $\bar{\nu}_x$ fluxes (and more parameters if the flux distribution is not exactly Fermi-Dirac). The small number of events and the sensitivity to the experimental efficiency make it impossible to do this reliably (Bahcall, 1987; Kahana *et al.*, 1987; Krauss, 1987). More statistically significant fits can be obtained if one makes assumptions to constrain some of these four parameters. If mixing is neglected and the data are fit to a single temperature, a value of the initial temperature $T_{\bar{e}}^t \approx 5$ MeV is indicated. Since this is larger than the value in Eq. (3.22), it suggests the possibility of some neutrino mixing (we note that the predicted neutrino temperatures of supernova models after SN 1987A have increased). If one assumes the values in Eq. (3.22), then a value of $P(\bar{\nu}_e \to \bar{\nu}_e) \approx 0.30$ yields a fit to the data that is better than the single temperature fit. With the present uncertainty in supernova models, neither $P(\bar{\nu}_e \to \bar{\nu}_e)$ nor the flux temperature can be obtained without making assumptions.

Summarizing, although the relative difference between fluxes of different neutrino flavors is expected to be large, because the expected absolute neutrino fluxes are uncertain by a large percentage and because only a small number of $\bar{\nu}_e$ were detected, it is not possible to significantly constrain neutrino mass and mixing parameters from the neutrino detection of SN 1987A (except for a large, kinetmatic mass limit). A future supernova may yield important information on neutrino flavor mixing if future experiments are sensitive to many different neutrino species.

4. Supernova dynamics and neutrino mixing

The dynamics of a supernova are very sensitive to small details. Because neutrinos account for almost all of the energy released, the dynamics depend sensitively on the properties of neutrinos. Here we will qualitatively describe some of the ways that neutrino mixing can influence supernova dynamics and attempt to identify the relevant range of neutrino mass and mixing parameters.

In a supernova, neutrino mixing becomes relevant for flavor-dependent scattering processes. We can thus ignore neutral-current effects. Only mixing between ν_e ($\bar{\nu}_e$) and ν_μ ($\bar{\nu}_\mu$) or ν_τ ($\bar{\nu}_\tau$) needs to be considered. Furthermore, the typical neutrino wavelength in a medium [Eq. (2.36)],

$$\lambda_0 = 4\pi E_\nu / A \approx \sqrt{2}\pi/(\rho_e G_F) , \tag{3.30}$$

is much shorter than the nonforward, flavor-dependent scattering length

$$l_s = 1/(\rho_n \sigma_{\text{capture}}) \approx 1/(\rho_n G_F^2 E_\nu^2) , \tag{3.31}$$

where $\rho_{n(e)}$ is the nucleon (electron) density. Thus we may ignore phase effects and, to a very good approximation, use classical probabilities for describing neutrino mixing.

Using the neutrinosphere density of about 3×10^{11} g/cm^3, we may consider the cases of "light" and "heavy" neutrinos, depending on whether neutrino resonances happen outside or inside the neutrinosphere, respectively.

Outside the collapsed core, the escaping neutrinos can deposit energy on the surrounding matter and contribute

to the supernova explosion. This is especially important for the so-called delayed shock mechanism (Bethe and Wilson, 1985; Wilson, 1985). If neutrino mixing occurs, the temperature of the ν_e and $\bar{\nu}_e$ fluxes will increase, with a corresponding loss in luminosity [Eq. (3.22)]. The cross sections for charged-current processes are strongly dependent on the neutrino energy, and this tends to enhance the energy deposition. For adiabatic resonant conversion to occur outside the neutrinosphere and before the typical region where the shock may stall (Fuller *et al.*, 1987), we have

$$10 < m_2 < 300 \text{ eV} ; \tag{3.32}$$

for the range of mixing angle given in Fig. 17,

$$\Delta^{4/3}\sin^2 2\theta > 10^{-6} \text{ eV}^{4/3} . \tag{3.33}$$

For such a "light" neutrino, the supernova will be enhanced.

Inside the collapsed core there is a large degenerate sea of trapped electron neutrinos. This acts to prevent further neutronization and helps to keep the nucleons in large nuclei, thereby enhancing neutrino trapping. These things are crucial to the "prompt" supernova mechanism where the kinetic energy of the material surrounding the core comes primarily from the "bounce" of a large core. A paper by Fuller *et al.* (1987) and unpublished calculations by Cooperstein (Kahana *et al.*, 1987; Brown *et al.*, 1988) suggest that a resonance inside the core would be fatal to the prompt supernova mechanism. An adiabatic resonance inside the core would occur for a "heavy" neutrino mass in the range

$$300 \text{ eV} < m_2 < 2 \text{ keV} \tag{3.34}$$

and neutrino mixing parameters approximately the same as those given by Eq. (3.33) (we note that in the core there is a contribution to the induced electron-neutrino mass due to background electron neutrinos, see Table II). Thus for a "heavy" neutrino, the supernova will likely not occur.

It is to be hoped that neutrino mixing will be incorporated in future supernova calculations, so that its quantitative impacts can more accurately be assessed.

D. Early universe

There is a long history of using the success of big-bang nucleosynthesis to constrain the properties of neutrinos. The standard model of the early universe successfully predicts the primordial abundances of ^{2}H, ^{3}He, ^{4}He, and ^{7}Li. These predictions are sensitive to neutrinos because (1) the neutron-to-proton ratio is fixed by neutrino decoupling from beta equilibrium with the nucleons and (2) the expansion rate of the universe at that time is dominated by the neutrino energy density. A famous example of such a constraint on neutrino properties is the limit on the number of light-neutrino flavors to be less than or equal to 4. Thus it is a reasonable question to ask what types of constraints big-bang nucleosynthesis places on neutrino oscillations.

1. Changes in the ^{4}He abundance

The expansion of the universe causes the density to monotonically decrease; hence a resonant conversion of neutrino species as described in Sec. II is possible. Matter-enhanced neutrino oscillations in the early universe have been considered in detail by Langacker *et al.* (1987). They estimate the maximum possible change in the ^{4}He abundance from matter-enhanced oscillations. Here we describe the physical scenario and quote their results.

As the early universe cools, the neutrino interaction rate falls below the expansion rate of the universe at a temperature of a few MeV. The tau and muon (anti)neutrinos only interact via the neutral currents, so they decouple first at a temperature of about 5 MeV. The electron (anti)neutrinos can scatter off the electron background via the charged current, so they decouple a little later at a temperature of about 3 MeV. At temperatures around 1 MeV, the electrons and positrons annihilate out. The nucleons decouple from beta equilibrium with the neutrinos at a temperature of about 0.7 MeV.

Because the electron (anti)neutrinos decouple later than the others, they are heated to a slightly higher temperature as a result of early e^+e^- annihilation. Thus there is a difference generated between the electron (anti)neutrino and muon or tau (anti)neutrino densities. A resonant conversion between these neutrino flavors would interchange the number densities and hence affect the subsequent nucleosynthesis. To have an effect, the resonant conversion must occur at a temperature after the density difference is generated, 3 MeV, but before the neutrinos decouple from beta equilibrium, 0.7 MeV.

The change in the ^{4}He abundance Y can be ascribed to two different types of deviations from the standard nucleosynthesis model. One type of deviation is that the neutrino temperatures are altered by resonant conversion. This can lead to a change of the ^{4}He mass fraction of at most $\delta Y = 1.0 \times 10^{-4}$. The other type of deviation from standard nucleosynthesis is that there may now be generated a difference between the ν_e and $\bar{\nu}_e$ densities. Assuming that only the neutrino, and not the antineutrino, densities undergo resonant conversion leads to a change of the ^{4}He mass fraction of at most $\delta Y = 1.4 \times 10^{-3}$. The inferred primordial ^{4}He mass fraction is $Y = 0.24$. Thus matter-enhanced resonant conversion in the early universe produces only small deviations from the standard nucleosynthesis predictions.

2. Neutrino propagation in the early universe

Despite the small size of the changes found above, it is interesting to consider neutrino oscillations in the unusu-

al environment of the early universe. These considerations might be relevant for using standard big-bang nucleosynthesis to constrain more exotic neutrino physics than considered above. For instance, resonant conversion into a sterile neutrino species (Kristev *et al.*, 1986) or magnetically induced helicity oscillations (Fukugita *et al.*, 1988) depend on the matter-induced neutrino potentials. Thus we shall make some brief comments on neutrino propagation through a medium like the early universe.

The medium of the early universe is very different from the relatively normal matter in the sun or a supernova. In the early universe, the particle and antiparticle densities are expected to be equal up to about 10^{-10}, which is roughly the present-day ratio of baryons to photons. Thus there is a cancellation to order 10^{-10} for the induced mass of the neutrino (see Table II). At this level, effects that are higher order in G_F may be relevant, since $G_F T^2 \approx 10^{-10}$ for $T \approx 3$ MeV. Examples of such effects are nonforward neutrino scattering, photon-neutrino scattering, and radiative corrections to neutrino-electron and neutrino-neutrino scattering. If these corrections do not cancel out in a *CP* symmetric plasma, then they may be comparable to the leading-order term. In general, these effects have not been calculated precisely.

One type of correction that has been calculated comes from nonzero-momentum transfer in the leading-order process (Notzold and Raffelt, 1988). These corrections were discussed in Sec. II.B.2 and are given in Table II. The terms are of order $3(T/M_W)^2 \approx 10^{-10}$ for $T \approx 0.5$ MeV. They do not vanish when the plasma is *CP* symmetric and the particle and antiparticle densities are equal.

Nonforward neutrino scattering can also be very important, since it does not cancel in a *CP* symmetric plasma. By the optical theorem, it leads to an imaginary part in the forward-scattering amplitude and hence in the matter-induced mass A. Before neutrino decoupling, nonforward neutrino scattering keeps all neutrino species in equilibrium; hence any neutrino mixing is irrelevant. After decoupling, one expects nonforward neutrino scattering to have little effect on resonant conversion. To see this explicitly in terms of the imaginary part of the induced mass, we note that decoupling occurs when $1/(N\sigma) > R$; the neutrino scattering length is greater than the radius of the universe. However, for resonant conversion to occur, the adiabatic condition can be written as $R > \lambda_{\rm res} = 4\pi E/(\Delta \sin 2\theta)$; the radius of the universe must be greater than the oscillation wavelength at resonance. Combining these two conditions and writing them in terms of A yields $\mathrm{Im}(A) < \Delta \sin 2\theta$. Thus after decoupling, we should expect little effect on resonant conversion from an imaginary part of the induced mass which is smaller than the smallest scale in the problem, the mass splitting at resonance.

IV. SUMMARY AND CONCLUSIONS

Neutrino flavor mixing offers the most sensitive method to determine the masses and mixing angles of the neutrinos. The appeal of this method is enhanced by the recent discovery that matter (MSW) effects can alter neutrino flavor mixing in dramatic ways. The electrons in normal matter give rise to a difference in the index of refraction between electron neutrinos and muon or tau neutrinos. This difference can lead to significant changes in the flavor content of the neutrino after it has propagated through enough matter, typically an astrophysical length scale. The resulting neutrino flavor mixing takes on a resonant character and is fundamentally different from vacuum flavor mixing. In a constant-density medium, two neutrino flavors can mix maximally at the resonant density even if the vacuum mixing angle is quite small. In a medium with smooth, monotonically varying density, total conversion from one neutrino species to another can occur as the neutrino propagates through the resonant density. It results in a drastic reduction in the initial neutrino flavor content, something which is impossible to accomplish by propagation in vacuum for any mixing angle. Thus matter effects must be accounted for when considering neutrino flavor mixing during propagation, and, in fact, they provide a useful tool for probing new ranges of neutrino parameters.

A quantitative description of resonant neutrino conversion can be done very precisely. Although numerical integration of the propagation equations is always an option, it is rather cumbersome due to the necessity of integrating the result over the neutrino energy and due to the desire to know the result for many different neutrino masses and mixing parameters. Fortunately, numerical integration of the wave equation is seldom necessary, since resonant conversion can be described quite accurately in an analytic fashion for any number of neutrino flavors. Although phases are essential for the very existence of the MSW effect, almost all of its applications can be described in terms of the much simpler classical probabilities. Then the electron-neutrino survival probability, $P(\nu_e \rightarrow \nu_e)$, factors into independent probabilities at the production, resonance, and detection regions. The probabilities at the production and detection positions are given by the (matter-dependent) mixing matrices at those points. The description of the probability in the region around the resonance point, P_c, can be borrowed (with some important modifications) from other areas of physics. The mathematics of the MSW effect is identical to that of the level-crossing problem in atomic and nuclear physics. Thus one can be very confident in the basic description of the MSW effect.

Once we have the function $P(\nu_e \rightarrow \nu_e)$, it is straightforward to use it in physical applications. The most important application is to electron neutrinos produced in the sun, since they have been studied theoretically for several decades and experimentally for two decades. The MSW effect offers a reasonable solution to the long-standing solar neutrino problem—that the solar neutrino signal observed in the ^{37}Cl detector is about $\frac{1}{4}$ of the predicted signal. This solution is relatively insensitive to neutrino parameters. For two flavors, it works for neutrino mass

differences and mixing angles spanning a range of roughly $10^{-4} \leq m_2^2 - m_1^2 \leq 10^{-8}$ eV^2 and $10^{-4} \leq \sin^2\theta < O(1)$. With three flavors, there are generally two neutrino resonances that can deplete the ν_e flux, with each resonance somewhat similar to the two-flavor case. It is well to keep in mind that there are many possibilities for which the two-flavor solution cannot account, especially when one tries to combine the ^{37}Cl data with other future experiments.

The MSW solution to the solar neutrino problem is very appealing theoretically. It is very much in line with expectations of our current understanding of particle physics. Nevertheless, one must not lose sight of the fact that many other possibilities exist, not the least of which is that given a slight change in the standard solar model, things can be drastically different. Thus more experiments are needed to test whether neutrino mixing, and in particular the MSW effect, is the correct solution to the solar neutrino problem.

The most straightforward test of flavor mixing, be it matter enhanced or just vacuum, is to look for ν_μ or ν_τ in the solar neutrino flux. The heavy-water detector, a ^{11}B detector, and possibly the liquid-argon detector or a very large H_2O Cherenkov detector, should be capable of doing that. One may also look for clues in the neutrino energy spectra. The gallium detector and the water Cherenkov detector can be used for these purposes. Deviation from the expected neutrino energy spectra would be an unmistakable sign of matter effects. An even more dramatic effect would be a diurnal variation due to the neutrino passing through matter in the Earth. However, it should be emphasized that such variations can only occur if the neutrino parameters fall in a rather narrow range.

Besides the solar neutrinos, one could also look for flavor mixing in the atmospheric neutrinos. In addition, the recent detection of neutrinos from SN 1987A offers new ways to study neutrino mass and mixing parameters. Supernova calculations are still not accurate enough to offer detailed constraints. However, with improved theoretical models and experimental techniques, the next observation is likely to be extremely informative and valuable.

The future holds considerable promise for improving our knowledge of neutrino mass and mixing parameters. New experiments sensitive to the various neutrino sources are under construction and many more are being discussed. Neutrino propagation through matter provides a tool for probing a range of neutrino mass and mixing parameters that are not accessible by any other means and offers an attractive solution to the long-standing solar neutrino problem. The range of neutrino masses that are explored using this technique is theoretically very interesting, since similar values follow naturally from simple extensions of the standard model. It is to be hoped that the phenomenon of neutrino mixing will shortly lead us to a definitive and quantitative understanding of neutrinos.

ACKNOWLEDGMENTS

We are grateful to D. Arnett, T. Clark, J. Gaidos, T. Gaisser, W. Haxton, T. Leung, J. LoSecco, S. Love, S. Parke, S. Petcov, P. Rosen, and A. Smirnov for many helpful discussions. This work was supported in part by the United States Department of Energy.

REFERENCES

Aardsma, G., *et al.*, 1987, Phys. Lett. B **194**, 321.
Abela, R., M. Daum, G. H. Eaton, R. Frosch, B. Jost, P. R. Kettle, and E. Steiner, 1984, Phys. Lett. B **146**, 431.
Alberini, C., *et al.*, 1986, Nuovo Cimento C **9**, 237.
Albrecht, H., *et al.*, 1988, Phys. Lett. B **202**, 149.
Alekseev, E. N., L. N. Alekseeva, I. V. Krivosheina, and V. I. Volchenko, 1988, Phys. Lett. B **205**, 209.
Alekseev, E. N., L. N. Alekseeva, V. I. Volchenko, and I. V. Krivosheina, 1987, Pis'ma Zh. Eksp. Teor. Fiz. **45**, 461 [JETP Lett. **45**, 589 (1987)].
Arafune, J., and M. Fukugita, 1987, Phys. Rev. Lett. **59**, 367.
Arafune, J., M. Fukugita, T. Yanagida, and M. Yoshimura, 1987a, Phys. Rev. Lett. **59**, 1864.
Arafune, J., M. Fukugita, T. Yanagida, and M. Yoshimura, 1987b, Phys. Lett. B **194**, 477.
Arnett, W. D., 1987, Astrophys. J. **319**, 136.
Auriemma, G., M. Felcini, P. Lipari, and J. L. Stone, 1988, Phys. Rev. D **37**, 665.
Babu, K. S., E. Ma, and J. Pantaleone, 1989, Phys. Lett. B **218**, 233.
Bahcall, J. N., 1978, Rev. Mod. Phys. **50**, 881.
Bahcall, J. N., 1987, Rev. Mod. Phys. **59**, 505.
Bahcall, J. N., M. Baldo-Ceolin, D. B. Cline, and C. Rubbia, 1986, Phys. Lett. B **178**, 324.
Bahcall, J. N., R. Davis, Jr., and L. Wolfenstein, 1988, Nature (London) **334**, 487.
Bahcall, J. N., J. M. Gelb, and S. P. Rosen, 1987, Phys. Rev. D **35**, 2976.
Bahcall, J. N., and B. R. Holstein, 1986, Phys. Rev. C **33**, 2121.
Bahcall, J. N., W. F. Huebner, S. H. Lubow, P. D. Parker, and R. K. Ulrich, 1982, Rev. Mod. Phys. **54**, 767.
Bahcall, J. N., K. Kubodera, and S. Nozawa, 1988, Phys. Rev. D **38**, 1030.
Bahcall, J. N., T. Piran, W. H. Press, and D. N. Spergel, 1987, Nature (London) **327**, 682.
Bahcall, J. N., and R. K. Ulrich, 1988, Rev. Mod. Phys. **60**, 297.
Balantekin, A. B., S. H. Fricke, and P. J. Hatchell, 1988, Phys. Rev. D **38**, 935.
Baldini, A., and G. F. Giudice, 1987, Phys. Lett. B **186**, 211.
Baltz, A. J., and J. Weneser, 1987, Phys. Rev. D **35**, 528.
Baltz, A. J., and J. Weneser, 1988a, Comments Nucl. Part. Phys. **18**, 227.
Baltz, A. J., and J. Weneser, 1988b, Phys. Rev. D **37**, 3364.
Barabanov, I. R., *et al.*, 1985, in *Solar Neutrinos and Neutrino Astronomy*, AIP Conference Proceedings No. 126, edited by M. L. Cherry, K. Lande, and W. A. Fowler (AIP, New York), p. 175.
Barger, V., R. J. N. Phillips, and K. Whisnant, 1986, Phys. Rev. D **34**, 980.
Barger, V., K. Whisnant, S. Pakvasa, and R. J. N. Phillips, 1980, Phys. Rev. D **22**, 2718.
Bethe, H. A., 1939, Phys. Rev. **55**, 434.
Bethe, H. A., 1984, *Highlights of Modern Astrophysics* (Wiley-Interscience, New York).
Bethe, H. A., 1986, Phys. Rev. Lett. **56**, 1305.

Bethe, H. A., and J. R. Wilson, 1985, Astrophys. J. **295**, 14.
Bilenky, S. M., and S. T. Petcov, 1987, Rev. Mod. Phys. **59**, 671.
Bilenky, S. M., and B. M. Pontecorvo, 1977, Usp. Fiz. Nauk **123**, 181 [Sov. Phys. Usp. **20**, 776 (1977)].
Bionta, R. M., *et al.*, 1987, Phys. Rev. Lett. **58**, 1494.
Bionta, R. M., *et al.*, 1988, Phys. Rev. D **38**, 768.
Booth, N. E., 1987, Appl. Phys. Lett. **50**, 293.
Boris, S., *et al.*, 1987, Phys. Rev. Lett. **58**, 2019.
Botella, F. J., C. S. Lim, and W. J. Marciano, 1987, Phys. Rev. D **35**, 896.
Bouchez, J., M. Cribier, J. Rich, M. Spiro, S. Vignaud, and W. Hampel, 1986, Z. Phys. C **32**, 499.
Bratton, C. B., *et al.*, 1988, Phys. Rev. D **37**, 3361.
Brown, G.E., *et al.*, 1988, Phys. Rep. **163**, 1.
Bugaev, E. V., G. V. Domogatsky, and V. A. Naumov, 1986, in *Cosmic Ray Muon and Neutrino Physics/Astrophysics Using Deep Underground/Underwater Detectors,* Proceedings of the Japan-U.S. Seminar, edtied by Y. Ohashi and V. Z. Peterson (Institute for Cosmic Ray Research, University of Tokyo).
Cabrera, B., L. M. Krauss, and F. Wilczek, 1985, Phys. Rev. Lett. **58**, 2498.
Caldwell, D. O., 1989, Int. J. Mod. Phys. A **4**, 1851.
Carlson, E. D., 1986, Phys. Rev. D **34**, 1454.
Chang, L. N., and R. K. P. Zia, 1988, Phys. Rev. D **38**, 1669.
Chen, H. H., 1985, Phys. Rev. Lett. **55**, 1534.
Cheng, T. P., and L.-F. Li, 1980, Phys. Rev. Lett. **45**, 1908.
Cowan, G. A., and W. C. Haxton, 1982, Science **216**, 51.
Cribier, M., W. Hampel, J. Rick, and D. Vignaud, 1986, Phys. Lett. B **182**, 89.
Cribier, M., J. Rich, M. Spiro, D. Vignaud, W. Hampel, and B. T. Cleveland, 1987, Phys. Lett. B **188**, 168.
Dadykin, V. L., *et al.*, 1987, Pis'ma Zh. Eksp. Teor. Fiz. **45**, 464 [JETP Lett. **45**, 593 (1987)].
Dar, A., and A. Mann, 1987, Nature (London) **325**, 790.
Dar, A., A. Mann, Y. Melina, and D. Zajfman, 1987, Phys. Rev. D **35**, 3607.
Davis, R., Jr., 1988, in Neutrino '88, proceedings of the XIII International Conference, Boston, unpublished.
Davis, R., Jr., D. S. Harmer, and K. C. Hoffman, 1968, Phys. Rev. Lett. **20**, 1205.
de Bellefon, A., P. Espigat, and G. Waysand, 1985, in *Solar Neutrinos and Neutrino Astronomy,* AIP Conference Proceedings No. 126, edited by M. L. Cherry, K. Lande, and W. A. Fowler (AIP, New York), p. 227.
De Rújula, A., S. L. Glashow, R. Wilson, and G. Charpak, 1983, Phys. Rep. **99**, 342.
Eichler, R., 1988, in *Lepton and Photon Interactions,* Proceedings of the International Symposium on Lepton and Photon Interactions at High Energies, Hamburg, West Germany, 1988, edited by R. Rückl and W. Bartel [Nucl. Phys. B (Proc. Suppl.) **3**, 389].
Elliot, S. R., A. A. Hahn, and M. K. Moe, 1987, Phys. Rev. Lett. **59**, 2020.
Ermilova, V. K., V. A. Tsarev, and V. A. Chechin, 1986, Pis'ma Zh. Eksp. Teor. Fiz. **43**, 353 [JETP Lett. **43**, 453 (1986)].
Flaminio, V., and B. Saitta, 1987, Riv. Nuovo Cimento **10**(8), 1.
Friedlander, G., and J. Weneser, 1987, Science **235**, 760.
Fritschi, M., E. Holzschuh, W. Kundig, J. W. Petersen, R. E. Pixley, and H. Stussi, 1986, Phys. Lett. B **173**, 485.
Fukugita, M., D. Notzold, G. Raffelt, and J. Silk, 1988, Phys. Rev. Lett. **60**, 879.
Fuller, G. M., R. W. Mayle, J. R. Wilson, and D. N. Schramm, 1987, Astrophys. J. **322**, 795.
Gaisser, T. K., T. Stanev, and G. Barr, 1988, Phys. Rev. D **38**, 85.
Gell-Mann, M., P. Ramond, and R. Slansky, 1979, in *Supergravity,* edited by P. Van Nieuwenhuizen and D. Z. Freedman (North-Holland, Amsterdam), p. 315.
Gilman, F., 1986, Comments Nucl. Part. Phys. **16**, 231.
Gronau, M., C. N. Leung, and J. L. Rosner, 1984, Phys. Rev. D **29**, 2539.
Grotz, K., H. V. Klapdoor, and J. Metzinger, 1986, Astron. Astrophys. **154**, L1.
Halprin, A., 1986, Phys. Rev. D **34**, 3462.
Haxton, W. C., 1986, Phys. Rev. Lett. **57**, 1271.
Haxton, W. C., 1987a, Phys. Rev. D **35**, 2352.
Haxton, W. C., 1987b, Phys. Rev. D **36**, 2283.
Haxton, W. C., and C. W. Johnson, 1988, Nature (London) **333**, 325.
Haxton, W. C., and G. J. Stephenson, Jr., 1984, Prog. Part. Nucl. Phys. **12**, 409.
Hirata, K., *et al.*, 1987, Phys. Rev. Lett. **58**, 1490.
Hirata, K., *et al.*, 1988a, Phys. Rev. D **38**, 448.
Hirata, K., *et al.*, 1988b, Phys. Lett. B **205**, 416.
Hiroi, S., H. Sakuma, T. Yanagida, and M. Yoshimura, 1987a, Phys. Lett. B **198**, 403.
Hiroi, S., H. Sakuma, T. Yanagida, and M. Yoshimura, 1987b, Prog. Theor. Phys. **78**, 1428.
Ito, M., T. Kaneko, and M. Nakagawa, 1988, Prog. Theor. Phys. **79**, 13.
Joshipura, A. S., and M. V. N. Murthy, 1988, Phys. Rev. D **37**, 1374.
Kahana, S. H., J. Cooperstein, and E. Baron, 1987, Phys. Lett. B **196**, 259.
Kaneko, T., 1987, Prog. Theor. Phys. **78**, 532.
Kawakami, H., *et al.*, 1987, Phys. Lett. B **187**, 198.
Kim, C. W., J. Kim, and W. K. Sze, 1988, Phys. Rev. D **37**, 1072.
Kim, C. W., S. Nussinov, and W. K. Sze, 1987a, Phys. Lett. B **184**, 403.
Kim, C. W., S. Nussinov, and W. K. Sze, 1987b, Phys. Rev. D **35**, 4014.
Kim, C. W., and W. K. Sze, 1987, Phys. Rev. D **35**, 1404.
Kirsten, T., 1986, in *'86 Massive Neutrinos in Astrophysics and in Particle Physics,* Proceedings of the VI Moriond Workshop, Tignes-Savoie, France, 1986, edited by O. Fackler and J. Tran Thanh Van (Editions Frontières, Gif-sur-Yvette), p. 119.
Kolb, E. W., M. S. Turner, and T. P. Walker, 1986, Phys. Lett. **B175**, 478.
Krastev, P. I., and S. T. Petcov, 1988a, Phys. Lett. B **207**, 64.
Krastev, P. I., and S. T. Petcov, 1988b, in *5th Force Neutrino Physics,* proceedings of the Moriond Workshop, Les Arcs, France, 1988, edited by O. Fackler and J. Tran Thanh Van (Editions Frontières, Gif-sur-Yvette), p. 179.
Krastev, P. I., and S. T. Petcov, 1988c, Phys. Lett. B **205**, 84; **214**, 660(E).
Krauss, L., 1987, Nature (London) **329**, 689.
Kuo, T. K., and J. Pantaleone, 1986, Phys. Rev. Lett. **57**, 1805.
Kuo, T. K., and J. Pantaleone, 1987a, Phys. Rev. D **35**, 3432.
Kuo, T. K., and J. Pantaleone, 1987b, Phys. Lett. B **198**, 406.
Kuo, T. K., and J. Pantaleone, 1988, Phys. Rev. D **37**, 298.
Kuo, T. K., and J. Pantaleone, 1989, Phys. Rev. D **39**, 1930.
Lagage, P. O., M. Cribier, J. Rich, and D. Vignaud, 1987, Phys. Lett. B **193**, 127.
Landau, L., 1932, Phys. Z. Sowjetunion **2**, 46.
Landau, L. D., and E. M. Lifshitz, 1977, *Quantum Mechanics: Non-Relativistic Theory* (Pergamon, New York).
Langacker, P., 1981, Phys. Rep. **72**, 185.

Langacker, P., J. P. Leveille, and J. Sheiman, 1983, Phys. Rev. D **27**, 1228.
Langacker, P., S. T. Petcov, G. Steigman, and S. Toshev, 1987, Nucl. Phys. B **282**, 589.
Lanou, R. E., H. J. Maris, and G. M. Seidel, 1987, Phys. Rev. Lett. **58**, 2498.
Lim, C. S., and W. J. Marciano, 1988, Phys. Rev. D **37**, 1368.
Longo, M. J., *et al.*, 1987, in *Neutrino Masses and Neutrino Astrophysics,* edited by V. Barger *et al.* (World Scientific, Singapore), p. 463.
LoSecco, J. M., 1986, Phys. Rev. Lett. **57**, 652.
LoSecco, J. M., *et al.*, 1987, Phys. Lett. B **184**, 305.
Maki, Z., M. Nakazawa, and S. Sakata, 1962, Prog. Theor. Phys. **28**, 870.
Mann, A., *et al.*, 1988, in Neutrino '88, proceedings of the XII International Conference, Boston, unpublished.
Mannheim, P. D., 1988, Phys. Rev. D **37**, 1935.
Mathews, G. J., S. B. Bloom, G. M. Fuller, and J. L. Bahcall, 1985, Phys. Rev. C **32**, 796.
Mayle, R., J. R. Wilson, and D. Schramm, 1986, Nuovo Cimento C **9**, 443.
Messiah, A., 1986, in *'86 Massive Neutrinos in Astrophysics and in Particle Physics,* Proceedings of the VI Moriond Workshop, Tignes-Savoie, France, edited by O. Fackler and J. Tran Thanh Van (Editions Frontières, Gif-sur-Yvette), p. 373.
Mikheyev, S. P., and A. Yu. Smirnov, 1985, Yad. Fiz. **42**, 1441 [Sov. J. Nucl. Phys. **42**, 913 (1985)].
Mikheyev, S. P., and A. Yu. Smirnov, 1986a, Nuovo Cimento C **9**, 17.
Mikheyev, S. P., and A. Yu. Smirnov, 1986b, Zh. Eksp. Teor. Fiz. **91**, 7 [Sov. Phys. JETP **64**, 4 (1986)].
Mikheyev, S. P., and A. Yu. Smirnov, 1987a, Pis'ma Zh. Eksp. Teor. Fiz. **46**, 11 [JETP Lett. **46**, 10 (1987)].
Mikheyev, S. P., and A. Yu. Smirnov, 1987b, in *New and Exotic Phenomena,* Proceedings of the VII Moriond Workshop, Les Arcs–Savoie, France, edited by O. Fackler and J. Tran Thanh Van (Editions Frontières, Gif-sur-Yvette), p. 405.
Mikheyev, S. P., and A. Yu. Smirnov, 1987c, Usp. Fiz. Nauk **153**, 3 [Sov. Phys. Usp. **30**, 759 (1987)].
Mikheyev, S. P., and A. Yu. Smirnov, 1988, Phys. Lett. B **200**, 560.
Minakata, H., and H. Nunokawa, 1988, Phys. Rev. D **38**, 3605.
Minakata, H., H. Nunokawa, K. Shiraishi, and H. Suzuki, 1987, Mod. Phys. Lett. A **2**, 827.
Nakanata, M., 1988, doctoral thesis (University of Tokyo).
Nicolaidis, A., 1988, Phys. Lett. B **200**, 553.
Nieves, J. F., 1987, Puerto Rico University Preprint No. 87-1064.
Notzold, D., 1987a, Phys. Lett. B **196**, 315.
Notzold, D., 1987b, Phys. Rev. D **36**, 1625.
Notzold, D., and G. Raffelt, 1988, Nucl. Phys. B **307**, 924.
Nussinov, S., 1976, Phys. Lett. B **63**, 201.
Parke, S. J., 1986, Phys. Rev. Lett. **57**, 1275.
Parke, S. J., and T. P. Walker, 1986, Phys. Rev. Lett. **57**, 2322; **57**, 3124(E).
Petcov, S. T., 1987, Phys. Lett. B **191**, 299.
Petcov, S. T., 1988a, Phys. Lett. B **200**, 373.
Petcov, S. T., 1988b, Phys. Lett. B **207**, 64.
Petcov, S. T., 1988c, Phys. Lett. B **214**, 139.
Petcov, S. T., 1988d, Phys. Lett. B **214**, 259.
Petcov, S. T., and S. Toshev, 1987, Phys. Lett. B **187**, 120.
Pizzochero, P., 1987, Phys. Rev. D **36**, 2293.
Pontecorvo, B., 1958, Zh. Eksp. Teor. Fiz. **34**, 247 [Sov. Phys. JETP **7**, 172 (1958)].
Pontecorvo, B. M., 1968, Zh. Eksp. Teor. Fiz. **53**, 1717 [Sov. Phys. JETP **26**, 984 (1968)].
Raghaven, R. S., X. G. He, and S. Pakvasa, 1988, Phys. Rev. D **38**, 1317.
Raghavan, R. S., and S. Pakvasa, 1988, Phys. Rev. D **37**, 849.
Raghavan, R. S., S. Pakvasa, and B. A. Brown, 1986, Phys. Rev. Lett. **57**, 1801.
Rosen, S. P., 1988, Phys. Rev. D **37**, 1682.
Rosen, S. P., and J. M. Gelb, 1986, Phys. Rev. D **34**, 969.
Sato, K., and H. Suzuki, 1987, Phys. Rev. Lett. **58**, 2722.
Schafer, A., and S. E. Koonin, 1987, Phys. Lett. B **185**, 417.
Schramm, D. N., 1987, Comments Nucl. Part. Phys. **17**, 239.
Shapiro, S. L., and S. A. Teukolsky, 1983, *Black Holes, White Dwarfs and Neutron Stars* (Wiley-Interscience, New York).
Smirnov, A. Yu., 1987, in *New and Exotic Phenomena,* Proceedings of the VII Moriond Workshop, Les Arcs–Savoie, France, edited by O. Fackler and J. Tran Thanh Van (Editions Frontières, Gif-sur-Yvette), p. 275.
Stacey, F. D., 1985, *Physics of the Earth,* 2nd ed. (Wiley, New York).
Stodolsky, L., 1987, Phys. Rev. D **36**, 2273.
Stueckelberg, E. C. G., 1932, Helv. Phys. Acta **5**, 369.
Sun, C. P., 1988, Phys. Rev. D **38**, 2908.
Suzuki, A., 1987, talk at the Workshop on Elementary Particle Picture of Universe, Tsukuba, Japan, University of Tsukuba Preprint No. UT-ICEPP-87-06.
Terry, D., and T. K. Kuo, 1981, Phys. Rev. D **24**, 2523.
Toshev, S., 1986, Phys. Lett. B **180**, 285.
Toshev, S., 1987a, Phys. Lett. B **185**, 177; **192**, 478(E).
Toshev, S., 1987b, Phys. Lett. B **196**, 170.
Toshev, S., 1988a, Mod. Phys. Lett. A **3**, 71.
Toshev, S., 1988b, Phys. Lett. B **198**, 551.
Volkova, L. K., 1980, Yad. Fiz. **31**, 1510 [Sov. J. Nucl. Phys. **31**, 784 (1980)].
Walker, T. P., and D. Schramm, 1987, Phys. Lett. B **195**, 331.
Weneser, J., and B. Friedlander, 1987, Science **235**, 755.
Whisnant, K., 1988, Phys. Rev. D **38**, 692.
Wilkerson, J. F., T. J. Bowles, J. C. Browne, M. P. Maley, R. G. H. Robertson, J. S. Cohen, R. L. Martin, D. A. Knapp, and J. A. Helffrich, 1987, Phys. Rev. Lett. **58**, 2023.
Wilson, J. R., 1985, in *Numerical Astrophysics,* edited by J. M. Centrella, J. M. Leblanc, and R. L. Bowers (Jones and Bartlett, Boston) p. 422.
Wilson, J. R., R. Mayle, S. E. Woosley, and T. Weaver, 1986, Ann. N.Y. Acad. Sci. **470**, 267.
Wolfenstein, L., 1978a, Phys. Rev. D **17**, 2369.
Wolfenstein, L., 1978b, in *Neutrino '78,* Proceedings of the International Conference on Neutrino Physics and Astrophysics, edited by E. C. Fowler (Purdue University, West Lafayette), p. C3.
Wolfenstein, L., 1979, Phys. Rev. D **20**, 2634.
Wolfenstein, L., 1987, Phys. Lett. B **194**, 197.
Wolfsberg, K., *et al.*, 1985, in *Solar Neutrinos and Neutrino Astronomy,* AIP Conference Proceedings No. 126, edited by M. L. Cherry, K. Lande, and W. A. Fowler (AIP, New York), p. 196.
Yanagida, T., 1979, Proceedings of the Workshop on Unified Theory and Baryon Number of the Universe, Tsukuba, Ibaraki, Japan, unpublished.
Zaglauer, H. W., and K. H. Schwarzer, 1987, Phys. Lett. B **198**, 556.
Zaglauer, H. W., and K. H. Schwarzer, 1988, Z. Phys. C **40**, 273.
Zener, C., 1932, Proc. R. Soc. London, Ser. A **137**, 696.